CHARACTERIZATION AND PHARMACOGENETICS OF HEPATIC PHASE I EXEMESTANE METABOLISM

By

AMITY PETERSON

A dissertation submitted in partial fulfillment of
the requirements for the degree of

DOCTOR OF PHILOSOPHY

WASHINGTON STATE UNIVERSITY
College of Pharmacy

MAY 2017

To the Faculty of Washington State University:

The members of the Committee appointed to examine the dissertation of AMITY PETERSON find it satisfactory and recommend that it be accepted.

Philip Lazarus, Ph.D., Chair

Sayed S. Daoud, Ph.D.

Gang Chen, Ph.D.

John White, Pharm.D., PA-C

ACKNOWLEDGMENTS

I would like to extend my sincerest thanks to the members of my advisory committee for their support of my professional development. Dr. Zuping Xia deserves special acknowledgment for his considerable work as the synthetic chemist for this project.

I would also like to acknowledge the funding agencies that made my doctoral work possible. Thank you to the National Institutes of Health for its generous financial support of this research. Graduate student teaching and research assistantships were kindly provided by the Washington State University Department of Pharmaceutical Sciences.

Most of all, I would like to thank my family and friends for their unwavering support. Thank you to my dad, Kenneth Peterson, for working so hard to make achieving a college education a possibility and for encouraging me to apply myself from a young age. My work ethic and curiosity are a direct result of my father's example. Thank you to my mom, Kelly Peterson, for the love and optimism that has sustained me throughout difficult times. Thank you to my sister, Chelsea Peterson, for inspiring me with her resilience and for taking care of me when I needed it most. Thank you to my dear friend, Beverly Wareham, for her warmth and words of encouragement. Finally, thank you to my friends, Kelly Ezell and Xiaomeng Jiang, for all of the good times and for lending a sympathetic ear during the bad times. I could not have done this without all of you.

CHARACTERIZATION AND PHARMACOGENETICS OF

HEPATIC PHASE I EXEMESTANE METABOLISM

Abstract

by Amity Peterson, Ph.D.
Washington State University
May 2017

Chair: Philip Lazarus

Exemestane (EXE) is an endocrine therapy used to combat postmenopausal breast cancer. Several studies have reported substantial differences in clinical outcomes between EXE-treated patients, as well as inexplicable variability in serum concentrations of EXE and its major metabolite, 17β-dihydroexemestane (17β-DHE). For many pharmaceuticals, drug response is influenced by patient-specific genetic factors related to xenobiotic metabolism. Thus, it is possible that allelic variation in genes involved in EXE metabolism contributes to inter-individual differences in patient outcomes, possibly through differential EXE clearance or varied rates of metabolite formation. Historically, knowledge of phase I EXE metabolism has been extremely limited with significant ambiguity surrounding the identity of the specific hepatic enzymes involved. To address this gap in knowledge, *in vitro* studies were undertaken to better characterize hepatic phase I EXE metabolism and in particular, to assess the impact of genetic variation in drug-metabolizing enzymes on the production of EXE metabolites with inhibitory activity against aromatase.

The first part of this dissertation describes the identification of phase I EXE metabolites and details their capacity to suppress estrogen synthesis. Four metabolites, including 17β-DHE, were detected in incubations of EXE with pooled human liver microsomes. 17β-DHE and a novel metabolite, 17α-DHE, were formed in incubations of EXE with pooled human liver

cytosol. The identities of phase I EXE metabolites were confirmed through comparison to reference compounds using UPLC/MS/MS. Anti-aromatase activity assays (AAA) revealed that 17β-DHE is the only phase I EXE metabolite formed by human liver fractions that appreciably impedes estrogen formation. AAA also suggest that the inhibitory potency of EXE is unaffected by common nonsynonymous polymorphisms in aromatase. The latter half of this dissertation identifies hepatic enzymes that are likely to participate in phase I EXE metabolism. *In vitro* assays show that CBR1, AKR1Cs, and multiple hepatic CYP450s predominantly reduce EXE to 17β-DHE with minor formation of additional inactive metabolites. Kinetic assays comparing 17β-DHE formation by each wildtype enzyme to its common variant allozymes show that specific genotypes are associated with altered EXE metabolism *in vitro*. However, additional investigations are needed to determine the prognostic value of these associations for predicting *in vivo* EXE response.

TABLE OF CONTENTS

CHAPTER FIVE: CONCLUSIONS AND FUTURE DIRECTIONS

LIST OF TABLES

CHAPTER ONE

CHAPTER TWO

CHAPTER THREE

CHAPTER FOUR

LIST OF FIGURES

CHAPTER ONE

CHAPTER TWO

CHAPTER THREE

CHAPTER FOUR

ABBREVIATIONS AND SYMBOLS

˚C	Degrees Celsius
5α-DHT	5-Alpha-dihydrotestosterone
6-HME	6-Hydroxymethylandrosta-1,4,6-triene-3,17-dione
17α-DHE	17-Alpha-dihydroexemestane
17β-DHE	17-Beta-dihydroexemestane
α	Alpha
β	Beta
µg	Microgram
µl	Microliter
µmol	Micromole
µM	Micromole per liter
AAA	Anti-aromatase activity
ACS	American Chemical Society grade
ADME	Absorption, distribution, metabolism, and excretion
ADR(s)	Adverse drug reaction(s)
AI	Aromatase inhibitor
AKR	Aldo-keto reductase
ANA	Anastrozole
APS	Ammonium persulfate
Arg	Arginine
Asn	Asparagine

Asp	Aspartate
AUC	Area under the curve
BCA	Bicinchoninic acid
BEH	Ethylene bridged hybrid
BL21	Chemically competent E. coli cell line
BMD	Bone mineral density
B-PER	Bacterial protein extraction reagent
C6	Carbon 6
C17	Carbon 17
cDNA	Complementary deoxyribonucleic acid
CL_{INT}	Intrinsic clearance of substrate
C_{max}	Maximum concentration
CPIC	Clinical Pharmacogenetics Implementation Consortium
CPR	NADPH-Cytochrome P450 oxidoreductase
CYP/CYP450	Cytochrome P450
Cys	Cysteine
dbSNP	Single nucleotide polymorphism database
dbVar	Short genetic variations database
DMEM	Dulbecco's modified Eagle's medium
DTT	Dithiothreitol
EBI	European Bioinformatics Institute
EDTA	Ethylenediaminetetraacetic acid

ER	Estrogen receptor
EXE	Exemestane
FDA	Food and Drug Administration
G418	Aminoglycoside antibiotic for selection of transfected HEK293
g	Relative centrifugal force
GC-MS	Gas chromatography coupled to mass spectrometry
Gln	Glutamine
Glu	Glutamate
Gly	Glycine
GWAS	Genome-wide association study
h	Hour
HEK293	Epithelial cell line derived from human embryonic kidney
His	Histidine
HLC	Human liver cytosol
HLM	Human liver microsomes
HMG-CoA	3-hydroxy-3-methylglutaryl-coenzyme A
HRP	Horseradish peroxidase
IC_{50}	Half maximal inhibitory concentration
IES	Intergroup Exemestane Study
IGNITE	Implementing Genomics in Practice
Ile	Isoleucine
kb	Kilobase

K_M	Michaelis constant; substrate concentration at 50% of V_{max}
l	Liter
LC	Liquid chromatography
LET	Letrozole
Leu	Leucine
Log-phase	Exponential phase of bacterial growth
Lys	Lysine
MAF	Minor allele frequency
MAP.3	Mammary Prevention 3 clinical trial
Met	Methionine
mg	Milligram
$MgCl_2$	Magnesium chloride
min	Minute
ml	Milliliter
mm	Millimeter
mmol	Millimole
MRM	Multiple reaction monitoring
MS/MS	Tandem mass spectrometry
m/z	Mass-to-charge ratio
NaCl	Sodium chloride
NADPH	Nicotinamide adenine dinucleotide phosphate
NaH_2PO_4	Sodium dihydrogen phosphate

NBP	(-)-N-3-benzylphenobarbital
NCBI	National Center for Biotechnology Information
ng	Nanogram
NHGRI	National Human Genome Research Institute
NHT	Neoadjuvant hormonal therapy
NIH	National Institutes of Health
Ni-NTA	Nitrilotriacetic acid loaded with divalent nickel ions
nl	Nanoliter
nM	Nanomole per liter
NSAID	Nonsteroidal anti-inflammatory drug
OFS	Ovarian function suppression
PBS	Phosphate-buffered saline
PCR	Polymerase chain reaction
PDA	Photodiode array detector
pH	Negative logarithmic value of the hydrogen ion concentration
Phe	Phenylalanine
PINP	Amino terminal propeptide of type I collagen
PREDICT	Pharmacogenomic Resource for Enhanced Decisions in Care and Treatment
Pro	Proline
PVDF	Polyvinylidene fluoride
QTof	Quadropole time-of-flight mass spectrometer

RNA	Ribonucleic acid
rpm	Revolutions per minute
s	Second
SDM	Site-directed mutagenesis
SDR	Short-chain dehydrogenase/reductase
SDS	Sodium dodecyl sulfate
SDS-PAGE	Sodium dodecyl sulfate polyacrylamide gel electrophoresis
Ser	Serine
SERM	Selective estrogen receptor modulator
SNP	Single nucleotide polymorphism
SOFT	Suppression of Ovarian Function Trial
$t_{1/2}$	Half-life
TAM	Tamoxifen
Taq	DNA polymerase from *Thermus aquaticus*
TBST	Tris-buffered saline with 0.1% Tween 20
TCP	Tranylcypromine
TEAM	Tamoxifen Exemestane Adjuvant Multinational phase 3 trial
TEMED	Tetramethylethylenediamine
TEXT	Tamoxifen and Exemestane Trial
Thr	Threonine
T_{max}	Time to maximum concentration
TNFα	Tumor necrosis factor alpha

Tyr	Tyrosine
U	Enzyme unit of activity
UGT	Uridine diphosphoglucuronosyl transferase
U-PGx	Ubiquitous Pharmacogenomics
UPLC	Ultra performance liquid chromatography
UTR	Untranslated region
V	Volt
Val	Valine
V_{max}	Maximum rate of reaction
wt	Wildtype

CHAPTER ONE

Literature review and background

1.1 INTRODUCTION

The first section of this chapter highlights the utility of pharmacogenetic information in improving healthcare. A brief review of aromatase, the enzyme targeted by the synthetic androgen, exemestane (EXE), is also presented. To impart relevant context to the reader, the physiological role of aromatase in healthy human tissues, as well as its pathological overexpression in cancerous breast tissue will be discussed. The second portion of this chapter reviews the pharmacology of exemestane, including its chemical structure, mechanism of action, toxicity, and clinical use in varying stages of hormone-responsive breast cancer. The final section summarizes the limited literature regarding EXE metabolism and discusses significant gaps in the existing knowledge of the drug's metabolic pathway.

1.2 PHARMACOGENETICS

1.2.1 Rationale for genotype-guided personalized medicine

One compelling tool for the advancement of personalized medicine is pharmacogenetics, which studies the influence of host-specific genetic factors on drug disposition [1]. From the analysis of clinical trials in human subjects, it is readily apparent that responses to pharmaceuticals often vary considerably between individuals [1]. Therefore, approval of a substance for clinical use may cautiously be interpreted as a general indication of sufficient drug safety and efficacy in an "average" individual of the selected test population [1]. However, the paradigm that one drug or dosage is uniformly appropriate to treat a particular disease in a genetically heterogeneous population is deeply flawed and unfortunately, often persists into clinical practice under the false assumption that an individual patient will respond in a predictable, standardized way characteristic of the drug's pharmacology [2, 3]. Suboptimal

patient outcomes, including a lack of therapeutic efficacy and toxicity are frequent, unintentional consequences of this prescriptive method [2, 3]. Ultimately, pharmacogenetic studies seek to improve healthcare by better informing the prescription of pharmaceuticals through the identification of clinically relevant gene-drug interactions [3].

1.2.2 Genetic screenings for the prevention of adverse drug reactions

Adverse drug reactions (ADRs) are broadly defined as noxious, unintentional responses to appropriately administered pharmaceutical products used at approved therapeutic doses [4]. Following administration of a drug, ADRs often manifest as predictable dose-dependent toxicities reflective of its therapeutic mechanism (intrinsic or type A) or arise from the complex interplay of patient-specific factors, such as nutritional status, environmental exposure to viral or chemical agents, and genetic predispositions (idiosyncratic or type B) [5]. Although largely preventable, serious ADRs requiring immediate medical intervention remain alarmingly common and tax healthcare systems worldwide [6, 7]. An estimated 3.6-6.5% of hospital admissions are a direct result of pharmaceutical-related toxicity [6, 8]. One recent study suggests that approximately 1 out of every 100 ADR-related hospitalizations in Europe culminates in the death of the patient [8]. Furthermore, a prospective analysis of nearly 19,000 individuals admitted to two hospitals in the United Kingdom found that patients admitted for ADRs required a median hospital stay of 8 days, utilized nearly 4% of the total bed capacity, and generated $847 million of direct medical costs [6].

Aside from the direct financial costs incurred by patients and health insurance providers, drug toxicity is associated with indirect costs to society at large, such as lost productivity in the workforce [9]. In addition to the economic incentive to reduce healthcare expenditures, it is

ethically imperative to systematically reduce ADRs as they are a cause of substantial physical and psychological suffering and a source of imminent danger to vulnerable patient populations, including children and the elderly [10-12]. One promising strategy for reducing pharmaceutical-related morbidity and mortality is the development and implementation of personalized medicine or individuated medical interventions [13].

Automated genotype-guided clinical decision support, which relies on prognostic markers of drug response, could decrease ADRs and improve overall patient care by preemptively suggesting dose modifications or use of an alternative therapeutic agent [14-16]. With sufficient knowledge of gene-drug interactions, treatments may be tailored for each patient prior to drug exposure by considering the likelihood of efficacy or toxicity based on their unique, genetically determined metabolic capacity and concomitant use of other medications [17]. In particular, clinical use of pharmacogenetic information could translate into a significant reduction in the incidence of idiosyncratic ADRs, which often have an underlying genetic component and typically remain undetected prior to drug approval due to an insufficient number of participants in most preclinical and clinical trials [5, 12, 13]. A recent pharmacoeconomic study by *Alagoz et al.* strongly supports one-time genetic testing as an effective means of reducing ADRs, which are associated with direct medical costs of approximately $2,400 per event [12, 18]. Interestingly, the same study projected that preemptive genetic testing of 1,000 40-year old patients would prevent 3 ADR-related deaths, 6 hospitalizations, and 95 emergency department or outpatient visits [12].

1.2.3 Use of genetic screenings to improve drug dosing and response

The efficacy and response rate of many drugs can be increased through the genotype-guided identification of patients most likely to exhibit a favorable response [12]. Unfortunately, it is estimated that 25-50% of pharmacological interventions produce undesirable side effects or fail to provide therapeutic relief [19]. Rapid identification of the safest, most effective course of treatment is especially important for pharmaceuticals with narrow therapeutic indices, as well as those used to treat life-threatening conditions in which poor efficacy may allow continued disease progression [20, 21]. Warfarin dosing serves as a prominent example of the clinical utility of using genetic information to adjust dosages to better suit the need of a particular individual. *Klein et al*. have shown that preventing one instance of suboptimal warfarin dosing, as defined by a deviation of 20% from the desired therapeutic dosage, required preemptive genotyping of only about 13 patients [22]. Moreover, a recent proof-of-concept study by *Hall-Flaven et al.* alludes to the opportunity to drastically improve psychiatric patient outcomes through routine genotype-guided prescribing [23]. Two hundred and twenty-seven individuals diagnosed with major depressive disorder were recruited to receive to outpatient treatment and assigned to one of two groups [23]. Prior to initiating psychiatric medication, one group of participants was preemptively genotyped for five genes associated with response to psychotropic drugs [23]. The prescribing physician of the genotyped patients had access to these results to guide choice of therapy while the other group of participants were prescribed treatment in the absence of genetic information [23]. Following 8 weeks of medication, the genotyped patients had a higher rate of response and showed greater overall improvement in their symptoms relative to the non-genotyped patients [23]. Interestingly, the initially non-genotyped patients were also genotyped at the end of the study, which revealed that the patients with the least improvement had been prescribed medications suboptimal for their genotype [23]. These results augment a

growing body of evidence suggesting that genotype-guided prescribing can improve clinical outcomes for multiple illnesses.

1.2.4 Challenges in the clinical implementation of personalized medicine

Despite its tremendous promise, personalized medicine has yet to become standard practice largely due to logistical issues, such as the high initial overhead required and difficulty in effectively communicating actionable genotype-drug interactions to clinicians [14, 24, 25]. Establishing point of care genetic testing requires not only the identification of reliable prognostic biomarkers but also the creation of an extensive infrastructure, including construction of a properly accredited laboratory [25, 26]. In addition to laboratory staff and genetic counselors, considerable technical support is needed to ensure proper data entry into electronic health records (EHRs) and to oversee the storage of large volumes of sequencing data [20, 25]. Additionally, automatic prescription advising software needs to be incorporated into EHRs prior to the widespread implementation of personalized medicine as it is unreasonable to expect healthcare workers to exhibit mastery of the ever-increasing volume and complexity of pharmacogenetic data [15, 16, 25].

Several other key factors limit the widespread accessibility of personalized medicine, including poor insurance coverage and slow turnaround times for DNA processing [24]. Typically, about 3-7 days elapse between the time of DNA collection and delivery of the results to the ordering clinician [24]. In instances requiring immediate medical intervention, this delay precludes genotyping and could lead to the unintentional selection of a suboptimal treatment [20]. One possible solution is to preemptively genotype patients for a panel of relevant pharmacogenes, which in addition to making genetic information accessible at the point of care,

may expedite the delivery of test results by reducing the total number of DNA samples processed [20]. Data collected at the Vanderbuilt University Medical Center suggests that reactive genetic testing actually increases the analytical burden placed on laboratories compared to preemptive panel-based testing of patients at high risk of undergoing coronary artery stenting [23]. Any potentially actionable gene-drug interactions detected with panel-based screenings could then be reflected in an EHR and reviewed prior to all future prescriptions [20, 27]. Nonetheless, coverage of panel-based genetic testing is minimal even in countries with universal healthcare [27, 28]. Without reimbursement, out-of-pocket costs are a significant obstacle to the implementation of routine clinical pharmacogenetics and will likely discourage many patients from seeking informative genetic testing [24, 27].

1.2.5 Recent progress in the implementation of personalized medicine

Despite considerable hurdles, significant headway has been made in the clinical implementation of precision medicine. The availability of next generation sequencing platforms has allowed studies of genotype-drug interactions to be performed and published at a rapid pace [29]. This abundance of information is reflected in the National Human Genome Research Institute-European Bioinformatics Institute Genome Wide Association Study (NHGRI-EBI GWAS) Catalog, which curated 177 studies reporting genetic markers associated with drug response as of January 2017 [30]. In accordance with this surge in clinically actionable data, the Food and Drug Administration recommends or requires genetic testing prior to the prescription of about 40 drugs, although information concerning genetic testing is now included in patient leaflets dispensed with nearly 120 pharmaceuticals [12, 31].

Likewise, the importance of continuing to expand and refine pharmacogenetic knowledge to improve human health has been increasingly recognized by the private sector. It has been suggested that genetic stratification in clinical trials could shorten the duration of drug development from 10-12 years to 3-5 years [32]. Furthermore, genetic stratification of subjects might differentiate genotypes prone to favorable responses or severe adverse events that would otherwise go undetected prior to FDA approval and possibly lead to toxicity-related withdrawal of the product from the market [33]. Interestingly, scientists from GlaxoSmithKline recently suggested that ~10% of pharmaceuticals have a single genetic biomarker with sufficiently strong association with patient response as to potentially influence choice of treatment [1]. For other drugs, it is feasible that the collective consideration of multiple biomarkers with more modest individual effect sizes could also inform therapeutic decisions [1].

Remarkable largescale efforts are currently underway to promote the advancement of personalized medicine. In 2015, President Barack Obama announced the implementation of the Precision Medicine Initiative, which seeks to enroll a diverse cohort of at least 1 million United States citizens beginning in 2017 [34]. Lifestyle information and biological samples, including DNA, will be collected from each participant and linked with their electronic medical record [34]. Correlational analyses of the dataset will then be performed to identify significant relationships between these variables and observed patient outcomes [34]. Several notable consortia have also assembled to facilitate the implementation of clinical pharmacogenetics, including the NIH-funded Implementing Genomics in Practice (IGNITE) initiative, the Dutch Pharmacogenetics Working Group, and the Clinical Pharmacogenomics Implementation Consortium (CPIC), which releases guidelines to assist clinicians in interpreting the results of genetic testing [35-38].

Although previous analyses support one-time preemptive genotyping as a cost-effective means of reducing adverse events, additional data confirming long-term savings will likely be required to persuade insurance providers to expand coverage to include routine genetic testing [12]. To address this issue, several consortia are embarking on detailed pharmacoeconomic analyses of genotype-guided medicine. Indiana University, for instance, has received funding for a large clinical trial comparing a genotyped cohort with non-genotyped individuals in terms of clinical outcomes and incurred medical costs [27]. The Ubiquitous Pharmacogenomics Consortium (U-PGx) will perform similar analyses in European populations in the coming years [26]. The results of these efforts are eagerly awaited, however, encouraging results have already been reported by the Pharmacogenomic Resource for Enhanced Decisions in Care and Treatment (PREDICT) program at Vanderbuilt University, including significant improvements in safety using genotype-guided prescription for patients receiving statins [14, 25].

1.3 AROMATASE

1.3.1 Role of aromatase in estrogen biosynthesis

Aromatase is a highly conserved cytochrome P450 monoxygenase (CYP450) required for estrogen biosynthesis in chordate animals [39]. In humans, aromatase is expressed in numerous tissues, including adipose, brain, placenta, ovary, and testis and encoded by the structurally complex gene, *CYP19A1*, which comprises over 100 kb of the long arm of chromosome 15 [40-45]. The primary RNA sequence of aromatase transcripts varies in a tissue-specific manner due to the existence of ten distinct first exons, which are alternatively spliced to nine shared coding exons [46-52]. Nonetheless, the variable first exon occurs upstream of the translation start site leading to the production of an identical 503 amino acid protein in multiple tissues with subsequent glycosylation [52-55]. Like other human CYP450s, aromatase is a heme-containing

enzyme localized to the endoplasmic reticulum [54, 56, 57]. Although tethered to the outer leaflet of the endoplasmic reticulum by its hydrophobic N-terminus, the active site of the enzyme protrudes into the cytosol where it catalyzes the conversion of androgens to estrogens in a process known as aromatization [56-61].

Despite four decades of research, the three-step catalytic mechanism of aromatase in estrogen biosynthesis remains unclear [62]. It is generally agreed that the first two steps are sequential hydroxylations of the C19 position of an androgen, but the third monoxygenation reaction continues to be a subject of much debate [62-66]. The net result is the creation of an aromatic phenol from the A ring in the steroid backbone [63]. Aromatization of androstenedione yields estrone while testosterone is converted to estradiol (Figure 1-1) [67]. In addition to an androgen substrate, aromatization requires NADPH, molecular oxygen, and NADPH-cytochrome P450 oxidoreductase (CPR), which transfers electrons to the heme prosthetic group of aromatase [39].

Aromatase-mediated estrogen production is noteworthy considering the involvement of estrogens in diverse physiological processes in both men and women alike, such as maintenance of bone density, carbohydrate metabolism, and cognitive functioning [62]. In premenopausal women, serum levels of estradiol typically exceed 80 pg/ml but decline to 2-10 pg/ml in postmenopausal women due to the cessation of ovarian estrogen synthesis [68, 69]. Following menopause, estrogens are produced locally by aromatase in extragonadal tissues with negligible release into the systemic circulation [70]. Previous studies have shown that aromatase inhibition can be used medicinally to alleviate several conditions, including unexplained infertility, endometriosis, certain hormone-responsive cancers, and gynecomastia [71-74]. It is therefore unsurprising that several generations of aromatase inhibiting compounds (AIs) have been

developed to achieve marked decreases in estrogen production [75]. In particular, the third-generation aromatase inhibitors, EXE, anastrozole (ANA), and letrozole (LET) are widely prescribed to postmenopausal women with estrogen receptor-positive (ER+) breast cancer to slow disease progression [75].

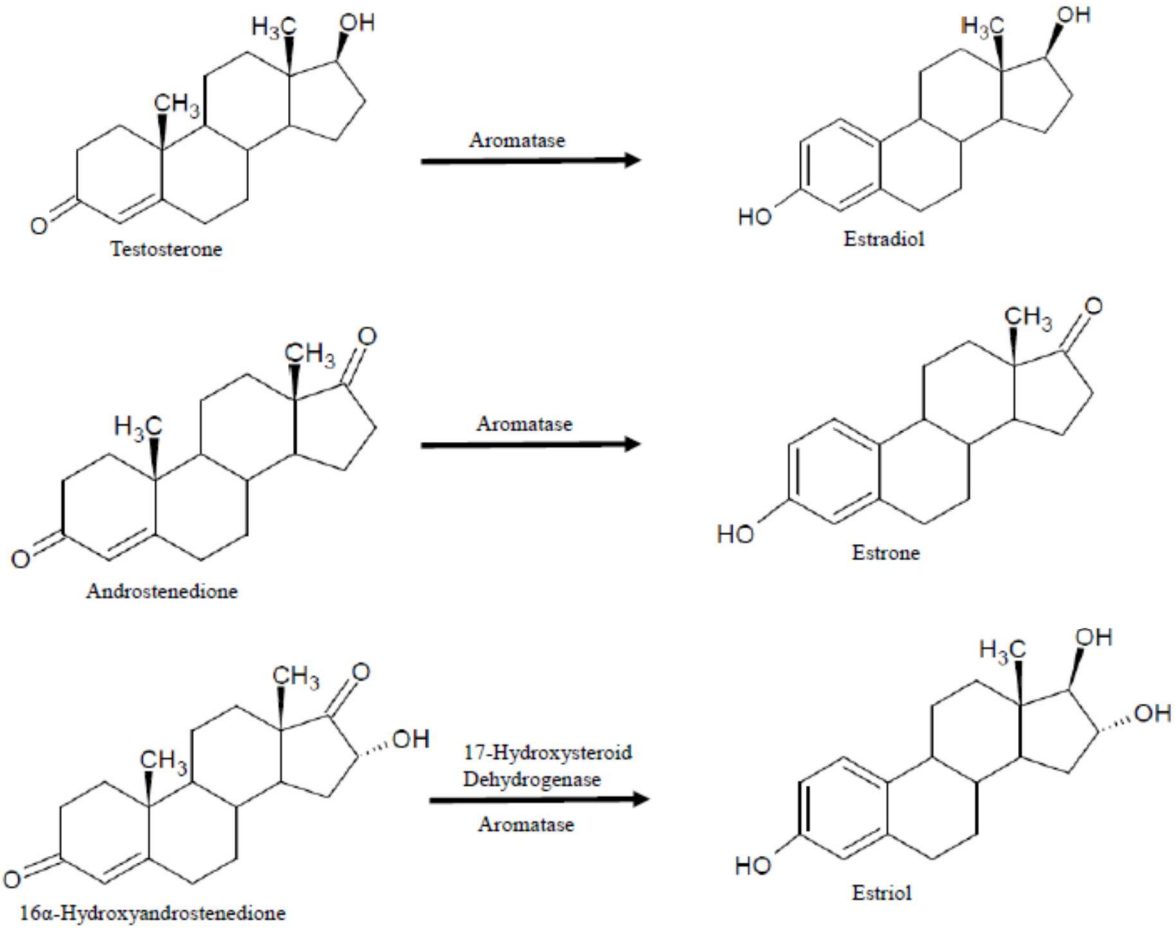

Figure 1-1: Aromatase-mediated estrogen biosynthesis [76].

1.3.2 Aromatase expression in healthy and cancerous breast tissue

Aromatase expression is regulated primarily at the transcriptional level via alternative

splicing [77-80]. Tissue-specific expression is driven by the synthesis of variable transcripts with one of ten distinct 5' untranslated regions (5' UTRs) joined to nine invariable coding exons at a shared junction [46-52]. Each promoter is responsive to a unique set of transcription factors, which facilitate tissue-specific expression in the presence of prostaglandin E2, tumor necrosis factor alpha (TNFα), glucocorticoids, and various pro-inflammatory cytokines [79]. To a lesser extent, aromatase levels are also determined by small non-coding RNAs and post-translational modifications [81, 82]. For instance, miR-378 regulates ovarian aromatase expression by seemingly altering transcript stability or the rate of protein synthesis [81]. Recent data indicates that post-translational phosphorylation decreases aromatase catalytic activity, as well as protein stability leading to increased degradation [82, 83]. Glycosylation, on the other hand, increases aromatase activity 35-40% [55]. Interestingly, studies using recombinant crystallized protein and fluorescence resonance energy transfer suggest that aromatase activity may be further modulated by the formation of homodimers or oligomers, which could increase efficiency by impeding intermediate release during the catalytic cycle [84, 85].

Pathological aromatase overexpression is common in hormone-responsive breast tumors, in which the availability of locally produced excess estrogen promotes aberrant intracellular signaling and metastasis [86-89]. A previous study detected a nearly 4-fold increase in aromatase transcripts in cancerous breast tissue with the greatest expression reported in the tumor-bearing quadrant [87]. Mean intratumoral estradiol levels have been studied extensively in postmenopausal breast cancer (46-480 pg/g) and greatly exceed plasma estrogen values previously reported in healthy postmenopausal subjects (2-10 pg/ml), further highlighting the clinical relevance of estrogen excess [69, 90].

Several mechanisms instigate deviant aromatase expression in breast cancer, including promoter switching [79, 91, 92]. In healthy breast tissue, basal aromatase activity is relatively low due to transcription driven primarily by the weak promoter I.4 and to a lesser extent, promoters I.3 and II [86]. Aromatase transcription markedly increases in cancerous breast and tumor-adjacent tissue due to upregulation of promoters I.3, I.4, I.7, and II [86, 93-97]. Aromatase overexpression in breast cancer is also partially attributed to the desmoplastic reaction, a process in which malignant epithelial cells use paracrine signaling to cultivate a favorable microenvironment [92]. The desmoplastic reaction occurs when tumor cells induce a fibrotic stromal response by copiously secreting various cytokines into the extracellular matrix [92]. Inhibitory signaling by malignant cells effectively discourages breast preadipocytes from maturing into differentiated adipocytes [92]. Instead, a layer of adipose fibroblasts forms to encapsulate the cancerous cell [92]. Aromatase overexpression is then reinforced in both compartments by mutually stimulatory paracrine signaling between the stromal breast tissue and cancerous cells [92]. Unfortunately, the immune response exacerbates estrogen excess by providing an additional source of intratumoral aromatase. Macrophages are known to express aromatase and heavily infiltrate cancerous breast tissue, comprising upwards of 25% of the cells therein [98, 99]. Furthermore, macrophages secrete prostaglandin E2, a potent inducer of aromatase expression in breast adipose fibroblasts [100-102].

1.4 EXEMESTANE PHARMACOLOGY

1.4.1 Chemical structure of EXE and other adjuvant anti-estrogens

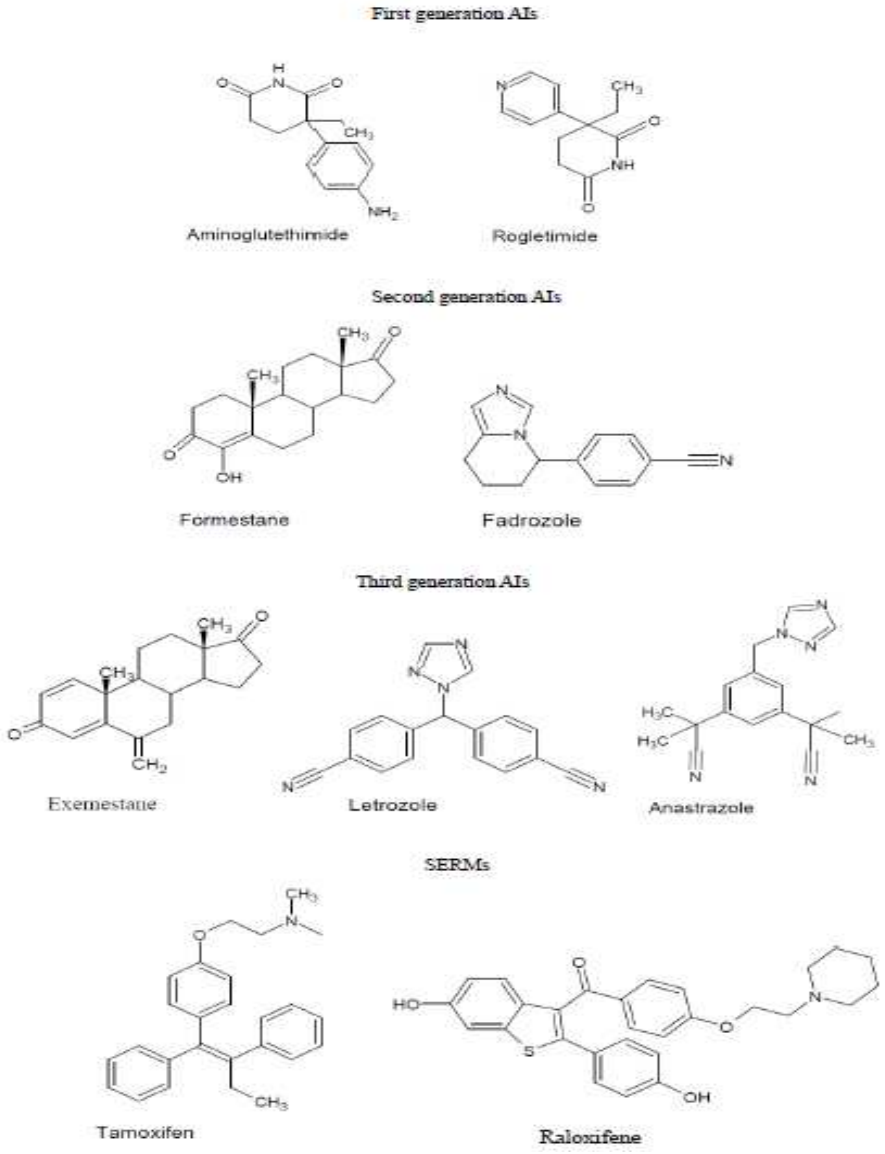

Figure 1-2: Chemical structures and classification of anti-estrogens used in breast cancer treatment [103].

Significant structural diversity exists among contemporary adjuvant anti-estrogens (Figure 1-2). Unlike the triazole derivatives LET and ANA, EXE features the planar, fused ring backbone characteristic of a steroid [104, 105]. Due to the high substrate specificity of aromatase, triazole derivatives are unable to access its androgen cleft and instead, cause reversible inhibition by interacting with other regions of the enzyme [104, 106, 107]. However,

the substantial molecular resemblance of EXE to androstenedione facilitates the entry of the AI into the androgen-binding pocket of aromatase resulting in irreversible inhibition [108, 109]. In contrast to the third-generation AIs, the widely used selective estrogen receptor modulators TAM and RAL are classified as triphenylethylene and benzotiophene derivatives, respectively [110].

1.4.2 Exemestane clinical pharmacology and pharmacokinetics

When administered to postmenopausal women, the pharmacological and pharmacokinetic parameters of EXE and TAM differ significantly. EXE has a half-life of approximately 24 hours in plasma (Table 1-1) [108]. Estrogen synthesis is maximally suppressed after 2-3 days with 25 mg/day EXE administered orally [108]. In postmenopausal subjects prescribed EXE, steady state kinetics are reached after 7 days [108]. In the plasma of healthy postmenopausal women, the mean AUC for EXE is 41.4 ng•h/ml with the maximum concentration of the drug detected about 2.9 h after its ingestion [108]. However, in the plasma of postmenopausal breast cancer patients, the mean AUC for EXE is increased to 75.4 ng•h/ml with its concentration peaking only 1.2 h after administration [108]. EXE is excreted equally in urine and feces [108]. TAM, however, is excreted primarily in feces (65%) and has a plasma half-life of 5-7 days [111]. TAM also takes considerably longer than EXE to reach peak plasma concentrations and steady state kinetics [111]. After administering a one-time 20 mg oral dose of TAM to postmenopausal women, maximum concentrations of the SERM occurred after about 5 hours [111]. Furthermore, four weeks of daily TAM (20 mg) is required to reach steady state kinetics, although its primary active metabolite N-desmethyl TAM may take up to 8 weeks to reach steady state in human subjects [111].

Table 1-1. Summary of EXE clinical pharmacology and pharmacokinetics.

Parameter	Reference
K_i = 4.3 nM	*Di Salle et al.* [112]
1.05 nM	*Ma et al.* [113]
26 nM	*Evans et al.* [114]
IC_{50} = 1.4 ± 0.42 μM for HEK293-expressed aromatase	*Sun et al.* [115]
IC_{50} = 30 nM for human placental microsomes	*Di Salle et al.* [112]
IC_{50} = 0.9 μM for androgen receptor binding	*Di Salle et al.* [112]
Plasma $t_{1/2}$ = 24 hours	*Pharmacia and Upjohn Co.* [108]
27 hours	*Spinelli et al.* [116]
Enzyme inactivation $t_{1/2}$ = 15.1 min	*Di Salle et al.* [114]
13.9 min	*Evans et al.* [114]
Mean C_{max} in plasma = 17 ng/ml	*Spinelli et al.* [116]
Mean plasma AUC in healthy postmenopausal women = 41.4 ng•h/ml	*Pharmacia and Upjohn Co.* [108]
Mean plasma AUC in postmenopausal breast cancer patients = 75.4 ng•h/ml	*Pharmacia and Upjohn Co.* [108]
Mean T_{max} in healthy postmenopausal women = 2.9 h	*Pharmacia and Upjohn Co.* [108]
Mean T_{max} in postmenopausal breast cancer patients = 1.2 h	*Pharmacia and Upjohn Co.* [108]
Time to maximum aromatase suppression = 2-3 days	*Pharmacia and Upjohn Co.* [108]
Time to steady-state = 7 days	*Zilembo et al.* [117]
Gastrointestinal absorption = 42%	*Pharmacia and Upjohn Co.* [108]
Plasma protein-bound EXE = 90%	*Pharmacia and Upjohn Co.* [108]
Fecal excretion in healthy postmenopausal women = 42%	*Pharmacia and Upjohn Co.* [108]
Urinary excretion in healthy postmenopausal women = 42%	*Pharmacia and Upjohn Co.* [108]

1.4.3 Mechanism of aromatase inhibition

Historically, the lack of an accurate three-dimensional conformation of aromatase has been a major hindrance in fully elucidating the mechanisms of aromatization and AI-mediated inhibition [118]. To address this significant gap in knowledge, several *in silico* homology studies were performed using CYP450s with known conformations as templates, including

soluble bacterial CYP450s, rabbit CYP2C5, and human CYP2C9 [119-121]. Although CYP450s share a characteristic tertiary fold, these models of aromatase were speculative and intrinsically limited by its low sequence homology (< 20%) with other CYP450s [118, 120]. Definitive structural analysis was delayed by technical challenges in crystallizing native aromatase, including overall hydrophobicity and a tendency to rapidly denature during extraction from the endoplasmic reticulum [118]. Owing to the persistence of researchers at the Hauptman-Woodward Medical Research Institute, conformational analysis of human placental aromatase was finally realized in 2009 [106, 122]. Like numerous other CYP450s, aromatase exhibits F-G loop flexibility, a property thought to regulate substrate occupancy of the active site by altering its accessibility [106, 118, 123, 124]. Nonetheless, aromatase structure and activity differ significantly from its most homologous relatives, CYP2D6 and CYP3A4, which accommodate numerous substrates via large, promiscuous active sites [106, 118, 125, 126].

The aromatase active site, in contrast, is small, rigid, and exhibits great specificity for androgen binding [106, 118, 122]. Structural analysis places the active site deep within the globular conformation of the enzyme, which has interesting repercussions for aromatase inhibitor design [118]. The embedment of aromatase into the outer endoplasmic reticulum orients the central active site in such a way that mechanism-based aromatase inhibitors must be sufficiently hydrophobic to traverse a phospholipid bilayer [106, 118]. As a steroid, EXE has strong hydrophobic character, which facilitates competition with androstenedione and other endogenous androgens for active-site binding [108]. Androstenedione and EXE share a steroid core structure comprised of four fused rings designated A, B, C, and D (Figure 1-3). However, EXE is distinguished by its C1-C2 double bond and exomethylene-substituted C6 [127]. Molecular modeling by *Ghosh et al.* strongly suggests that several hydrophobic residues (Thr310, Val370,

and Ser478) line the aromatase active site access channel forming a clamp around the C6 exomethylene [106]. During EXE docking, hydrogen bonds likely form between its C17 keto moiety and Arg115/Met374 [128]. An additional hydrogen bond is suspected between the C3 keto group and Asp309, which is protonated due to an unusually high pKa [128, 129].

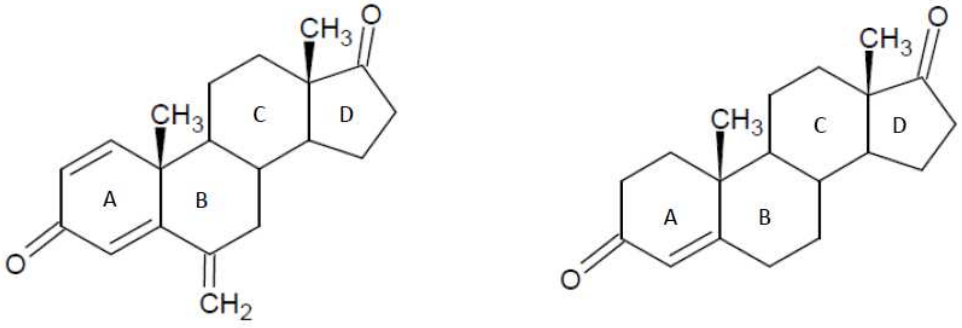

Exemestane Androstenedione

Figure 1-3: Chemical structures of EXE and androstenedione.

It is generally agreed that EXE is a pseudosubstrate capable of suicide inhibition [108, 109]. However, the exact mechanism by which EXE disrupts aromatase activity has been disputed in the literature. One early study suggested that the presence of a double bond between C1 and C2 allows A ring aromatization but prevents ejection from the catalytic site [130]. An alternative theory proposes that the movement or activity of Thr310, a residue located in the hydrophobic clamp, is limited by interaction with the C6 exomethylene of EXE [106]. According to prescriptive information disclosed by the drug's developer, EXE enters into the active site of aromatase where it is enzymatically converted to an undisclosed intermediate [108]. The reactive intermediate fails to release from the active site and instead remains tightly bound

to the enzyme [108]. In the absence of substrate release, aromatase-mediated estrogen synthesis comes to a standstill [108]. The data used to arrive at this conclusion has not been made publically available, prompting additional studies. A recent investigation by *Viciano et al.* was unable to pinpoint the exact mechanism of suicide inhibition but excluded EXE C19 hydroxylation as the immediate cause of irreversible binding to the active site [127]. Four aromatase residues (Trp224, Glu302, Asp309 and Ser478) are now believed to participate in EXE-mediated suicide inhibition, but precise mechanistic details are lacking at this time [131, 132].

1.4.4 Exemestane for breast cancer treatment and prevention

1.4.4.1 Chemoprevention

The National Cancer Institute of Canada Clinical Trials Group conducted an extensive investigation of the efficacy of EXE as a chemopreventative agent in the Mammary Prevention.3 clinical trial (MAP.3) [133]. The double-blind, placebo-controlled study enlisted a large cohort (n = 4,560) of healthy postmenopausal women with ≥ 1.66% chance of developing invasive breast cancer in the next 5 years according to the Gail risk criteria [133]. The participants were randomly assigned to ingest either 25 mg EXE/day or a placebo for up to 5 years [133]. After a median follow-up of 35 months, the risk of developing invasive breast cancer had decreased by 65% for EXE-treated women relative to the placebo group [133]. The literature shows that prophylactic tamoxifen (TAM), in contrast, reduces the incidence of breast cancer by only 50% in high-risk women [134, 135].

Due to its potentially serious side effects, uptake of TAM as a chemopreventative is poor with only 0.08% of American women between the ages of 40-79 utilizing it for this purpose

[135]. Clinical safety data from MAP.3 suggests that EXE is a less perilous alternative to TAM in the prevention setting [133]. MAP.3 participants taking EXE were more likely to experience side effects compared to the group receiving placebo (88% vs 85%), in particular hot flashes and arthritis [133]. However, no significant intergroup differences were observed for fracture risk, osteoporosis or cardiovascular adverse events, suggesting that EXE can be safely utilized for chemoprevention in postmenopausal women with an elevated risk of developing invasive breast cancer [133].

1.4.4.2 Neoadjuvant hormonal therapy

Neoadjuvant therapy has emerged as a highly effective tool in the treatment of early breast cancer. Administered prior to the primary medical intervention, neoadjuvant therapy attempts to reduce tumor burden in order to increase the efficacy of future pharmaceutical or surgical interventions [136]. For many patients with localized breast cancer, successful tumor down-staging can expand viable treatment options to include lumpectomy rather than complete mastectomy [136]. In addition to facilitating breast conservation, neoadjuvant therapies may render inoperable tumors amenable to surgical resection [137]. They are further prescribed in the palliative setting to women with locally advanced breast cancer and poor overall health, a population in which surgery is often unadvisable [138].

Neoadjuvant hormonal therapy (NHT), in particular, is an important element of early breast cancer treatment regimens [139]. Although neoadjuvant chemotherapy has long been a mainstay of breast cancer treatment, it is contraindicated in many patients on account of the high incidence of adverse events resulting from its considerable systemic toxicity [140]. Endocrine agents, in contrast, are generally better tolerated with clinical evidence demonstrating non-

inferior efficacy relative to neoadjuvant chemotherapy [136, 140]. TAM, a selective estrogen receptor modulator, is frequently employed as NHT, because it is highly effective in treating early breast cancer with clinical response rates of 33-67% [136]. Nonetheless, TAM use is associated with increased risk for potentially fatal adverse events, including ovarian cancer and thromboembolism [141, 142].

One method of circumventing the inherent toxicity of TAM in NHT is to expand the use of the third generation aromatase inhibitors, ANA, LET, and EXE. The side effects of aromatase inhibitors are generally mild and can often be managed with appropriate medical surveillance [143]. In addition to favorable safety profiles, several studies have deemed AIs superior to TAM in the preoperative treatment of ER+ breast cancer in postmenopausal women [140, 144-146]. A large meta-analysis bolstered these observations by examining the clinical outcomes of 1,160 postmenopausal women with ER+ breast cancer [140]. *Seo et al.* found that neoadjuvant treatment with an AI allowed for breast conservation surgery more frequently than preoperative TAM [140]. More recent results from the TEAM-IIA clinical trial reflect the potential utility of neoadjuvant EXE in treating postmenopausal women with ER+ breast cancer [138]. 64.5% of TEAM-IIA participants exhibited a partial or complete response following six months of neoadjuvant EXE while a similar study, PTEX46, reported a slightly lower response rate of 48% [138, 147]. Few serious side effects occurred in the TEAM-IIA cohort with 95.9% of adverse events classified as grade 1 or 2 [138]. Furthermore, many patients achieved significant decreases in tumor size (mean decrease = 47%), which likely contributed to the nearly 10% increase in the number of patients that could opt for breast conservation surgery rather than mastectomy [138]. These results suggest that EXE is a safe, efficacious alternative to TAM for the neoadjuvant treatment of ER+ breast cancer in postmenopausal patients.

1.4.4.3 Use in premenopausal women with ovarian function suppression

Reducing circulating estrogens via endocrine therapy is the standard endocrine treatment for hormone-responsive premenopausal breast cancer [148]. The efficacy of endocrine therapy can often be enhanced by the addition of ovarian function suppression (OFS) by gonadotropin-releasing hormone analogues (GnRHa), such as triptorelin [148]. At present, TAM is the most commonly used hormonal agent for estrogen suppression in premenopausal patients [148].

However, several studies indicate that concomitant use of EXE and OFS produces a more potent anti-estrogenic effect than TAM with OFS [148, 149]. A recent meta-analysis of the SOFT (Suppression of Ovarian Function Trial) and TEXT (Tamoxifen and Exemestane Trial) clinical trials, concluded that patients prescribed EXE + OFS had a significantly higher incidence of 5-year disease free survival than patients receiving TAM + OFS (91.1% versus 87.3%) [150]. After 5 years of treatment, 92.8% of patients given EXE + OFS were in remission while only 88.8% of patients taking TAM + OFS remained free of breast cancer [150]. The incidence of severe adverse events (grades 3 or 4), as well as attrition rates and patient-reported quality of life were similar between the two groups [150, 151]. Nonetheless, several significant differences in drug-induced side effects were noted. Patients receiving EXE + OFS were more likely to report joint pain or impaired sexual functioning than patients administered TAM + OFS, which was associated with increased severity of hot flushes and excessive sweating [151].

In 2015, the St Gallup expert panel issued new recommendations for the clinical use of combination therapy with EXE + OFS in accordance with the results of SOFT and TEXT clinical trials [152]. EXE with OFS was strongly recommended for women under the age of 35, as well as premenopausal women with 4 or more affected lymph nodes [152]. It should be noted that the

efficacy of EXE + OFS was not superior to that of TAM + OFS in individuals with HER2-positive tumors [150]. Moreover, a SOFT sub-study revealed a correlation between high body mass index and suboptimal estrogen suppression, which was detected in 17% of patients receiving EXE + OFS [153]. Further investigations are needed to fully understand what impact, if any, adiposity has on EXE efficacy in premenopausal women with breast cancer.

1.4.4.4 First-line endocrine therapy

Phase III clinical trials indicate that the third-generation AIs are more efficacious than TAM as first-line hormonal treatments for postmenopausal ER+ breast cancer [154-157]. One meta-analysis comparing TAM to third-generation AIs found that AI monotherapy reduced mortality by 11% relative to TAM in the first-line setting [158]. The EORTC-BCBG trial, in contrast, did not report significant differences in 1-year overall survival between women with hormone-receptor-positive metastatic breast cancer given EXE (82%) or TAM monotherapy (86%) [157]. In the same study, patients taking EXE were significantly more likely to respond to endocrine therapy than their TAM-treated peers with objective response rates of 46% and 31%, respectively [157].

Several large clinical trials have evaluated the so-called “switching strategy”. The TEAM study examined the relative efficacy of 5 years of upfront EXE monotherapy versus a switching strategy for treating postmenopausal women with hormone-responsive breast cancer [159]. Neither disease-free nor overall survival appreciably differed between the group receiving EXE and the group given sequential dosing with 2-3 years of TAM followed by 2-3 years of EXE for a total of 5 years of treatment [159]. Women following the sequential dosing regimen were twice as likely to report gynecological symptoms while patients that didn’t switch

medications had significantly more musculoskeletal adverse events [159]. The Intergroup Exemestane Study (IES) was similarly designed to include a TAM-to-EXE switching arm [73]. However, the IES compared the sequential treatment strategy with 5 years of first-line TAM in postmenopausal women with early breast cancer [73]. In this setting, women prescribed TAM monotherapy were 2-fold more likely to develop contralateral breast cancer during follow-up than women that had been switched to EXE after 2-3 years of TAM [160].

Compared to the nonsteroidal aromatase inhibitors, ANA and LET, EXE is prescribed as a first-line therapy less frequently [161]. This discrepancy has been attributed to a greater familiarity with the nonsteroidal AIs due to the delay between the marketing of ANA and LET and the subsequent release of EXE [161]. Results from MA.27 show that EXE and ANA exhibit similar efficacy and safety as upfront hormonal therapy [162]. A largescale phase III clinical trial directly comparing EXE and LET efficacy has yet to be undertaken. Nonetheless, indirect comparisons across published clinical trials suggest that the three third-generation AIs are superior in efficacy to TAM and roughly equipotent as first-line endocrine therapy for postmenopausal breast cancer [160, 163-166].

1.4.4.5 Second-line endocrine therapy

EXE is often used as a second-line treatment for postmenopausal women with metastatic hormone-responsive breast cancer that has progressed despite treatment with TAM, ANA or LET [167]. Relative to megestrol acetate as a second-line endocrine therapy, a phase III clinical trial concluded that EXE is more efficacious in prolonging both survival and time-to-progression in postmenopausal patients with advanced TAM-refractory breast tumors [168]. Several trials have shown that EXE can also be used to slow tumor progression through sequential use with a

non-steroidal AI [169-171]. The literature suggests that 24.3-46% of postmenopausal ER+ breast cancer patients may significantly benefit from therapy with EXE after failure of a non-steroidal AI [169-171]. In this setting, median time-to-progression after beginning treatment with EXE has been reported as 3-5 months [169-171]. Results from the BOLERO-2 study of advanced metastatic breast cancer further suggest that the progression-free survival of patients with ER+/HER- tumors may be significantly extended by concomitant use of EXE and an mTOR inhibitor, everolimus [172].

1.4.5 EXE-associated toxicity

1.4.5.1 Bone mineral density

As a result of drug-induced decreases in bone mineral density, postmenopausal women given EXE are 2.5-fold more likely to develop osteoporosis-related fractures than postmenopausal women not taking an AI [173-176]. One common side effect of EXE-induced estrogen suppression is increased bone turnover, which appears to compromise overall bone strength by altering its microarchitecture [164, 165, 173, 177-179]. Estrogen withdrawal leads to greater bone fragility and decreased mineral density by increasing osteoclast-mediated resorption [164, 165, 173, 177, 178]. Interestingly, EXE use is also associated with increases in biomarkers indicative of bone formation, such as alkaline phosphatase [180]. In light of the anabolic effect of androgens on bone formation, 17β-DHE, a phase I metabolite of EXE, may account for this observation [181]. In addition to decreased mineral density, excessive turnover causes deleterious changes in bone texture and morphology [174, 179]. Trabecularization is a common side effect of EXE in which strong cortical bone is remodeled to resemble weaker, porous trabecular bone [174, 179]. In a German sub-study of the TEAM clinical trial, clinically

significant trabecularization was evident in 39% of postmenopausal women with ER+ breast cancer after 2 years of adjuvant EXE [179].

Unlike EXE, TAM has a modest anabolic effect on bone mineral density (BMD) [182, 183]. As a partial estrogen agonist, it decreases the risk of osteoporosis-related bone fractures by impairing the resorptive activity of osteoclasts [76, 183, 184]. In a German TEAM sub-study of bone health, 2 years of adjuvant TAM decreased amino terminal propeptide of type I collagen (PINP), a well-established biomarker of turnover [185]. Structural alterations in bone texture were also observed in TAM-treated women and were thought to enhance fracture-resistance [179].

Clinical measurements collected during adjuvant endocrine therapy clinical trials are representative of the opposing effects of EXE and TAM on bone metabolism. In the Intergroup Exemestane Study (IES) of postmenopausal early breast cancer, participants were randomized to receive 5 years of hormonal therapy consisting of either EXE monotherapy or 2-3 years of TAM followed by a switch to 2-3 years of EXE [160]. After 58 months, 7% of the EXE monotherapy group had suffered a fracture compared to only 5% of the switch cohort [160]. The literature consistently shows that BMD, an important determinant of fracture risk in postmenopausal women, is compromised by AI use [186]. For instance, the TEAM clinical trial found that EXE decreased the BMD of lumbar spine 5.3% after 2 years while TAM increased it 1.9% [179]. A sub-study of the MAP.3 clinical trial reported widespread bone loss following 24 months of EXE use in healthy postmenopausal women at elevated risk for breast cancer [174]. Relative to women given placebo, the group receiving EXE experienced significant decreases in BMD in the distal radius (6.1%), distal tibia (5.0%), lumbar spine (2.4%), hip (1.8%), and femoral neck (2.4%) [174].

The risk of developing EXE-related bone loss varies between patients and necessitates the need for continued medical oversight throughout treatment [176]. To decrease the incidence of osteoporosis in postmenopausal women taking EXE, BMD should be reassessed every 6 months for patients that presented with low BMD (osteopenia) prior to initiating treatment [176]. Data from the IES and TEAM trials suggest that BMD loss plateaus in postmenopausal women within 2 years of beginning EXE [173, 185]. The IES trial further suggests that EXE-related decreases in BMD are partially reversible after treatment cessation [187, 188]. Nonetheless, it is preferable to preemptively reduce fracture risk during AI treatment by maintaining BMD through concomitant supplementation with vitamin D and calcium, as well as antiresorptive agents, such as zoledronic acid [176, 186]. Clinical guidelines state that osteoporotic patients should receive antiresorptive medications throughout the duration of EXE treatment [176]. However, most non-osteoporotic patients could also benefit from prophylactic BMD maintenance [176]. AI-associated bone loss can often be mitigated with appropriate medical supervision [176]. Nonetheless, baseline skeletal health and other patient-specific risk factors should be considered prior to initiating EXE use [176].

1.4.5.2 Lipid metabolism

Contemporary antiestrogens differ substantially with respect to their effects on lipid metabolism. In healthy postmenopausal women, as well as those diagnosed with early breast cancer, overall lipid metabolism is largely unchanged by endocrine therapy with daily EXE [161, 180, 189]. For instance, low-density lipoprotein cholesterol (LDL), lipoprotein, and serum triglyceride levels aren't significantly influenced by EXE use in postmenopausal women [180, 189-191]. A recent phase II clinical trial examined EXE as a chemopreventative agent for

healthy postmenopausal women at high-risk of developing breast cancer [190]. Although the mean total cholesterol of the subjects transiently increased, a return to near-baseline values occurred within 12 months of treatment [190]. As a first line treatment, 48 weeks of EXE use resulted in stable total cholesterol and high-density lipoprotein cholesterol (HDL) levels in postmenopausal patients with advanced breast cancer [191]. In several other studies, however, decreases of 6%-15% were reported in the mean serum HDL levels of postmenopausal women given EXE for 2 years [180, 190, 192]. Fortunately, data from the MAP.2 chemopreventative trial suggests that EXE-induced changes in HDL are reversible upon treatment cessation [189].

Unlike EXE, which has a minor impact on lipid metabolism, TAM induces favorable changes in lipid biomarkers. Numerous studies have reported significant decreases in levels of atherogenic LDL and total serum cholesterol in TAM-treated postmenopausal breast cancer patients [193-196]. This effect is attributed to inhibition of SD8I and ACAT, key enzymes in cholesterol biosynthesis and esterification, respectively [197-199]. As a result of this inhibition, absolute HDL formation can potentially decrease as well [200]. However, apolipoprotein upregulation resulting from the estrogen agonist activity of TAM may increase the ratio of HDL to LDL, a cardioprotective effect exhibited by statins [200-202]. Serum triglyceride levels, on the other hand, are not significantly impacted by six months of TAM treatment in postmenopausal women with advanced breast cancer [193]. The differential effects of TAM and EXE on lipid metabolism are well-established and could potentially inform the choice of endocrine therapy.

1.4.5.3 Cardio-cerebro-vascular health

AIs and TAM are divergent in their effect on cardiovascular health [161]. A recent meta-analysis of 19 randomized controlled clinical trials found that postmenopausal breast cancer patients (n = 62,345) treated with AIs were 19% more likely to experience cardiovascular adverse events compared to TAM-treated peers [203]. The same meta-analysis reported a 33% decrease in cardiovascular risk for patients prescribed TAM relative to those that received placebo [203]. Treatment with third generation AIs, however, was associated with a similar incidence of cardiovascular adverse events to that observed in the group taking placebo [203]. Results from the Intergroup Exemestane Study and MAP.3 chemopreventative trial indicate that exemestane use, in particular, is not associated with increased cardiovascular risk [133, 204]. Thus, the discrepancy between AIs and TAM in relative cardiovascular risk is attributed to the prophylactic properties of TAM rather than a cardiotoxic effect of AIs [161, 203-206]. TAM-mediated cardioprotection arises from several mechanisms. In addition to altering serum lipid levels through inhibition of multiple enzymes involved in cholesterol synthesis, TAM acts as an antioxidant to reduce harmful LDL oxidation and systemic inflammation [197-199, 207-210].

However, EXE is the preferred adjuvant hormonal therapy for many ER+ breast cancer patients for which TAM is contraindicated, including those with an increased risk of thromboembolism [73, 134, 141, 155, 156, 160]. Venous thromboembolic events, such as deep vein thrombosis and pulmonary embolism, are potentially fatal occurrences associated with SERM use [211]. In the IBIS-I chemopreventative clinical trial, participants taking TAM were 2.5-fold more likely to experience a venous thromboembolic event than healthy women taking placebo [134, 212]. The NSABP P-1 trial revealed that tamoxifen users had 1.6-, 3.0-, and 1.4-fold increases compared to nonusers in the incidence of deep vein thrombosis, pulmonary

embolism, and stroke, respectively [111]. EXE, in contrast, is not associated with an elevated risk for thromboembolism [73, 160]. In light of the differing cardio-cerebro-vascular toxicities of AIs and SERMs, careful consideration is warranted in the selection of an appropriate adjuvant hormonal therapy for breast cancer patients.

1.4.5.4 Musculoskeletal pain

Exemestane use is associated with the development of AIMSS (aromatase inhibitor induced-musculoskeletal symptoms), a characteristic cluster of symptoms that often includes musculoskeletal stiffness and bilateral pain in the joints of the hands, wrists or feet [76, 133, 160, 213-221]. In clinical trials of postmenopausal breast cancer patients, the incidence of AIMMS has been reported as 5-35% [222]. However, reports from the outpatient setting indicate that a majority of AI users may be adversely affected [223-228]. Adjuvant TAM, in contrast, induced significantly fewer musculoskeletal adverse events than AIs in numerous clinical trials, including the Intergroup Exemestane Study (IES) [222, 229-231]. The IES found that 38.5% of postmenopausal ER+ early breast cancer patients given 5 years of TAM had at least one musculoskeletal adverse event compared to 46.7% of the participants who had been switched to EXE following 2-3 years of initial TAM [229]. During the 5 years of treatment, EXE-treated patients were also significantly more likely to experience arthralgia (11.8% versus 18.6%) with a 10-fold increase in the incidence of carpel tunnel syndrome relative to women assigned to TAM monotherapy [73, 229]. Fortunately, AI-induced pain can often be ameliorated by weight-bearing exercises, over-the-counter analgesics, switching to a more tolerable AI or through supplementation with calcium, vitamin D, and glucosamine [232-234].

Several environmental and genetic risk factors are associated with an increased risk for AIMSS in postmenopausal women, including prior treatment with taxanes, pre-existing musculoskeletal dysfunction, and carrying variant *TCL1A* alleles [229, 235, 236]. Nevertheless, a scientific consensus has yet to be reached regarding the exact mechanism underlying musculoskeletal dysfunction in AI users. One widely held theory suggests that AIMMS are simply common menopausal symptoms magnified by potent systemic estrogen deprivation [213, 237]. The role of estrogen suppression in AIMSS pathology is supported by the elevated risk of developing severe musculoskeletal symptoms for women with certain genotypes of an estrogen-responsive immunomodulatory gene, *TCL1A* [236]. As estrogen interacts with opioid pain fibers to attenuate painful stimuli, a large decrease in serum estrogen could also contribute to increased musculoskeletal pain [238]. Potent aromatase inhibition could further explain the increased incidence of carpal tunnel syndrome in EXE users since estrogen receptors are expressed by both chondrocytes and the carpal ligament [239-241]. However, fluid accumulation around the digital flexor tendons is evident in radiological images of the wrists of EXE-treated women with carpal tunnel syndrome [242]. Any resultant nerve compression could explain the increased symptoms of carpel tunnel syndrome and may or may not be related to diminished estrogen levels through an unknown mechanism [242].

Unlike rheumatoid and osteoarthritis, AI-induced arthralgia is not inflammatory and cannot be attributed to structural damage of the articular surface or other tissues of the affected joint [234, 237]. Fascinating studies by *De Logu et al*. recently determined that AIMSS-like symptoms can be induced in mice via TRPA1, a cation channel expressed in the dorsal root ganglia [243]. In their experiments, androstenedione, which is frequently elevated in AI users, activated nociceptors by triggering TRPA1 [243]. Third-generation AIs are also believed to

activate TRPA1 [243]. Interestingly, the authors of the study speculate that exposure to androstenedione and oxidative stress byproducts lower the overall dose of AIs required to trigger neurogenic AIMSS-like symptoms, which could partially explain the interindividual variability in musculoskeletal symptoms in EXE-treated patients [243].

1.4.5.5 Gynecological health

In breast cancer patients, bothersome menopausal symptoms are a common consequence of blocking the activity or synthesis of estrogen with hormonal endocrine therapy [244]. However, there are key differences in the gynecological toxicity of the third-generation aromatase inhibitor, EXE, and the selective estrogen receptor modulator, TAM. AIs can cause or exacerbate vulvovaginal dryness and atrophy on account of its intense suppression of circulating estrogens to nearly undetectable levels [244-247]. In a sub-study of the phase III TEAM clinical trial, postmenopausal breast cancer patients that were switched to EXE after 2-3 years of TAM reported significantly lower libido and increased vaginal dryness one year after changing medications compared to the women that continued taking TAM for 5 years [248]. In the same study, however, patients in the TAM monotherapy arm had significantly more vaginal discharge than those receiving TAM/EXE sequential treatment [248].

Unlike EXE, TAM behaves as an estrogen agonist in certain tissues, which can promote the development endometrial abnormalities [249-253]. TAM exerts a well-established time-dependent proliferative effect on the endometrial lining [249, 250]. Endometrial thickening is widely regarded as an indication of increased risk for several gynecological afflictions [254]. As a result of endometrial thickening (> 5 mm), TAM-treated women have an increased incidence of uterine polyps and are 2-3-fold more likely to be diagnosed with endometrial cancer than

healthy postmenopausal women [251-253]. In a TEAM sub-study examining gynecological health of 143 postmenopausal ER+ breast cancer patients, transvaginal ultrasound showed that no women had endometrial lining thickness > 10 mm one year after switching to EXE, whereas 11 patients in the group given only TAM suffered from abnormal endometrial proliferation [255]. Results from the Intergroup Exemestane Study further suggest that EXE use following 2-3 years of initial TAM can reverse abnormal endometrial thickening in postmenopausal breast cancer patients [256]. However, these results should be interpreted with caution as they may be an artifact of TAM washout rather than a genuine effect of EXE. Overall, EXE and TAM are both associated with noxious menopausal symptoms, but the latter poses a much higher risk of causing serious secondary conditions.

1.4.5.6 Impact on adherence to adjuvant endocrine therapy

Poor adherence and early discontinuation of adjuvant endocrine therapy are significant obstacles in the treatment of breast cancer. Poor adherence is associated with decreased survival in TAM and AI-treated patients alike [257, 258]. Nonetheless, 31-73% of patients outside of clinical trials prematurely discontinue treatment [259]. Compliance with a medication regimen is influenced by multiple factors, including comorbidities and drug-induced adverse events [260]. The use of osteoporosis and cholesterol-lowering medications, for instance, is associated with increased compliance with oral hormonal therapy in elderly women (mean age = 76.4 years old) with breast cancer [260]. The literature suggests that breast cancer patients displaying symptoms of poor sleep quality, fatigue or forgetfulness prior to beginning adjuvant AI therapy are more likely to discontinue therapy within 12 months of initiating treatment [228]. A study of AI use in a community-based setting further found that musculoskeletal pain contributes

significantly to noncompliance with upwards of 20% of all treatment discontinuations attributed to joint pain [261]. Results from the ELPh trial of adjuvant AIs suggest that age may also influence adherence rates [228]. Younger women were significantly more likely to discontinue EXE or LET treatment than older participants [228]. Moreover, older women comply well with AI treatment in outpatient settings outside of clinical trials [262].

TAM persistence is poor, especially in younger patients, the majority of whom do not complete 5 years of endocrine therapy [263]. Several other studies report overall early discontinuation rates of approximately 30% in TAM-treated breast cancer patients [262, 264]. Patients harboring negative beliefs about the risks and potential benefits of treatment are at an elevated risk for TAM noncompliance [264, 265]. Carriers of functional CYP2D6 alleles are also more likely to stop taking TAM due to their extensive metabolizer status, which is thought to increase the severity of hot flashes and other treatment-related side effects [263].

In a cohort study of over 13,000 breast cancer patients, 19% and 31% of patients treated with AIs or TAM, respectively, had discontinued adjuvant hormonal therapy before completing the recommended 5 years of treatment [262]. When drawing comparisons in compliance rates between medications, it is important to consider that estimates of adherence and persistence can vary significantly between studies as a result of methodological differences [266]. Thus, caution should be exercised in comparing the outcomes of clinical trial participants with significant demographic differences. Notwithstanding these limitations, several trials have reported both EXE and TAM compliance and consistently suggest that EXE is associated with superior adherence [266]. These results are particularly interesting considering that many physicians are more knowledgeable in managing the side effects of TAM relative to those of EXE [260].

1.5 EXEMESTANE METABOLISM

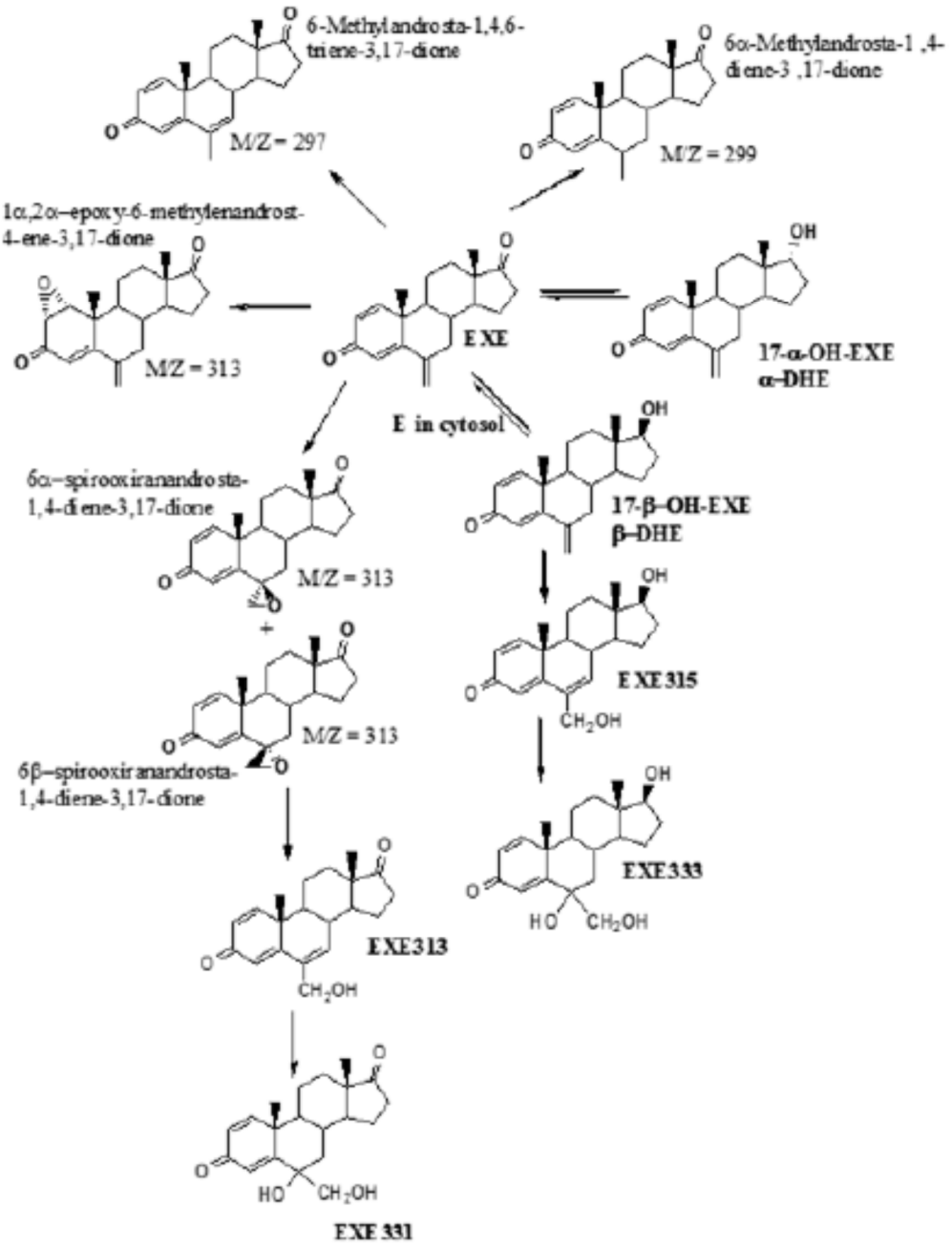

Figure 1-4: Proposed phase I metabolic pathways of EXE. Schematic courtesy of Dr. Zuping Xia.

Although EXE is highly effective *in vivo*, suppressing circulating estrogen levels in postmenopausal breast cancer patients by 98%, its complete metabolic pathway is as of yet uncharacterized nor is it known the extent to which genetic variation impacts phase I EXE metabolism [115, 267]. Prescriptive information states that EXE is extensively metabolized, but the chemical structures of its primary metabolites, as well as detailed information regarding their capacity to inhibit aromatase are omitted from the product leaflet dispensed with EXE tablets [108]. Based on the steroidal structure of EXE, two principal phase I metabolic pathways are predicted, each yielding several potential secondary metabolites (Figure 1-4) [268]. The first expected route of metabolic attack is oxidation of the C6 exomethylene, a moiety believed to be conducive to CYP450 activity [268]. The C17 keto group of EXE is also vulnerable to enzymatic reduction to form 17β-DHE [268].

The limited literature available describes 17β-dihydroexemestane (17β-DHE) as a prominent phase I EXE metabolite with both anti-aromatase and androgen agonistic activities *in vitro* [114, 115, 269-272]. One study concluded that 17β-DHE concentrations were ~35–40% those of the parent drug in the plasma of healthy individuals taking EXE, whereas another smaller study found that the amount of 17β-DHE relative to EXE in human plasma varied five-fold in a pool of only three participants [114, 273]. These observations support 17β-DHE as a major metabolite and highlight interindividual variations in EXE metabolism.

Although drug disposition is undoubtedly multifactorial, it has been estimated that 20–95% of variability in drug response is attributable to genetic factors [274]. A previous study by *Sun et al*. found that phase II EXE metabolism is profoundly affected by genetic variation in the drug-metabolizing enzyme, UGT2B17 [115]. In incubations with human liver microsomes, UGT2B17 genotype significantly correlated with levels of 17β-DHE conjugation with glucuronic

acid, which forms a water soluble glucuronide (glucuronidation) for urinary excretion [115]. Overall glucuronidation (V_{max}/K_M) of 17β-DHE in the HLM panel was 36-fold lower in UGT2B17-null homozygotes (*2/*2) compared to wildtype homozygotes (*1/*1) [115]. At present, it is unknown whether polymorphisms in phase I drug-metabolizing enzymes could likewise alter EXE clearance or the production of metabolites with anti-aromatase activity.

Discovering any genetic polymorphisms that contribute to inter-individual variation in phase I EXE metabolism is of great interest as they may be predictive of drug response in patients. However, finding useful biomarkers requires that enzymes participating in phase I EXE metabolism first be definitively identified. According to the original manufacturer, EXE (Aromasin®) is metabolized hepatically by CYP3A4 and aldo-keto reductases [108]. It is unclear whether the term aldo-keto reductases specifically refers to members of the aldo-keto reductase superfamily (AKRs), of which there are 15 human members with varying tissue expression patterns [108, 275, 276]. In this context, the term could also generically refer to enzymes from other families that can act as aldo-keto reductases, such as the short-chain dehydrogenase/reductases (SDRs). Furthermore, the results of an *in vitro* study using baculosome-expressed CYP450s suggest that CYP450s other than CYP3A4 may also metabolize EXE [277]. In light of this ambiguity, additional studies are needed to resolve the identity of phase I drug-metabolizing enzymes involved in EXE metabolism and to assess the effect of allelic variation on the catalytic activity of these enzymes.

1.6 HYPOTHESES AND OBJECTIVES

1.6.1 Hypotheses

1. It is hypothesized that hepatic xenobiotic-metabolizing enzymes from the aldo-keto reductase and cytochrome P450 superfamilies metabolize EXE to form multiple C6- and C17-modified phase I metabolites, and furthermore, naturally-occurring nonsynonymous variants in these enzymes may alter the production of metabolites that contribute to the drug's therapeutic effect of estrogen biosynthesis inhibition. If this is indeed the case, genetically-determined differential metabolite production may explain the substantial inter-individual variability seen in the clinical responses of women taking EXE for breast cancer treatment and prevention.

1.6.2 Objectives

1. To characterize the potency of wildtype aromatase inhibition by predicted and known phase I EXE metabolites *in vitro* utilizing an overexpressing HEK293 cell line (Chapter 2).

2. To assess if the potency of EXE-mediated inhibition of wildtype aromatase differs significantly from its potency in inhibiting common nonsynonymous aromatase variants (Chapter 2).

3. To definitively identify phase I EXE metabolites produced *in vitro* by hepatic ketosteroid reductases, xenobiotic-metabolizing cytochrome P450s, human liver cytosol, and human liver microsomes (Chapters 3 & 4).

4. To identify the hepatic ketosteroid reductases and cytochrome P450s most likely to be involved in *in vivo* EXE metabolism by calculating kinetic parameters for the formation of active metabolites by each enzyme (Chapters 3 & 4).

5. To identify functional polymorphisms prevalent at ≥ 1% in ketosteroid reductases and cytochrome P450s and to assess their impact on the catalytic activity against EXE substrate by calculating kinetic parameters for comparison to wildtype (Chapters 3 & 4).

CHAPTER TWO

Anti-aromatase activity of exemestane and its phase I metabolites

**A version of this chapter has been accepted for publication:
Peterson A, Xia Z, Chen G and Lazarus P. Exemestane Potency is unchanged by Common Nonsynonymous Polymorphisms in CYP19A1: Results of a Novel Anti-aromatase Activity Assay examining Exemestane and its Derivatives.

2.1 INTRODUCTION

This chapter describes the results of a rapid, novel UPLC tandem mass spectrometry assay that was developed to measure the ability of EXE and its putative phase I metabolites to inhibit estrogen synthesis by wildtype aromatase. The anti-aromatase activity of EXE against two common aromatase variants is also presented to evaluate what effect, if any, genetic variation has on EXE potency. The identity of several phase I EXE metabolites formed by human liver microsomes is also revealed.

2.2 BACKGROUND

Comprehensively identifying phase I EXE metabolites is of considerable interest, because EXE derivatives, such as 17β-DHE, may contribute to systemic estrogen blockade through aromatase inhibition. A previous pharmacokinetics study found that the maximum plasma concentration of EXE in postmenopausal women with a prior history of breast cancer ranged from 3.0-15.6 ng/ml following 2 weeks of oral dosing (25 mg/day) while the maximum amount of its 17β-DHE metabolite varied 7-fold with reported values of 0.22-1.58 ng/ml [76]. However, past attempts to identify less-studied metabolites have been speculative due to the lack of standard reference compounds. Using GC-MS, three peaks likely corresponding to C6-oxidized metabolites were detected in the urine of healthy male volunteers [278]. Another study found six metabolites, including 17β-DHE, in human urine following administration of radiolabeled EXE [279]. However, both studies of urinary EXE metabolites were hampered by a lack of comparison of physiochemical properties between the suspected metabolites and known standards. Six possible metabolite peaks were observed in human liver microsomes presented with EXE substrate [277]. One peak was confirmed to be 17β-DHE and another was tentatively

designated as 6-HME [277]. The identities of the remaining four peaks could not be established [277].

This study addresses methodological issues that have historically undermined phase I EXE metabolite identification. First, a reference library of C6 and C17-modified EXE analogs was synthesized to confirm the identity of suspected metabolites observed in incubations of EXE with human liver microsomes. Secondly, a newly-developed UPLC/MS/MS method eliminates the need for organic extraction to remove residual substrate prior to analysis unlike previous scintillation-based studies of AAA [280]. Instead, low levels of estrone formation are quantitated directly rather than extrapolated from tritiated water release during the aromatization of radiolabeled androstenedione. Interestingly, aromatase from human placental microsomes is used in traditional AAA screenings [280]. CYP1A1 is well-expressed in human placenta and extensively metabolized EXE in an *in vitro* assay using recombinant baculosome-expressed CYP450s [277, 281]. Background phase I metabolism in human placental microsomes may complicate the analysis of AAA assays. However, expression analysis has shown that HEK293 are CYP450 and UGT-null (data not shown). To circumvent potential confounding from endogenous enzymes in placental preparations, aromatase-overexpressing HEK293 were created in the present study to evaluate the potency of EXE analogs in impeding estrogen biosynthesis.

While it is well-accepted that genetic differences may influence an individual's drug disposition for many pharmaceuticals, the extent to which polymorphisms in aromatase explain inter-individual variation in EXE metabolism in unclear. Interestingly, aromatase has several common nonsynonymous variants, which might contribute to variability in drug disposition by altering EXE affinity or the velocity of its reduction to 17β-DHE [76]. It is possible that variant alleles causing differential metabolite production are predictive biomarkers for EXE efficacy or

toxicity risk. Consequently, we also compared the efficacy of EXE in inhibiting two allozymes, aromatase^{Thr201Met} and aromatase^{Arg264Cys} relative to the wildtype enzyme.

2.3 MATERIALS AND METHODS

2.3.1 Chemicals and materials

Hangzhou DayangChem Co. (Hanzhou City, China) supplied the androgens boldenone, testosterone, and 4-andostene-3,17-dione for the synthesis of EXE and its analogs. Tokyo Chemical Industry Co. (Tokyo, Japan), Thermo Fisher Scientific (Waltham, MA), and Sigma-Aldrich (St. Louis, MO) produced all other reagents (ACS grade or higher) needed for synthesis. Steroid purification required silica columns (Yamazen Corp., Osaka, Japan) and thin-layer chromatography plates (Bonna-Agela Technologies Inc., Wilmington, DE). LC/MS grade methanol, acetonitrile, and formic acid was purchased from Thermo Fisher Scientific. XenoTech (Lenexa, KS) supplied pooled mixed gender human liver microsomes (Cat no. H0610, n = 50). Corning (Corning, NY) and Integrated DNA Technologies (Coralville, IA) manufactured the NADPH regeneration system and oligonucleotide primers, respectively. A QuikChange II Site-Directed Mutagenesis Kit was purchased from Agilent (Santa Clara, CA) to produce aromatase variant overexpression vectors. The HEK293 cell line was procured from ATCC (Manassas, VA). G418, penicillin/streptomycin, fetal bovine serum, Opti-MEM, and DMEM supplemented with 4.5 g/L glucose, 110 mg/L sodium pyruvate, and L-glutamine was purchased from Invitrogen (Carlsbad, CA) along with an XCell electrophoresis system. Lipofectamine 2000, PVDF membranes, Pierce BCA protein assay kit, SuperSignal West Femto Maximum Sensitivity Substrate, sodium dodecyl sulfate (SDS), glycine, tris base, ammonium persulfate (APS), goat anti-rabbit HRP-conjugated antibody (cat. No. 31466), and tetramethylethylenediamine

(TEMED) were also purchased from Thermo Fisher Scientific. Nonfat dry milk was prepared by BioRad (Hercules, CA). Sigma-Aldrich (St. Louis, MO) supplied Ponceau staining solution, Tween 20, acrylamide/bis-acrylamide solution, 2-mercaptoethanol, estrone, androstenedione substrate, and estrone-2,3,4-^{13}C3. Rabbit monoclonal anti-aromatase antibody (cat. no. ab124776) was purchased from Abcam (Cambridge, MA).

2.3.2 Reference library synthesis

EXE and ten C6-oxidized or C17-reduced EXE analogs were resuspended in ethanol and stored at -80˚C following synthesis at Washington State University (Spokane, WA). For a thorough description of 17α-DHE synthesis, the reader is directed to recent work by *Platt et al* [282]. However, a brief summation of 17α-DHE synthesis is provided in Figure 2-1 [282]. Previous studies provide detailed descriptions of the synthesis, purification, and NMR-based identity verification of each remaining compound [268, 282-284].

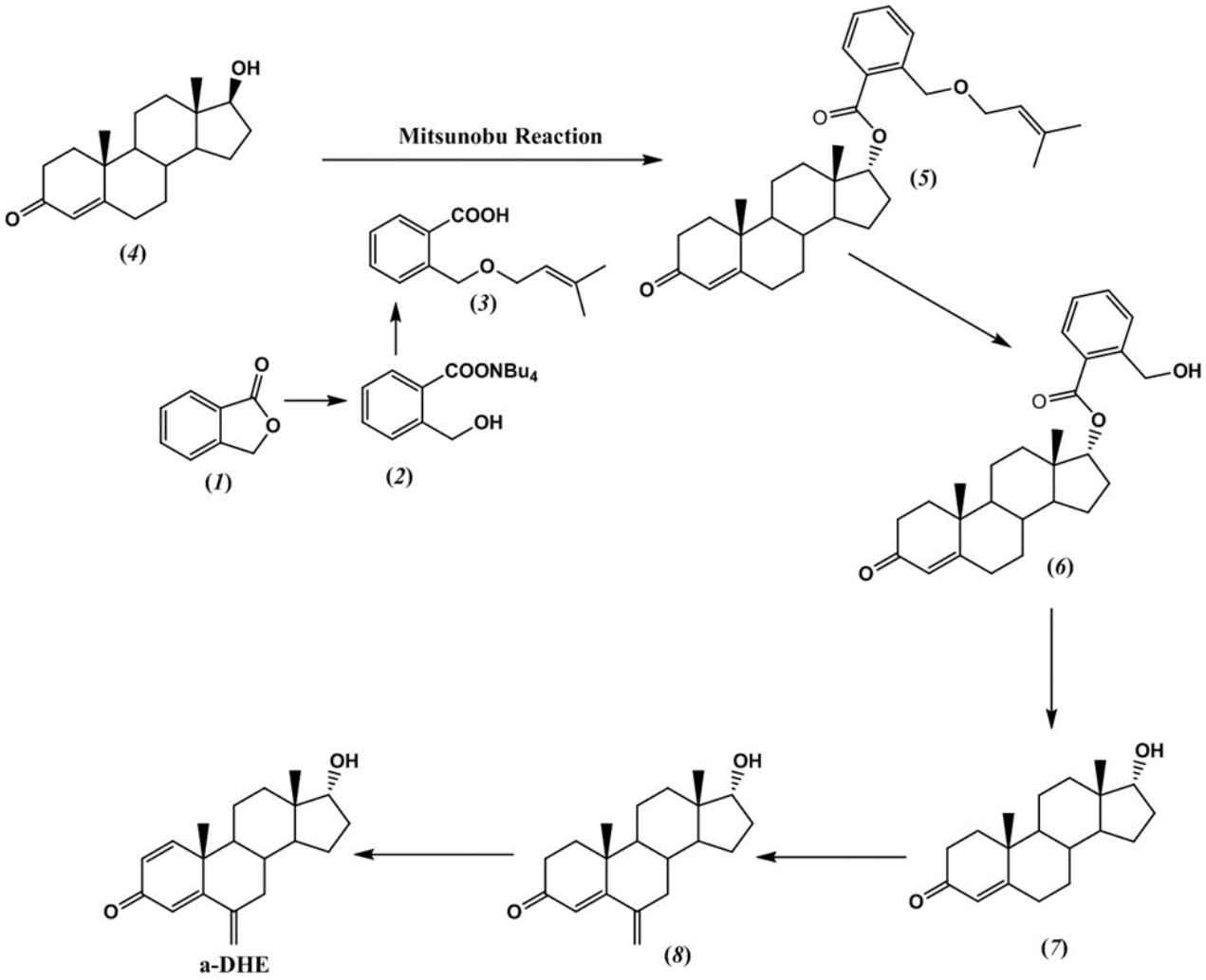

Figure 2-1: Synthesis of 17α-DHE from testosterone [282].

2.3.3 Creation of aromatase-overexpressing HEK293

Stable overexpression of wildtype aromatase in HEK293 was driven by a pcDNA3.1/V5-His-TOPO mammalian expression vector as previously described [115]. Constitutive overexpression vectors encoding common aromatase variants Thr201Met and Arg264Cys were produced via site-directed mutagenesis using the wildtype plasmid as template. Variant expression vectors were amplified in BL21 grown under ampicillin selection for 16 h at 37˚C. Sanger sequencing was used to confirm successful mutagenesis. Lipofectamine 2000 was used

to transfect HEK293 with variant overexpression plasmids. Transfected HEK293 were grown in high-glucose DMEM containing 700 μg/ml G418, 10% FBS, and penicillin/streptomycin for at least three weeks. The cells were then harvested by resuspension in PBS, lysed via 4 freeze-thaw cycles, and centrifuged for 15 min at 13,200g at 4˚C. Microsomes for each cell line were prepared from the supernatant through differential centrifugation (1 h, 34000 g) in a chilled Beckman L7-65 ultracentrifuge (Brea, CA), resuspended in PBS, and stored at -80˚C. To normalize the amount of aromatase included in AAA assays, its relative expression was quantitated in triplicate by subjecting 20 μg of protein from each overexpressing cell line to SDS-PAGE in a 10% tris-glycine polyacrylamide gel. Following transfer to PVDF for 90 min at 30 V, the membrane was blocked overnight at 4˚C in 5% nonfat dry milk, washed for 30 min in 0.1% Tween, and probed overnight with anti-aromatase primary antibody (1:2500). The next day, the membrane was again washed for 30 min, and probed with HRP-conjugated goat anti-rabbit antibody (1:7500) for 1 h at ambient temperature. Following another 30 min wash, the blot was incubated with SuperSignal West Femto Maximum Sensitivity Substrate per the manufacturer instructions and imaged on a ChemiDoc Imager (BioRad, Hercules, CA). Image J software (NIH, Bethesda, MD) was used to measure band density while Ponceau staining was used to validate even loading between lanes.

2.3.4 Anti-aromatase activity assays.

Per 50-μl reaction in PBS (pH 7.4), 5 μM androstenedione, a NADPH regeneration system (1.55 mM NADP+, 3.3 mM glucose-6-phosphate, 3.3 mM MgCl2, 0.5 μl of 40 U/ml glucose-6-phosphate dehydrogenase), and 15 μg of microsomes from HEK293 overexpressing wildtype or variant aromatase were individually incubated with varying concentrations of each

steroid. Organic solvent comprised < 1% of the total volume of each enzymatic incubation, which proceeded at 37˚C for 2 h. Reactions were terminated with 50 µl of ice cold acetonitrile and centrifuged at 4˚C for 15 min at 13,200 g. Supernatants were collected and spiked with 50 ng of estrone-2,3,4-^{13}C3 as an internal standard. An incubation with microsomes derived from non-transfected HEK293 was also performed to serve as a negative control. Aromatization catalyzed by wildtype or variant aromatase was likewise monitored in the presence of vehicle rather than EXE or compounds from the reference library to reflect maximal uninhibited estrone formation. Estrone was measured using a novel 6-minute direct detection UPLC/MS/MS method on the Waters Acquity platform using m/z transitions 271.17→133.09 as a marker for estrone and 274.15→162.00 for estrone-2,3,4-^{13}C3. Mobile phase (57% methanol in 0.1% formic acid) was infused isocratically from 0-4 min at a flow rate of 0.4 ml/min. The column was then washed with methanol for 1 min followed by 1 min of re-equilibration with mobile phase. Cone and collision voltages were set at 35 V and 20 V, respectively. Dwell time for both compounds was 0.1 s. IC50 values from incubations with wildtype aromatase were calculated for each compound in GraphPad Prism 6 (La Jolla, CA). One-way ANOVA was used to compare the IC50 value for EXE incubated with wildtype aromatase with IC50 values for EXE incubated with overexpressed aromatase allozymes.

2.3.5 Exemestane metabolite identification

A 50-µl incubation containing 50 µg of HLM in PBS (pH 7.4), 400 µM EXE, and an NADPH regeneration system was placed in a 37˚C water bath for 4 h before termination with 50 µl of cold acetonitrile. After a 15-min refrigerated centrifugation at 13,200 g, the supernatant was examined for phase I EXE metabolites. A 10-min UPLC method was used to separate and

detect EXE and the ten other reference compounds through multiple reaction monitoring with positive mode electrospray ionization on a Waters ACQUITY UPLC/MS/MS system (Milford, MA). The 1.7 μm ACQUITY UPLC BEH C18 column (2.1 mm x 50 mm, Ireland) used for these analyses was protected by a 0.2 μm in-line filter. The UPLC gradient conditions used (Table 2-1) have previously been described in the literature [282]. The fragmentation characteristics and retention time of suspected metabolite peaks were compared to compounds from the reference library.

Table 2-1. UPLC conditions for detection of phase I EXE metabolites [282].

Time (min)	% A[a]	% B	% C	Curve
initial	70	20	10	initial
0.5	70	20	10	11
9	30	60	10	6
9.5	0	90	10	6
10	70	20	10	6

[a] Mobile phase A, 0.1% formic acid; mobile phase B, 100% methanol; mobile phase C, 100% acetonitrile. Flow rate = 0.4 mL/min.

2.4 RESULTS AND DISCUSSION

2.4.1 Wildtype aromatase inhibition by EXE and its metabolites

A reference library of purified androgens was assayed for *in vitro* inhibition of wildtype aromatase by monitoring estrone formation (Figure 2-2). In the present study, EXE (IC_{50} = 0.92 ± 0.17 μM) and its major metabolite 17β-DHE (IC_{50} = 4.3 ± 0.56 μM) were potent and moderate inhibitors of aromatase, respectively. These results agree with an earlier study which found that 17β-DHE was approximately 2.6-fold less potent than EXE [268]. Manufacturer data also references the diminished potency of C6-oxidized or C17-reduced EXE derivatives [108]. Interestingly, the epoxide 6α-spirooxiranandrosta-1,4-diene-3,17-dione was the most potent EXE analog assayed (IC_{50} = 1.2 ± 0.19 μM), exhibiting nearly 5-fold greater potency than its 6β stereoisomer (IC_{50} = 5.7 ± 1.6 μM). 17α-DHE and three additional compounds exhibited negligible aromatase inhibition with IC_{50} values exceeding 100 μM (Figure 2-3). According to *Buzzetti et al.* (1993), 6-HME was 21-fold less potent than EXE [268]. However, we measured 6-HME as 67-fold less potent (IC_{50} = 61 ± 20 μM) perhaps due to methodological differences. The remaining androgens assayed were 4 to 8-fold less potent than EXE (IC_{50} = 3.3-7.1 μM). In keeping with the observations of *Buzzetti et al*., non-epoxide C6-oxidized metabolites exhibited minimal AAA [268].

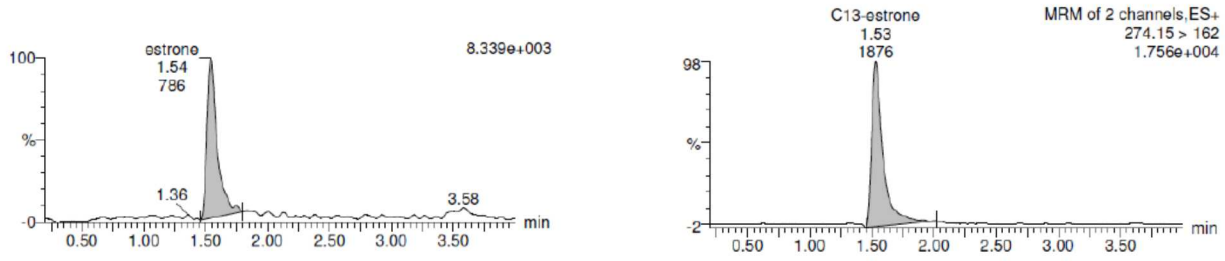

Figure 2-2: Chromatograms showing estrogen detection. Left, estrone; right, estrone-2,3,4-$^{13}C3$ internal standard.

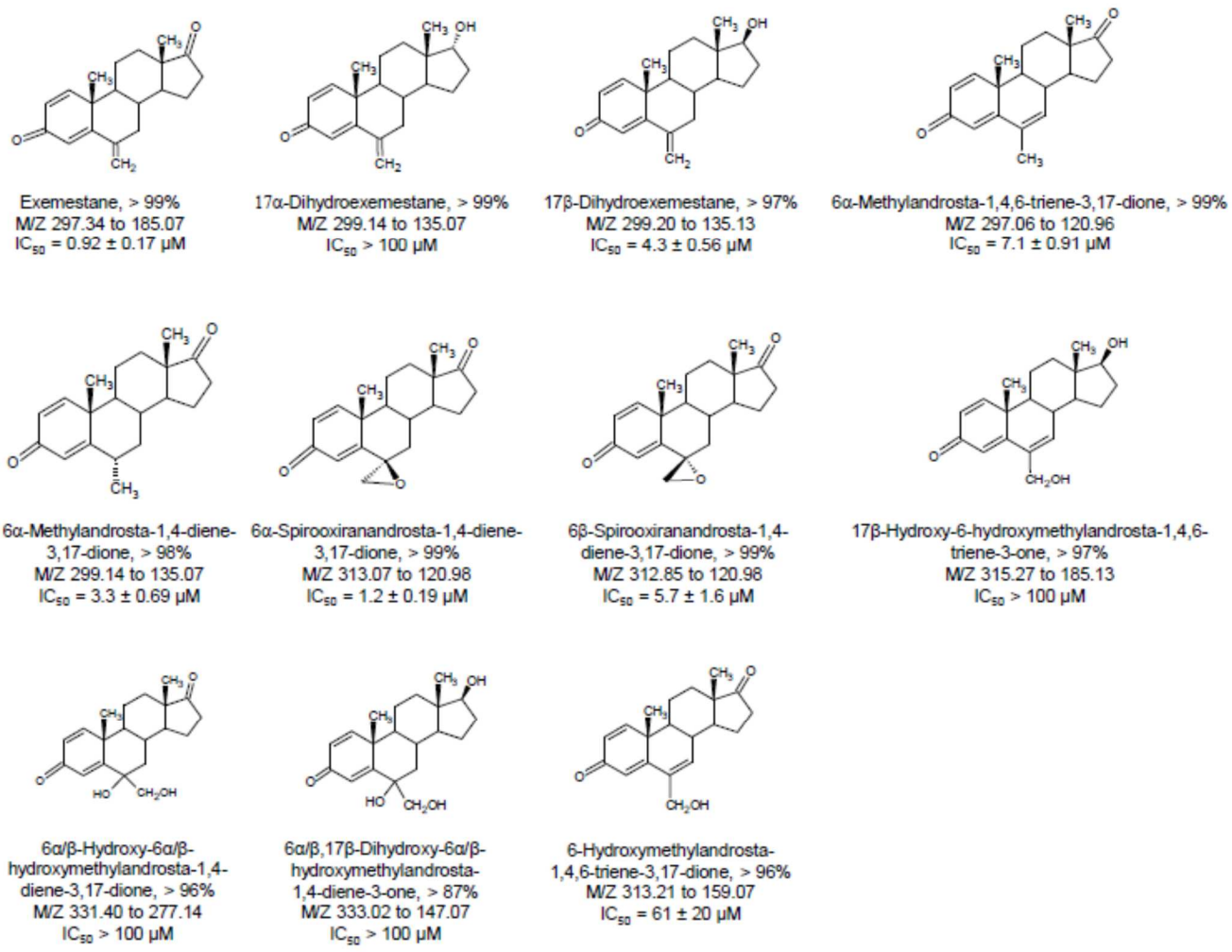

Figure 2-3: Chemical structures of species included in the synthesized reference library of EXE analogs. % purity is provided for each compound. Mass transitions used for UPLC/MS/MS-based detection are listed, as well as IC_{50} values for wildtype aromatase as determined by anti-aromatase activity assay.

2.4.2 Impact of nonsynonymous polymorphisms on EXE potency

IC_{50} values describing EXE-mediated aromatase inhibition did not significantly differ ($p = 0.71$) between wildtype enzyme (0.92 ± 0.17 µM), aromatase^{Thr201Met} (0.86 ± 0.12 µM), and aromatase^{Arg264Cys} (0.97 ± 0.09 µM) in AAA assays normalized for relative aromatase expression

(Figure 2-4). Many aromatase polymorphisms exist, but data regarding the functional significance of variant alleles on human health is inconsistent [76, 113, 285]. The prevalence of the Thr201Met allele is estimated as 5% in Caucasians and African Americans while the frequency of the Arg264Cys allele is 2.5% and 22.5% in Caucasian and African Americans, respectively [113]. One study of variant aromatase found that enzyme activity strongly correlated with expression levels in transiently transfected COS-1 and further concluded that any differences from wildtype in the overall activity of the Thr201Met and Arg264Cys allozymes are likely mediated by differential expression [113].

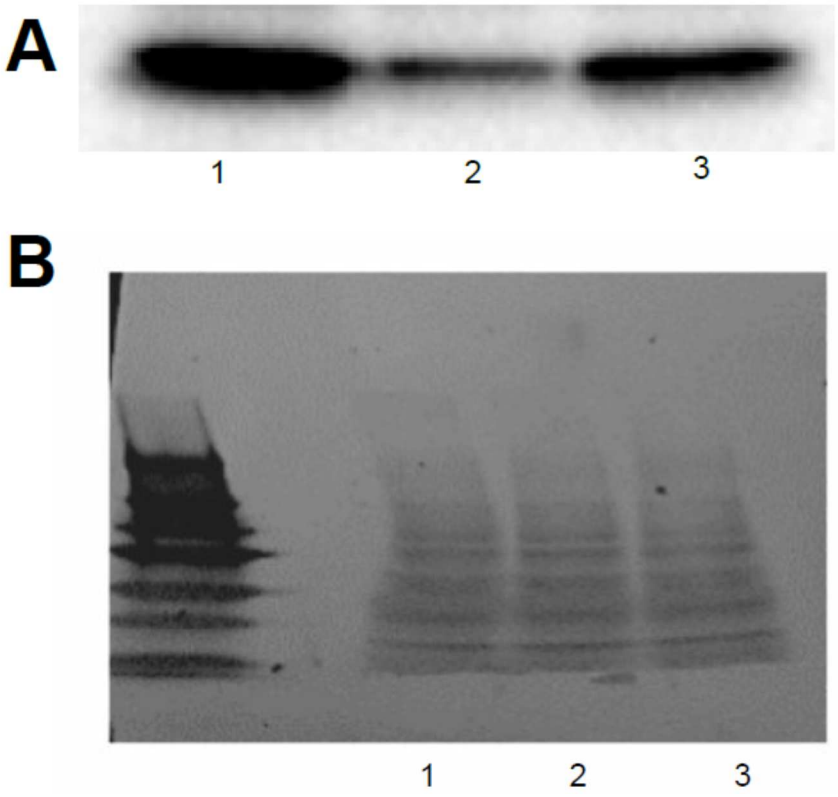

Figure 2-4: Relative quantification of overexpressed wildtype and variant aromatase in HEK293 microsomes by Western blotting. (A) Lane 1, wildtype aromatase; lane 2, aromatase^{Thr201Met}; lane 3, aromatase^{Arg264Cys}. (B) Ponceau total protein staining for aromatase normalization.

2.4.3 EXE metabolite identification

17β-DHE, 6-HME, 6α/β-hydroxy-6α/β-hydroxy-methylandrosta-1,4-diene-3,17-dione, and 6α/β,17β-dihydroxy-6α/β-hydroxymethyl-androsta-1,4-diene-3-one were identified in incubations of EXE with pooled human liver microsomes through comparison to reference compounds (Figure 2-5). Although we found four EXE metabolites, an *in vitro* study of EXE metabolism by *Kamdem et al.* detected six peaks corresponding to putative metabolites [277]. Our assay was not designed to identify phase II metabolites suggesting that the two additional peaks observed in the previous study may correspond to conjugated metabolites, such as the 17β-DHE-glucuronide produced by UGT2B17 [115]. Considering their low abundance and limited capacity to inhibit aromatase, the three C6-oxidized metabolites detected are unlikely to contribute to the overall pharmacology of EXE *in vivo*. However, these results show that 17β-DHE is not only the predominant EXE metabolite formed in human liver microsomes, but also capable of inhibiting aromatase with moderate potency suggesting that it may make clinically relevant contributions to the overall response to EXE in women with ER+ breast cancer [282]. However, additional studies are needed to discern the relevance of these findings to the clinical outcomes of EXE-treated postmenopausal women.

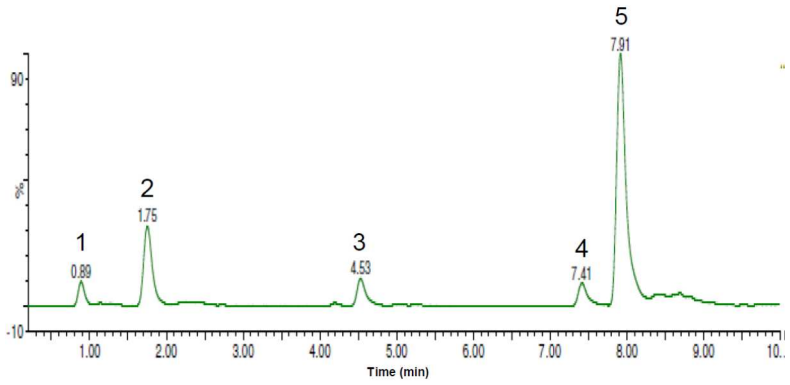

Figure 2-5: Identification of EXE metabolites in human liver microsomes. EXE metabolite profile was examined after a 4 h incubation of pooled mixed gender human liver microsomes with EXE (n = 50). Peak 1, 6α/β,17β-dihydroxy-6α/β-hydroxymethylandrosta-1,4-diene-3-one; peak 2, 6α/β-hydroxy-6α/β-hydroxymethylandrosta-1,4-diene-3,17-dione; peak 3, 6-HME; peak 4, EXE; peak 5, 17β-DHE.

CHAPTER THREE

Impact of nonsynonymous single nucleotide polymorphisms on in vitro metabolism of exemestane by hepatic cytosolic reductases

**A version of this chapter has previously been published:
Platt A, Xia Z, Liu Y, Chen G and Lazarus P. Impact of nonsynonymous single nucleotide polymorphisms on in-vitro metabolism of exemestane by hepatic cytosolic reductases. Pharmacogenet Genomics. 2016 Aug;26(8):370-80.

3.1 INTRODUCTION

This chapter describes EXE metabolite production by human liver cytosol, as well as five purified hepatic ketosteroid reductases. Wildtype enzyme kinetics data is presented to gauge the potential contribution of each enzyme to the drug's overall metabolism via production of its major metabolite, 17β-DHE. Common enzyme variants were also assayed to assess the impact of nonsynonymous polymorphisms on affinity for EXE substrate and metabolite production.

3.2 BACKGROUND

Modification of the steroid scaffold at C17 is a well-documented phenomenon central to the regulation of human steroid hormone potency [286]. One early study predicted that EXE, like many steroids, is vulnerable to phase I metabolism at the carbonyl group occupying this position [268]. Carbonyl-reducing enzymes catalyze similar reactions despite contributions from two distinct protein phylogenies: the AKR and short-chain dehydrogenase/reductase (SDR) superfamilies [287]. These enzymes play a prominent role in endogenous steroid metabolism by transforming ketosteroids into hydroxysteroid alcohols, altering their ligand affinities and rendering them available for conjugative reactions with phase II enzymes, such as the uridine diphosphoglucuronosyl transferases [288]. Reduction of EXE at C17 to form a reactive beta hydroxyl has been confirmed and is known to facilitate additional metabolism by UGT2B17 and ultimately, excretion [115].

In total, 12 NADP(H)-dependent enzymes from the AKR and SDR superfamilies are believed to participate in carbonyl-containing xenobiotic reduction [287]. Of these enzymes, AKR1C1, 1C2, 1C3, and 1C4 (termed AKR1C1–4) as well as CBR1 are soluble, hepatically expressed and active against ketosteroids. Thus, it stands to reason that these reductases may be

responsible for functionalizing the C17 carbonyl group of EXE to produce the 17β-DHE metabolite in human liver cytosol [287]. Numerous nonsynonymous polymorphisms have been described in hepatic xenobiotic-metabolizing enzymes, including the AKRs [289]. Naturally occurring variations in enzymes active in EXE metabolism could lead to differential metabolite production between individuals, potentially altering the overall duration of exposure to antiestrogen therapy in vivo and thus, clinical outcomes. The present study aims to clarify the metabolic pathway of EXE by identifying cytosolic hepatic reductases active in its biotransformation as well as any phase I metabolites produced. For the first time, the functional consequences of common polymorphisms on reductase-mediated production of the active metabolite, 17β-DHE, are also explored.

3.3 MATERIALS AND METHODS

3.3.1 Chemicals and materials

The 4-androstene-3,17-dione, boldenone, and testosterone used in EXE and 17-DHE synthesis were purchased from Hangzhou DayangChem Co. (Hangzhou, Zhejiang, China). All other reagents used in steroid synthesis were ACS grade or higher and purchased from Sigma-Aldrich (St Louis, Missouri, USA), Tokyo Chemical Industry Co. (Tokyo, Japan), or Thermo Fisher Scientific (Waltham, Massachusetts, USA). Thin-layer chromatography plates from Bonna-Agela Technologies Inc. (Wilmington, Delaware, USA) and silica columns from Yamazen Corp. (Osaka, Japan) were used for purification following synthesis. Codon-optimized pQE-T7 overexpression plasmids for wildtype AKR1C1–4 as well as CBR1 were purchased from Qiagen (Germantown, Maryland, USA). The QuikChange II Site-Directed Mutagenesis Kit that was used to make variant reductase expression vectors was acquired from Agilent (Santa

Clara, California, USA). Oligonucleotides to prime site-directed mutagenesis were manufactured by Integrated DNA Technologies (Coralville, Iowa, USA). Kanamycin, chlorophenicol, isopropyl β-D-1-thiogalactopyranoside, and imidazole were obtained from Sigma-Aldrich. Pooled human liver cytosol collected from 50 individuals was procured from XenoTech (Lenexa, Kansas, USA). 86% of the human liver cytosol donors were Caucasian, whereas 4 and 10% were African American or Hispanic, respectively. The NADPH regeneration system used for activity assays was purchased from Corning (Corning, New York, USA). B-PER complete protein extraction reagent, Halt EDTA-free protease inhibitor cocktail, Ni-NTA affinity purification columns, and Slide-a-Lyzer G2 dialysis cassettes (10 kDa MWCO) were purchased from Thermo Fisher Scientific. All solvents used for mass spectrometry were LC/MS grade and also obtained from Thermo Fisher Scientific. Luria broth base and 4–20% tris-glycine gels for SDS-PAGE were acquired from Invitrogen (Carlsbad, California, USA). The BCA protein assay and silver staining kits used in protein purity assessment were purchased from Pierce (Rockford, Illinois, USA).

3.3.2 Synthesis of exemestane and 17-dihydroexemestane

EXE, 17α-DHE, and 17β-DHE were synthesized on site at Washington State University to a purity of greater than 99%. EXE and 17-DHE were prepared and authenticated in accordance with published methods [76, 268, 283]. A Yamazen AI-580s flash chromatography system was used to purify each compound following synthesis. Purity was determined by PDA spectrum (210–400 nm) on an Acquity I Class UPLC platform from Waters (Milford, Massachusetts, USA). Before resuspension in ethanol and storage at −80°C, the structure of each steroid was verified by reviewing nuclear magnetic resonance spectra recorded on a Bruker

AV300 instrument (Billerica, Massachusetts, USA) with the kind permission of the Department of Chemistry at Gonzaga University (Spokane, Washington, USA).

3.3.3 Identification of nonsynonymous polymorphisms

Functional polymorphisms for the AKR1C subfamily and CBR1 were derived from the National Center for Biotechnology Information (NCBI) Variation Viewer using filters to search dbSNP and dbVar for any missense or nonsense gene variants arising from single nucleotide variations, insertions, deletions, or frameshifts [290]. For the purpose of this study, common functional polymorphisms were those detected at a minor allele frequency (MAF) of greater than 1% in the human population according to the 1000 Genomes Project or GO-ESP datasets. Data on interethnic differences in MAF for common ketosteroid reductase variants identified were extracted from NCBI's 1000 Genomes Browser and organized into Table 3-1.

Table 3-1: Interethnic differences in the incidence of common AKR1C variants [282].

Variant Enzyme	NCBI dbSNP Identifier	South Asian MAF	European MAF	African MAF	Hispanic MAF	East Asian MAF
AKR1C2 Phe46Tyr	rs2854482	0.0235	0.0368	0.1831	0.0231	0.0069
AKR1C3 His5Gln	rs12529	0.3395	0.5954	0.5431	0.4553	0.1389
AKR1C3 Glu77Gly	rs11551177	0.0174	0.0825	0.028	0.0663	0.001
AKR1C3 Lys104Asn	rs12387	0.1759	0.1481	0.1263	0.1916	0.1379
AKR1C3 Pro180Ser	rs34186955	0.0082	0.0308	0	0.0058	0
AKR1C3 Arg258Cys	rs62621365	0.002	0.003	0	0.1225	0.0724
AKR1C4 Gly135Glu	rs11253043	0	0	0.0953	0.013	0
AKR1C4 Ser145Cys	rs3829125	0.1115	0.1203	0.025	0.2017	0.1111
AKR1C4 Leu311Val	rs17134592	0.1094	0.1203	0.025	0.2017	0.1111

3.3.4 Recombinant protein production

Overexpression vectors encoding common variant ketosteroid reductases (MAF > 0.01) were created from wildtype AKR1C and CBR1 plasmids by site-directed mutagenesis. Oligonucleotide sequences used to prime mutagenesis are provided in the Table 3-2. Each expression vector was transformed into chemically competent BL21. Transformants were grown on kanamycin selection plates and confirmed by Sanger sequencing. Isolated bacterial colonies were scraped into 150 ml Luria broth supplemented with 7.5 mg kanamycin and 3.75 mg

chlorophenicol and grown at 37°C for 16 h in a table-top shaker with gentle aeration (200 rpm). A total of 750 ml fresh Luria broth containing 37.5 mg kanamycin and 18.75 mg chlorophenicol was inoculated with 120 ml of the overnight culture and grown for an additional 1.75 h to reach log-phase growth. Protein expression was induced by the addition of 0.5 mmol/l isopropyl β-D-1-thiogalactopyranoside, followed by 3 h of growth at 37°C. BL21 were pelleted by centrifugation and lysed with 25 ml B-PER complete with an EDTA-free protease inhibitor cocktail.

Table 3-2: Oligonucleotides used in the creation of variant ketosteroid reductase overexpression vectors by site-directed mutagenesis [282]. Top, sense oligonucleotide sequence; bottom, antisense oligonucleotide sequence.

AKR1C Polymorphism	5' → 3' Oligonucleotide Sequence
AKR1C2 Phe46Tyr	actggcaattgaagcaggctatcatc cgctatcaatatgatgatagcctgct
AKR1C3 His5Gln	cattcagtttcacgcactgttgtttgctatcctgtttca tgaaacaggatagcaaacaacagtgcgtgaaactgaatg
AKR1C3 Glu77Glu	tgctggtataaaaaatatctccgcgtttcacgctaccatc gatggtagcgtgaaacgcggagatatttttataccagca
AKR1C3 Pro180Ser	cggtttatatttcagaccacttttattcagaatcatttccagctgacgacgat atcgtcgtcagctggaaatgattctgaataaaagtggtctgaaatataaaccg
AKR1C3 Arg258Cys	cgttgcagctgataacacagtgcaatcagtgcc ggcactgattgcactgtgttatcagctgcaacg
AKR1C4 Gly135Glu	atcaacggtatcaaaaataacttttttcattttcatctttcggcagcggtg caccgctgccgaaagatgaaaatgaaaaagttatttttgataccgttgat
AKR1C4 Ser145Cys	cactggcaaaaaaacataaacggaca tcagtgccggtgtccgtttatgtttt
AKR1C4 Leu311Val	aattatcgttatgtggtgatggatttt cggatgatccatcacaaaatccatca

Polyhistidine-tagged recombinant protein was bound to Ni-NTA resin and then affinity purified through the sequential addition of increasing concentrations of imidazole suspended in PBS, pH 7.4. Purification columns were initially equilibrated with wash buffer containing 50 mmol/l NaH_2P0_4, 300 mmol/l NaCl, and 10 mmol/l imidazole, pH 8.0. Each bacterial lysate was mixed with equilibration buffer 1:1, loaded onto a dedicated column, and allowed to drain by gravity. Columns were incubated at room temperature for 30 min to promote maximum protein binding. Columns were then successively washed with 20, 60, 100, and 250 mmol/l imidazole. Each imidazole wash was allowed to drain from the resin bed completely by gravity. Flow-through was discarded. Recombinant enzyme was eluted using 500 mmol/l imidazole wash buffer. Dialysis was performed against PBS for 12 h at 4°C. PBS was changed 90 min after

initiating dialysis and then again after 3 h to ensure complete removal of imidazole before use in kinetic assays. A total of 750 ng of each enzyme was subjected to SDS-PAGE on 4–20% tris-glycine polyacrylamide gel and found to be greater than 80% pure by silver staining (Figure 3-2).

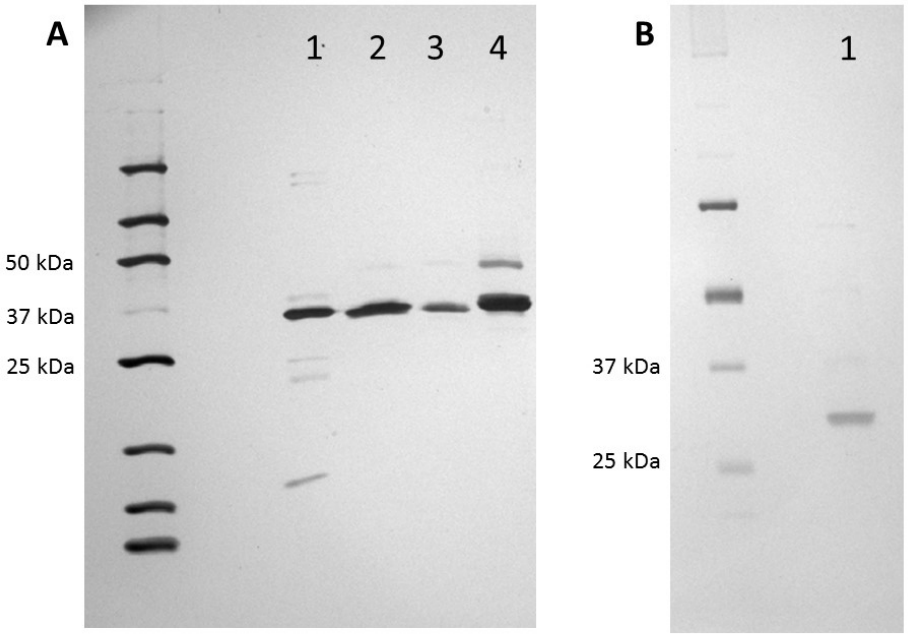

Figure 3-1: Silver staining of purified recombinant reductases. Panel (A), AKR1C1; lane 1, AKR1C2; lane 2, AKR1C3; lane 3, AKR1C4; lane 4. Panel (B), CBR1; lane 1 [282].

3.3.5 Metabolite identification

EXE-derived metabolites were identified in 18 h enzymatic incubations with 200 µmol/l EXE in PBS, pH 7.4, at 37°C. Each 50 µl incubation was supplemented with the NADPH regeneration system (1.55 mmol/l NADP+, 3.3 mmol/l glucose-6-phosphate, 3.3 mmol/l $MgCl_2$, 0.5 µl of 40 U/ml glucose-6-phosphate dehydrogenase) and included 7.5 µg pooled human liver cytosol or 1.5 µg of recombinant wildtype reductase. Overnight incubations with 200 µmol/l 17β-DHE and 17α-DHE were also performed under the same conditions to assess the

reversibility of EXE reduction. Following termination with ice-cold acetonitrile, each incubation was centrifuged at 4°C for 15 min at 13,200 g. Supernatant was collected and analyzed by ultra-pressure liquid chromatography coupled with tandem mass spectrometry using an ACQUITY UPLC/MS/MS system (Waters; Milford, Massachusetts) equipped with a protective 0.2 μm in-line filter in series with a 1.7 μm ACQUITY UPLC BEH C18 column (2.1 × 50 mm; Waters). The UPLC conditions used in these analyses are detailed in Table 2-1. Each supernatant was initially screened for the presence of EXE metabolites using UPLC/MS and electrospray ionization to detect positively charged molecular ions with m/z ranging from 100 to 450. To confirm the identity of peaks observed in the comprehensive scan, a second targeted UPLC/MS/MS scan was performed using mass transitions m/z 297.34→185.07, 299.14→135.07, and 299.20→135.13 to monitor EXE, 17α-DHE, and 17β-DHE, respectively. Desolvation temperature was 500°C with 800 l/h nitrogen gas used for drying. Collision energy was optimized at 25 V for EXE and 20 V for 17-DHE. A cone voltage of 25 V and 0.01 s dwell time resulted in high-sensitivity detection of all three compounds. Retention times of metabolites observed in the enzymatic incubations were compared with EXE metabolite standards.

3.3.6 Enzyme kinetic assays

Varying concentrations of EXE (0.5–400 μmol/l) were included as substrate for reductase-mediated DHE production in 2-h incubations. Each reaction was performed in PBS, pH 7.4, at 37°C in the presence of an NADPH regeneration system. Recombinant AKR1C protein of 1000 ng was used per reaction, whereas 250 ng recombinant CBR1 was used to avoid substrate depletion, which would have precluded Michaelis–Menten modeling. Similar

incubations were performed using 5 μg pooled human liver cytosol (HLC) in 90 min incubations. Protein concentration and incubation length fell within the linear range of reaction velocity curves for EXE reduction (data not shown). All reactions were terminated with cold acetonitrile, centrifuged at 4°C for 15 min at 13,200 g, and then dried for 2 h at ambient temperature. 20 μl of water/acetonitrile (1:1) was used to ensure complete resuspension before analysis. The formation of 17β-DHE was monitored using the UPLC/MS/MS method described above and quantified against a reference curve of known concentrations.

3.3.7 Statistical analysis

Kinetic parameters were determined according to the Michaelis–Menten equation using GraphPad Prism 6 software (GraphPad Software Inc., San Diego, California, USA). V_{max} values derived from kinetic assays were normalized to account for recombinant protein purity and expressed as picomoles/min/mg. All reported values represent the results of independent assays run in triplicate. The activity of each variant enzyme was compared with its respective wildtype using Student's t-test or one-way analysis of variance supplemented with Sidak's test for multiple comparisons, as appropriate. A two-tailed *p* value of less than 0.05 was considered the threshold for statistical significance.

3.4 RESULTS AND DISCUSSION

3.4.1 Identification of cytosolic exemestane metabolites

The predominant metabolite formed in overnight incubations of EXE with pooled human liver cytosol was 17β-DHE, although a lesser amount of 17α-DHE was also detected (Fig. 3-3). When presented with 17α-DHE or 17β-DHE as a substrate, neither exemestane nor secondary

metabolite formation was observed in HLC incubations (data not shown). Recombinant AKR1C4 and CBR1 catalyzed the reduction of EXE to both stereoisomers of DHE, whereas only 17β-DHE formation was mediated by AKR1C1–3.

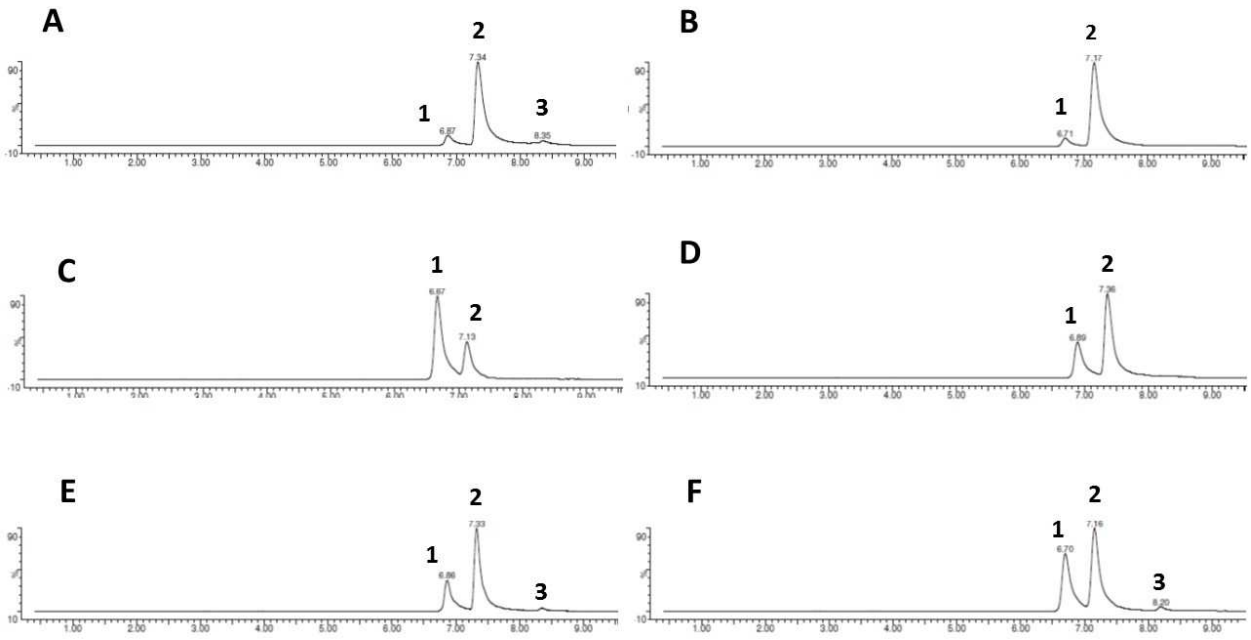

Figure 3-2: Identification of EXE metabolites in overnight incubations. Panel (A), Mixed gender liver cytosol pooled from 50 human donors; panel (B), AKR1C1; panel (C), AKR1C2; panel (D), AKR1C3; panel (E), AKR1C4; and panel (F), CBR1. Peak 1, Exemestane; peak 2, 17β-dihydroexemestane; peak 3, 17α-dihydroexemestane [282].

3.4.2 Kinetic analysis of 17β-dihydroexemestane formation

Assays monitoring the reduction of EXE to 17β-DHE by purified wildtype protein suggest that AKR1C4 has the highest affinity for EXE (K_M= 9.7 ± 1.9 μmol/l) followed by AKR1C3, AKR1C2, AKR1C1, and CBR1 with K_M values of 12.3 ± 1.1, 16.4 ± 0.6, 35.3 ± 3.8, and 265 ± 21 μmol/l, respectively. The apparent K_M for HLC was established to be 55.7 ± 1.9 μmol/l (results not shown). Representative plots of 17β-DHE formation versus EXE substrate

concentration are shown in Figure 3-4. The formation of 17β-DHE catalyzed by pooled HLC proceeded at a maximum rate of 21 ± 4.8 pmol/min/mg. The observed V_{max} was similar for AKRs 1C1, 1C2, and 1C3 (71.1 ± 1.5, 84.2 ± 15.6, and 83.3 ± 15.4 pmol/min^{-1}/mg^{-1}, respectively). CBR1 reduced EXE about 11- to 13-fold faster than AKRs 1C1, 1C2 or 1C3 with an observed V_{max} of 928 ± 244 pmol/min^{-1}/mg^{-1}. The V_{max} for AKRs 1C1, 1C2, and 1C3 was about 31- to 36-fold higher than that of AKR1C4 (83.3 ± 15.4 vs. 2.3 ± 0.6 pmol/min^{-1}/mg^{-1}). Intrinsic clearance as calculated by V_{max}/K_M was highest for AKR1C3 (6.8), followed closely by AKR1C2 (5.1), CBR1 (3.5) and AKR1C1 (2.0). Recombinant AKR1C4 (0.24) showed the lowest overall activity of wildtype enzymes assayed (Table 3-4).

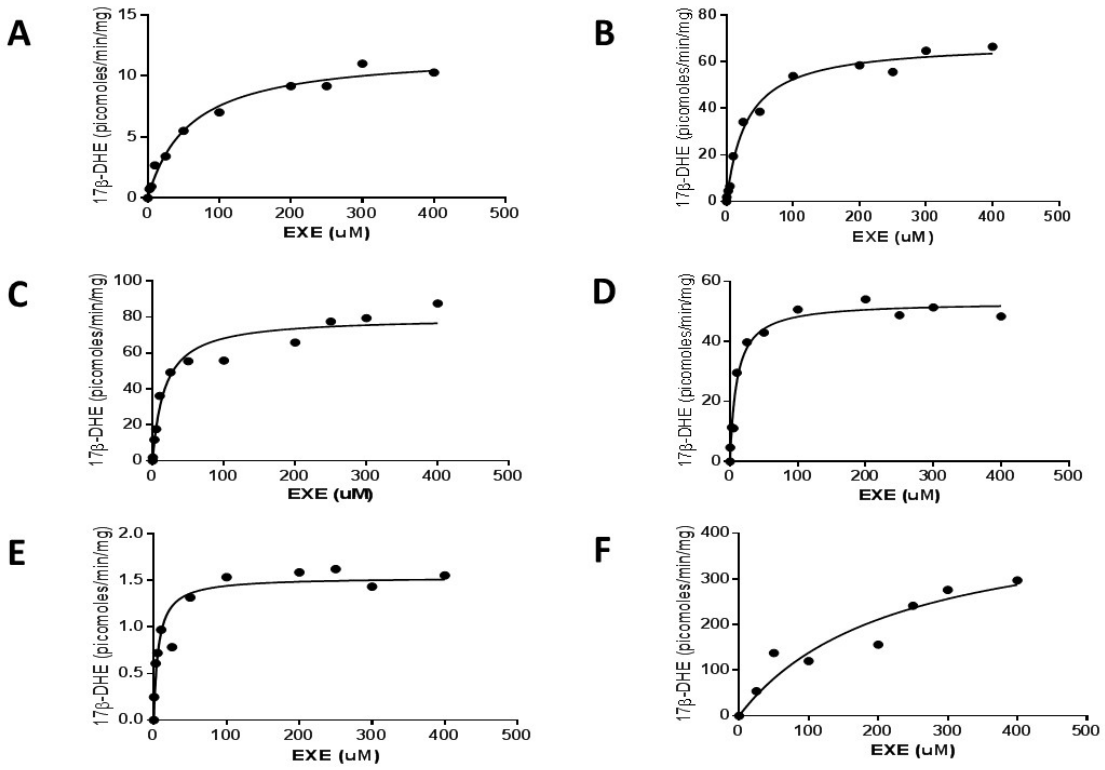

Figure 3-3: Representative kinetics curves for the reduction of EXE to 17β-DHE. Panel (A), pooled human liver cytosol; panel (B), AKR1C1; panel (C), AKR1C2; panel (D), AKR1C3; panel (E), AKR1C4; and panel (F), CBR1 [282].

Table 3-3: Kinetic analysis of wildtype and variant ketosteroid reductases active against EXE [282].

Reductase enzyme or variant	NCBI dbSNP Identifier	1000 Genomes Project (MAF)	GO-ESP (MAF)	K_M (μM)	V_{max} (picomoles·min^{-1}·mg^{-1})[a]	CL_{INT} (nl·min^{-1}·mg^{-1})
wt AKR1C1				35.3 ± 3.8	71.1 ± 1.5	2.0
wt AKR1C2				16.4 ± 0.6	84.2 ± 15.6	5.1
AKR1C2 Phe46Tyr	rs2854482	0.0649	0.07	13.5 ± 2.8	105.1 ± 6.3	7.8
wt AKR1C3				12.3 ± 1.1	83.3 ± 15.4	6.8
AKR1C3 His5Gln	rs12529	0.4203	0.43	17.9 ± 2.9	3.8 ± 0.1*	0.21
AKR1C3 Glu77Gly	rs11551177	0.0367	0.0503	13.9 ± 2.2	1.9 ± 0.2*	0.14
AKR1C3 Lys104Asn	rs12387	0.1518	0.1569	16.8 ± 1.0	6.4 ± 0.3*	0.38
AKR1C3 Pro180Ser	rs34186955	0.0086	0.0117	11.2 ± 3.1	3.6 ± 0.6*	0.32
AKR1C3 Arg258Cys	rs62621365	0.0325	0.001	75.8 ± 19.9*	2.3 ± 0.1*	0.03
wt AKR1C4				9.7 ± 1.9	2.3 ± 0.6	0.24
AKR1C4 Gly135Glu	rs11253043	0.027	0.0278	311.4 ± 75.7*	19.1 ± 4.2*	0.06
AKR1C4 Ser145Cys	rs3829125	0.1028	0.1143	9.6 ± 2.4	5.9 ± 1.1	0.61
AKR1C4 Leu311Val	rs17134592	0.1024	0.1143	11.9 ± 2.0	6.3 ± 0.8	0.53
CBR1				265 ± 21	928 ± 244	3.50

[a] All V_{max} values were normalized to reflect the purity of recombinant enzymes assayed. * Denotes that a variant exhibited statistically significant deviations ($p < 0.001$ in all cases) from the activity of its respective wildtype (wt).

3.4.3 Impact of functional polymorphisms on exemestane reduction

Screening the NCBI Variation Viewer for cytosolic ketosteroid reductase variants prevalent at 1% or greater yielded a single nonsynonymous polymorphism for AKR1C2, as well

as three common variants in AKR1C4. Although six AKR1C3 allelic variants were identified, only five underwent kinetic screening to characterize 17β-DHE formation. AKR1C3^{Glu36Term} (rs1804062) was excluded as it encodes a truncated protein lacking functional cofactor and substrate-binding domains. No polymorphisms matching our search criteria were detected for AKR1C1 or CBR1. K_M and V_{max} values were comparable between AKR1C2 and AKR1C2^{Phe46Tyr} (Table 3-4). Wildtype AKR1C3 showed affinity for EXE similar to its variants His5Gln, Glu77Gly, Lys104Asn, and Pro180Ser. However, AKR1C3^{Arg258Cys} recombinant protein had roughly six-fold lower affinity for EXE (K_M= 12.3 ± 1.1 vs. 75.8 ± 19.9 μmol/l). Furthermore, all AKR1C3 functional variants assayed showed markedly decreased velocity of EXE reduction, leading to sizable disparities from the wildtype in intrinsic clearance. The K_M was similar between wildtype AKR1C4 (9.7 ± 1.9 μmol/l) and its Ser145Cys (9.6 ± 2.4 μmol/l) and Leu311Val (11.9 ± 2.0 μmol/l) variants. The experimental K_M for AKR1C4^{Gly135Glu} using EXE as a substrate (311.4 ± 75.7 μmol/l) was 32-fold higher than that of the wildtype, indicative of significantly lowered affinity resulting from amino acid substitution. No notable difference was observed in the V_{max} of 17β-DHE formation between AKR1C4 and its Ser145Cys or Leu311Val allelic variants. Recombinant AKR1C4^{Gly135Glu} metabolized EXE 8-fold faster than its wildtype counterpart (V_{max} =19.1 ± 4.2 vs. 2.3 ± 0.6 pmol/min/mg).

3.4.4 Discussion of experimental results

Studies examining phase I EXE metabolism are scarce. However, the limited data available suggest that 17β-DHE is a major EXE metabolite produced by reduction of the C17 carbonyl moiety [114, 269-271]. Although the involvement of the AKR superfamily has been reported previously, specific enzymes catalyzing hepatic EXE metabolism have thus far been

unidentified [108]. The present study confirms that C17 reduction of EXE by cytosolic carbonyl reductases to yield 17β-DHE is indeed a major metabolic pathway (Figure 3-5).

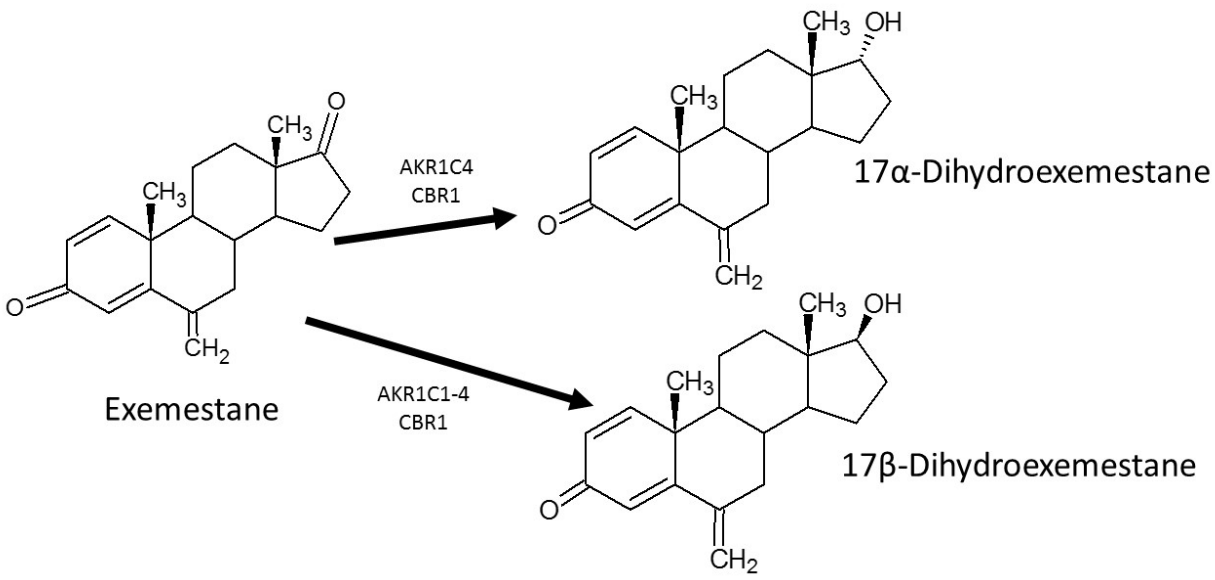

Figure 3-4: Schematic of *in vitro* EXE metabolism by hepatic cytosolic AKR and SDR ketosteroid reductases [282].

Formation of an additional stereoisomer, 17α-DHE, was detected in concert with 17β-DHE in the current study. Oxidation of DHE to form EXE was not observed in incubations of human liver cytosol with an abundance of 17α-DHE or 17β-DHE, suggesting that biotransformation of EXE by hepatic cytosolic reductases is irreversible (data not shown). A previous study exploring the ability of 17β-DHE to impede aromatase-mediated estrogen formation concluded that 17β-DHE inhibits aromatase with potency similar to its parent compound EXE [115]. However, 17α-DHE appears to be a subsidiary phase I metabolite with no appreciable aromatase-inhibiting properties (Refer to **Chapter 2**). As an active EXE

metabolite, 17β-DHE may contribute toward the therapeutic mechanism of systemic estrogen deprivation and thus influence *in vivo* efficacy of EXE in breast cancer treatment and prevention.

Although CBR1, as well as all 1C members of the AKR superfamily reduce EXE to 17β-DHE, only AKR1C4 and CBR1 produced detectable quantities of 17α-DHE. The current literature strongly suggests that human AKR1C isoforms are remarkably functionally plastic [276]. The stereochemistry of hydroxylated AKR1C products is known to be dependent on the initial docking position of substrate in the enzyme active site [291, 292]. Accommodation of multiple modes of substrate binding enables distinct hydroxysteroid products to be enzymatically derived from a single ketosteroid precursor, possibly explaining the production of both 17-DHE stereoisomers from parent EXE [276, 291, 292]. Furthermore, it has been reported that AKR1C4 reduces tibolone to both 3α-hydroxytibolone and 3β-hydroxytibolone *in vitro* using a single active site [291]. The same study suggests that AKR1C4 interconverts the two stereoisomers showing dual oxidoreductase and epimerase activities [291]. Whether the production of 17α-DHE by recombinant AKR1C4 in the present study is attributable to the innate promiscuity of the active site or epimerase activity is unknown.

Wildtype AKRs 1C2, 1C3, and 1C4 show similar affinity for EXE, whereas AKR1C1, which functions primarily as a 20-ketosteroid reductase, showed the lowest affinity of the AKRs assayed [293]. CBR1, a SDR, showed the lowest overall affinity for EXE, but catalyzed 17β-DHE formation much more rapidly (11–403-fold) than recombinant AKR1C enzymes. The kinetic mechanism of AKRs is strictly ordered with NADP(H) cofactor binding before docking of substrate and dissociating only after its release [294-296]. Cofactor release as well as substrate reduction are believed to be the primary determinants of overall catalytic rate [297].

However, the kinetic mechanism of CBR1 may differ from that of the AKRs, which could account for the accelerated rate of CBR1-mediated EXE reduction.

Although our *in vitro* data suggest that intrinsic clearance of EXE is highest for AKR1C3 followed by AKR1C2> CBR1 >AKR1C1≃AKR1C4, the *in vivo* contribution of each enzyme toward hepatic EXE metabolism is likely influenced by substrate availability, as well as relative expression. Although CBR1 produces 17β-DHE quickly *in vitro*, it has low affinity for EXE (K_M= 265 ± 21 μmol/l), implying that it may play a lesser role at therapeutic doses administered to patients. AKRs 1C1–4, in contrast, show much higher affinity for EXE, with K_M values ranging from 9.7 ± 1.9 to 35.3 ± 3.8 μmol/l. Quantitative reverse transcription-PCR data by Penning and colleagues suggest that transcripts encoding each AKR1C isoform are abundant and equally expressed in the human liver, the principal site of EXE metabolism [108, 276]. AKR1C1–3 are also well expressed in breast tissue, which is a primary site of estrogen synthesis in postmenopausal women [79, 276]. These findings allude to the potential contributions of soluble AKR1C carbonyl reductases in converting a potent AI into the active metabolite, 17β-DHE, *in vivo*.

Xenobiotic-metabolizing enzymes, including the AKRs, are highly polymorphic, with multiple high penetrance variants naturally found in the human populace [289]. Several AKR1C polymorphisms result in altered catalytic activity *in vitro* whereas other allelic variants are associated with an increased risk of life-threatening pathologies [298-300]. In the present study, a subset of common cytosolic reductase variants differed from their wildtype counterparts with respect to affinity for EXE as well as maximal velocity in its reduction to 17β-DHE.

AKR1C2^{Phe46Tyr} is similar to wildtype AKR1C2 in both affinity for the EXE substrate and maximum velocity of 17β-DHE formation. Although *Bains et al.* recorded reduction of the

anticancer drugs daunorubicin and doxorubicin comparable with the wildtype, tyrosine substitution at residue 46 decreased overall AKR1C2 activity against 1-acenaphthenol by ~30% [301]. *Takahashi et al.* reported a 40% decrease in V_{max} for 5α-DHT reduction relative to the wildtype enzyme [302]. These conflicting data suggest that deviations in catalytic activity could be substrate dependent. It has also been theorized that cofactor binding may be compromised in the Phe46Tyr variant, leading to reduced enzymatic activity [298]. If this is indeed the case, it is feasible that the use of supraphysiological concentrations of NADPH in the present study might mask moderately lowered cofactor affinity, resulting in similar V_{max} for EXE reduction by both wildtype and polymorphic AKR1C2 protein.

The AKR1C3 variants His5Gln, Glu77Gly, Lys104Asn, and Pro180Ser have comparable affinity for EXE, but hydroxylation of the ketosteroid is sluggish compared with their wildtype counterpart, whose CL_{INT} was 18–49-fold higher than that shown for the four AKR1C3 variants (Table 3-4). The Pro180Ser polymorphism occurs near α-helix 5 of the conserved $(\alpha/\beta)_8$-barrel conformation characteristic of the AKR superfamily and has been associated previously with decreased V_{max} using daunorubicin and doxorubicin as substrates for reduction [301, 303]. As it lies in close proximity to key cofactor binding residues (Ser166, Asp167, and Glu190), it has been proposed that NADPH binding may be adversely affected, thus decreasing the overall rates of catalysis [301].

The AKR1C3^{Arg258Cys} functional polymorphism is associated with a large (227-fold) decrease in CL_{INT} and a marked decrease in affinity for EXE substrate relative to wildtype (12.3 ± 1.1 vs. 75.8 ± 19.9 μmol/l), possibly because of its physical proximity to tryptophan residue 227 of the substrate-binding pocket. This variant maps to α-helix 7 and is likewise near multiple residues of the cofactor binding pocket, likely explaining decreased 17β-DHE production [303].

The catalytic tetrad of AKR1C3, in turn, is comprised of amino acid residues His117, Lys84, Tyr55, and Asp50 [303]. Substitution of negatively charged glutamic acid for nonpolar glycine at amino acid 77 decreases the overall rates of EXE reduction by recombinant protein 44-fold ostensibly by altering the chemical and conformational environment near the catalytic tetrad (83.3 ± 15.4 pmol/min/mg compared with 1.9 ± 0.2 pmol/min/mg). The results of a Swedish study found that Caucasian men heterozygous for the Glu77Gly genotype had lower serum testosterone levels than wildtype homozygotes, implying that this particular polymorphism may influence the risk of androgen-dependent pathologies [304].

Our experimental results, as well as the locations of the His5Gln and Lys104Asn functional polymorphisms, suggest that significantly reduced V_{max} for EXE reduction is mediated through changes in overall enzyme stability or folding rather than changes in EXE or cofactor binding. An inverse association between His5Gln and the risk of bladder cancer has been noted previously in patients of the Spanish Bladder Cancer Study [305]. If His5Gln shows decreased catalysis for substrates other than EXE, these observations may be attributable to decreased bioactivation of polyaromatic hydrocarbons by AKR1C3, thus modifying exposure to genotoxic compounds promoting tumorigenesis [305]. At this time, additional data are needed to fully explicate the role of common AKR1C3 polymorphisms in attenuating or enhancing the risk of cancer.

Although AKR1C4^{Ser145Cys} showed a slightly higher V_{max} compared with the wild-type (5.9 ± 1.1 vs. 2.3 ± 0.6 pmol/min/mg, respectively), it had an affinity for EXE similar to the wildtype, with K_M values of 9.6 ± 2.4 and 9.7 ± 1.9 μmol/l, respectively. V_{max} values for EXE reduction did not differ appreciably (6.3 ± 0.8 and 2.3 ± 0.6 pmol/min/mg), which is consistent

with a previous study concluding that the overall catalytic activity of the Ser145Cys variant is comparable with wildtype AKR1C4 using several test substrates [299].

However, the results of our current investigation contrast to previous reports describing altered catalytic activity in the common AKR1C4^{Leu311Val} and Gly135Glu functional polymorphisms. Valine substitution at amino acid 311 results in decreased activity against several substrates including daunorubicin, 1-acenaphthenol, as well as steroids androsterone and 5β-androstane-3α, 17β-diol [299, 301]. A mutagenesis study carried out by *Matsuura et al.* suggests that the leucine residue 311 is involved in substrate binding at the AKR1C4 active site, and valine substitution decreased the overall activity by almost 50% for several substrates [306]. Although several nearby amino acid residues (Asn306, Ala308, and Tyr310) contribute toward substrate binding on the C-terminal loop of human AKRs, significant deviations from the wild-type in EXE substrate affinity and overall velocity of catalysis were not observed in kinetic assays monitoring 17β-DHE formation [303]. AKR1C4^{Gly135Glu}, however, showed significantly less affinity for EXE (K_M=311.4 ± 75.7), and the maximum velocity of its reduction (V_{max} = 19.1 ± 4.2 pmol/min/mg) was eight-fold faster than wildtype AKR1C4. V_{max} and K_M values reported previously for AKR1C4 and the Gly135Glu variant do not differ for doxorubicin, daunorubicin, and 1-acenaphthenol substrates [301]. The extent to which functional polymorphisms impact catalysis is likely a complex interplay between the unique chemistry of each substrate and the specific nature of the amino acid deviations present. Thus, discrepancies between our observations and those reported in the literature may simply reflect a substrate-dependent effect on catalysis by variant AKR1C4 proteins.

In the present *in vitro* study, we attempted to clarify manufacturer claims of hepatic cytosolic EXE metabolism. Two isomers of DHE, the major phase I EXE metabolite, were

identified in reactions with human liver cytosol, and five ketosteroid reductases were shown to be capable of catalyzing EXE reduction to the major metabolite 17β-DHE. Several functional polymorphisms in AKR1Cs resulted in altered rates of 17β-DHE formation compared with their respective wildtype enzymes as well as showing markedly decreased affinity for EXE substrate. However, a limitation of the present study is that the cytosolic reductases examined were not overexpressed in a mammalian cell line. Kinetic assays examining exemestane metabolism were instead performed using purified reductases. Therefore, misfolding may have occurred, which could inadvertently affect the kinetic activities observed due to differential protein stability.

Functional polymorphisms resulting in impaired reductase activity may partially underlie the varied response between individuals administered EXE by facilitating differential metabolite production. It has been suggested previously that 17β-DHE may contribute toward the overall therapeutic mechanism of its parent compound [272]. Thus, it is feasible that genetic factors affecting the conversion of EXE into its active metabolite could potentially impact circulating 17β-DHE levels, and in turn, influence overall clinical benefit. Albeit a well-established endocrine therapy, to our knowledge, this is the first time that the novel EXE metabolite 17α-DHE has been described in the literature. It is evident that many unanswered questions remain in terms of EXE metabolism, and additional unidentified metabolites may still exist. Although the involvement of CYP3A4 is known, *in vitro* experiments by Kamdem and colleagues suggest that the overall CYP450-mediated metabolism of EXE may include contributions by additional isoforms [108, 277]. Therefore, future studies should examine the relative contributions of major hepatic CYP450s and soluble cytosolic ketosteroid reductases to phase I metabolism of this drug. Genotype–phenotype correlative studies are also needed to determine whether functional

AKR1C polymorphisms with deviant catalytic activity *in vitro* are associated with drug efficacy or incidence of adverse events in patients taking EXE for breast cancer treatment or prevention

CHAPTER FOUR

Impact of nonsynonymous single nucleotide polymorphisms on in vitro metabolism of exemestane by hepatic cytochrome P450s

**A version of this chapter has been accepted for publication:
Peterson A, Xia Z, Chen G and Lazarus P. In vitro metabolism of exemestane by hepatic cytochrome P450s: impact of nonsynonymous polymorphisms on formation of the active metabolite 17β-dihydroexemestane.

4.1 INTRODUCTION

This chapter qualitatively and quantitatively describes the *in vitro* metabolism of EXE by wildtype and variant hepatic xenobiotic-metabolizing cytochrome P450s. Phase I metabolites were identified in incubations of EXE with HEK293-overexpressed cytochrome P450s. The results of enzyme kinetic assays monitoring the formation of 17β-DHE are discussed with emphasis placed on the impact of genetic variation on enzyme catalytic activity and overall EXE metabolism. Isoform-specific cytochrome P450 experiments were performed to gauge the impact of each isoform on 17β-DHE formation. These results are also reported in this chapter.

4.2 BACKGROUND

Several studies have examined the pathways involved in the metabolism of EXE. 17β-dihydroexemestane (17β-DHE) is a major metabolite found in the plasma of individuals taking EXE, and several cytosolic reductase enzymes including CBR1 and members of the AKR1C subfamily were shown to be active in its formation [114, 273, 282]. Previous studies using cytochrome P450-overexpressing baculosomes have also suggested that several CYP450s may be involved in 17β-DHE formation [277]. Aside from its abundance in clinical samples, 17β-DHE is noteworthy for its ability to inhibit aromatase (Chapter 2). The concentration of 17β-DHE relative to EXE in human plasma may vary 5-fold between individuals although the mechanisms underlying this observation have not been fully resolved [114].

It is well-established that nonsynonymous polymorphisms in genes involved in drug absorption, distribution, metabolism, and excretion (ADME) can lead to genotype-dependent variability in clinical responses for certain drugs [274]. Regarding EXE pharmacogenetics, recent *in vitro* enzyme kinetics assays have shown that the hepatic cytosolic enzymes CBR1 and AKR1C1-4 reduce EXE with several nonsynonymous variants in AKR1C3 and AKR1C4

significantly altering overall 17β-DHE metabolism (Chapter 3) [282]. These observations bolster the possibility that genetically-determined differences in metabolic capacity contribute to variability in clinical responses in EXE-treated women by influencing 17β-DHE production and UGT-driven clearance.

Studies describing the impact of variant cytochrome P450 monoxygenases (CYP450s) on EXE metabolism are conspicuously absent from the literature. Xenobiotic-metabolizing members of the CYP450 family participate in the hepatic metabolism of hundreds of distinct substrates comprising approximately 75% of all currently marketed pharmaceuticals [307]. With over 2000 known genetic variants, CYP450s are highly polymorphic enzymes [308]. A subset of variant CYP450 isoforms have previously been associated with clinically significant alterations in drug metabolism and disease susceptibility as reviewed by *Preissner et al.* [308]. The present study seeks to deepen our understanding of phase I EXE metabolism by identifying metabolites produced by xenobiotic-metabolizing hepatic CYP450s and to quantitate the impact of common nonsynonymous variant CYP450s on formation of the active metabolite 17β-DHE.

4.3 MATERIALS AND METHODS

4.3.1 Chemicals and materials

Testosterone, boldenone, and 4-andostene-3,17-dione were purchased from Hangzhou DayangChem Co., China. All other reagents used for synthesis of exemestane and its phase I metabolites were ACS grade or higher and purchased from Thermo Fisher Scientific (Waltham, Massachusetts, US), Tokyo Chemical Industry Co. (Tokyo, Japan) or Sigma-Aldrich (St. Louis, Missouri, US). Thin-layer chromatography plates and silica columns used to purify the synthesized steroids were purchased from Bonna-Agela Technologies Inc. (Wilmington, DE,

US) and Yamazen Corp. (Osaka, Japan), respectively. Variant CYP450 overexpression vectors were made using a QuikChange II Site-Directed Mutagenesis Kit from Agilent (Santa Clara, California, US), as well as oligonucleotides manufactured by Integrated DNA Technologies (Coralville, Iowa, US). Negative control baculosomes, SuperScript II First-Strand Synthesis System for RT-PCR, cell culture medium, fetal bovine serum, penicillin/streptomycin, and G418 were acquired from Invitrogen (Carlsbad, California, US). Choice-Taq polymerase was purchased from Denville Scientific (Holliston, Massachusetts, US). LC/MS grade organic solvents, tris base, glycine, tetramethylethylenediamine (TEMED), ammonium persulfate (APS), sodium dodecyl sulfate (SDS), SuperSignal West Femto Maximum Sensitivity Substrate, Lipofectamine 2000, oligo(dT) primer, Pierce BCA protein assay kit, PVDF membranes, and monoclonal HRP-conjugated V5 epitope antibody (catalog # MA5-15253-HRP) were procured from Thermo Fisher Scientific (Waltham, Massachusetts, US). Nonfat dry milk used as a blocking agent for Western blotting was prepared by BioRad (Hercules, CA, US). The NADPH regeneration system included in kinetic assays was purchased from Corning (Corning, New York, US). Ampicillin, dithiothreitol (DTT), Tween 20, and acrylamide/bis-acrylamide solution were acquired from Sigma-Aldrich (St. Louis, Missouri, US). Pooled mixed gender liver microsomes from 50 human donors was obtained from XenoTech (Lenexa, Kansas, US). The ethnic composition of the pooled hepatic microsomes was 84% Caucasian, 8% Hispanic, 6% African American, and 2% Asian. (-)-N-3-benzylphenobarbital (NBP) is a product of Cypex Ltd (Dundee, United Kingdom) while all other compounds used for CYP450 isoform-specific inhibition were obtained from Sigma-Aldrich.

4.3.2 Synthesis of exemestane and phase I exemestane metabolites

EXE and its phase I metabolites were synthesized at Washington State University using previously published protocols [268, 282-284, 309]. A Yamazen AI-580s flash chromatography system was utilized in the purification of each compound following synthesis. Purity was estimated for each EXE derivative by PDA spectrum (210 nm-400 nm) using the Acquity I Class UPLC platform from Waters (Milford, Massachusetts, USA). With the kind permission of Gonzaga University's Department of Chemistry (Spokane, WA), the identity of each steroid was authenticated using nuclear magnetic resonance spectra generated by a Bruker AV300 instrument (Billerica, MA, US). High resolution mass spectra were also obtained on a Waters Xevo G2-S QTof Mass Spectrometer to confirm the parity of the experimental and theoretical mass-to-charge values for each compound prior to resuspension in ethanol and storage at -80˚C.

4.3.3 Identification of nonsynonymous polymorphisms

Common nonsynonymous polymorphisms for CYP450s 1A2, 2C8, 2C9, 2C19, 2D6, 3A4, and 3A5 were identified using the National Center for Biotechnology Information (NCBI) Variation Viewer [290]. Search filters were set to simultaneously screen dbVar and dbSNP for any missense or nonsense variants caused by single nucleotide variations, deletions, insertions or frameshifts. Low incidence variants were excluded from the current study and defined as those occurring with a minor allele frequency (MAF) of < 1% according to the GO-ESP dataset or 1000 Genomes Project. Interethnic differences in the occurrence of common CYP450 variants were examined using NCBI's 1000 Genomes Browser. These results are summarized in Table 4-1.

Table 4-1: Interethnic differences in the incidence of common CYP450 variants.

Polymorphism	NCBI dbSNP Identifier	1000G MAF	GO-ESP MAF	South Asian (SAS) MAF	European (EUR) MAF	African (AFR) MAF	Hispanic (AMR) MAF	East Asian (EAS) MAF
CYP1A2^{Ser298Arg}	rs17861157	0.0240	0.0239	0	0	0.0893	0.0029	0
CYP2C8^{Ile269Phe}	rs11572103	0.0547	0.0554	0.0123	0.004	0.1891	0.0115	0
CYP2C8^{Arg139Lys}	rs11572080	0.0457	0.0853	0.0297	0.1183	0.0083	0.0994	0.001
CYP2C8^{Lys399Arg}	rs10509681	0.0457	0.0854	0.0297	0.1183	0.0083	0.0994	0.001
CYP2C8^{Ile264Met}	rs1058930	0.0166	0.0406	0.0072	0.0577	0.0083	0.0187	0
CYP2C9^{Arg144Cys}	rs1799853	0.0479	0.0955	0.0348	0.1243	0.0083	0.0994	0.001
CYP2C9^{Ile359Leu}	rs1057910	0.0485	0.0484	0.1094	0.0726	0.0023	0.0375	0.0337
CYP2C9^{Arg150His}	rs7900194	0.0148	0.0201	0.001	0.002	0.053	0.0014	0
CYP2C9^{His251Arg}	rs2256871	0.0220	0.0268	0	0.001	0.0817	0.0014	0
CYP2C19^{Ile331Val}	rs3758581	0.0485	0.0473	0.1094	0.0686	0.0023	0.0346	0.0397
CYP2C19^{Glu92Asp}	rs17878459	0.0090	0.0231	0	0.0358	0.0038	0.0058	0
CYP2D6^{Arg296Cys}	rs16947	0.3592	0.4004	0.3620	0.3429	0.5537	0.3271	0.1399
CYP2D6^{Ser486Thr}	rs1135840	0.4012	0.4083	0.4724	0.4543	0.3238	0.5245	0.2956
CYP2D6^{Pro34Ser}	rs1065852	0.2380	0.1885	0.1646	0.2018	0.1127	0.1484	0.5714
CYP2D6^{Thr107Ile}	rs28371706	0.0591	0.0585	0	0.002	0.2179	0.0086	0
CYP3A4^{Arg162Gln}	rs4986907	0.0052	0.0103	0	0.001	0.0174	0.0029	0

4.3.4 Creation of CYP450-overexpressing HEK293 cell lines

Oligo(dT)$_{20}$ was used to prime reverse transcription of pooled hepatic total RNA from five human donors (Penn State Cancer Institute Biorepository). The resultant first-strand cDNA was further amplified using CYP450 isoform-specific primers and *Taq* polymerase. cDNA encoding wildtype CYP450s 1A2, 2C8, 2C9, 2C19, 2D6, 3A4 or 3A5 was introduced into the pcDNA3.1/V5-His-TOPO expression vector for stable overexpression in mammalian cells.

CYP2D6*2 and CYP2C19*1B cDNA were also amplified from pooled human liver RNA. Additional constitutive overexpression vectors encoding nonsynonymous variants with MAF > 0.01 were produced for CYP450s 1A2, 2C8, 2C9, 2C19, and 3A4 via site-directed mutagenesis (SDM) using wildtype plasmid as template. Two common CYP2D6 haplotypes were likewise derived from the CYP2D6*2 overexpression vector through SDM. Oligonucleotide pairs used to amplify wildtype CYP450 cDNA or prime mutagenesis are detailed in Table 4-2 and Table 4-3, respectively. Each expression vector was transformed into chemically competent BL21. Transformants were then grown overnight on ampicillin selection plates at 37˚C. Sanger sequencing was used for sequence confirmation prior to transfecting HEK293 with overexpression plasmids using Lipofectamine 2000 per the manufacturer instructions. Transfected HEK293 were grown for at least 3 weeks under 700 μg/ml G418 selective pressure in DMEM supplemented with 4.5 g/L glucose, L-glutamine, 110 mg/L sodium pyruvate, 10% FBS, and penicillin/streptomycin.

Table 4-2: Oligonucleotide pairs used to amplify wildtype CYP450 cDNA. Top, sense oligonucleotide sequence; bottom, antisense oligonucleotide sequence.

CYP450	**5' → 3' Oligonucleotide Sequence**
CYP1A2	tacagatggcattgtccca gttgatggagaagcgcag
CYP2C8	acaatggaacctttgtggtcc gacagggatgaagcagatctgg
CYP2C9	gagaaggcttcaatggattc gacaggaatgaagcacag
CYP2C19	acaatggatcctttgtggtcc gacaggaatgaagcacagctgat
CYP2D6	ttggtagtgaggcaggtatgg gcggggcacagcacaaa
CYP3A4	agtagtgatggctctcatcccag ggctccacttacggtgc
CYP3A5	gaagaaggaaagtggcgatgg ttctccacttagggttccatctct

Table 4-3: Oligonucleotide pairs used to produce variant CYP450s by site-directed mutagenesis of wildtype CYP450s. Top, sense oligonucleotide sequence; bottom, antisense oligonucleotide sequence.

Nonsynonymous CYP450	5' → 3' Oligonucleotide Sequence for Site-Directed Mutagenesis
CYP1A2 Ser298Arg	ggatgaggttgcctctggctctaggcc ggcctagagccagaggcaacctcatcc
CYP2C8 Ile264Met	tgatcaggaagcaatccataaagtcccgaggattg caatcctcgggactttatggattgcttcctgatca
CYP2C8 Ile269Phe	cttttcctgctccattttgaacaggaagcaatcgataaagt actttatcgattgcttcctgttcaaaatggagcaggaaaag
CYP2C8 Arg139Lys	cggtcctcaatgctcttcttccccatcccaa ttgggatggggaagaagagcattgaggaccg
CYP2C8 Lys399Arg	agatatttggattaggaaattccttgtcatcatgtagcacggaag cttccgtgctacatgatgacaaggaatttcctaatccaaatatct
CYP2C9 Arg144Cys	gcttcctcttgaacacagtcctcaatgctcctc gaggagcattgaggactgtgttcaagaggaagc
CYP2C9 Arg150His	cctccacaaggcagtgggcttcctcttga tcaagaggaagcccactgccttgtggagg
CYP2C9 His251Arg	gttgttcatgtccattgattcttggcgttcttttacttttttccaaaatata tatattttggaaaaagtaaaagaacgccaagaatcaatggacatgaacaac
CYP2C9 Ile359Leu	gtggggagaaggtcaaggtatctctggacctcg cgaggtccagagataccttgaccttctccccac
CYP2C19 Glu92Asp	cctcttccagaaaactcgtctccaagatcaatcag ctgattgatcttggagacgagttttctggaagagg
CYP2D6 Pro34Thr	gggggcctggtgtgtagcgtgcagc gctgcacgctacacaccaggccccc
CYP2D6 Ser486Thr	gtcagccaccactatgcgcaggttctcatcattga tcaatgatgagaacctgcgcatagtggtggctgac
CYP2D6 Thr107Ile	caggatctggatgatgggcacaggcggg cccgcctgtgcccatcatccagatcctg
CYP3A4 Arg162Gln	gcctgtctctgcttcctgcctcagatttctcac gtgagaaatctgaggcaggaagcagagacaggc

4.3.5 CYP450 quantification

Following antibiotic selection, the relative CYP450 content of each overexpressing cell line was assessed via Western blotting. Briefly, CYP450-overexpressing HEK293 cells were resuspended in PBS 1:1 followed by four flash freeze-thaw cycles. The homogenate was centrifuged at 9,000 g for 30 min at 4˚C. The supernatant was then subjected to 1 h centrifugation at 34,000 g in a chilled Beckman L7-65 ultracentrifuge. To remove cytosolic contamination, the supernatant was discarded before resuspending the microsomal fraction in 1.5 ml PBS. After an additional 60-min refrigerated centrifugation at 34,000 g, the supernatant was again discarded. The washed pellet was resuspended in PBS and stored at -80˚C. The bicinchoninic acid assay (BCA) was used to determine protein concentration prior to SDS-PAGE. 7.5 µg of microsomal protein from each wildtype or variant cell line was loaded onto a 10% tris-glycine polyacrylamide gel and run at 125 volts for approximately 1 h. Gel-embedded proteins were then transferred onto PVDF (0.45 µm pore size) for 90 minutes using 30 V. After a 1-h incubation in 5% milk in tris-buffered saline with 0.1% Tween (TBST) at room temperature, the membrane was incubated with HRP-conjugated anti-V5 antibody (1:7500) overnight at 4˚C. Following a 30-min wash in TBST to remove excess antibody, V5-tagged recombinant CYP450 proteins were visualized on a ChemiDoc Imager using SuperSignal West Femto Maximum Sensitivity Substrate. Ponceau staining served as a loading control. Band density was measured using Image J (NIH, Bethesda, MD, US).

4.3.6 Metabolite identification

CYP450-derived phase I EXE metabolites were identified in 45-min incubations performed at 37˚C. Each 50-µl reaction contained 2.5 mM EXE substrate, 3 µl NADPH

regeneration system, and 20 μg of microsomal protein from a wildtype CYP450-overexpressing HEK293 cell line in PBS, pH 7.4. Similar incubations were conducted to assess background activity of endogenous metabolizing enzymes in non-transfected HEK293, as well as commercially available negative control baculosomes. These incubations included 100 μM EXE, 50 μg of microsomes or 50 μg of baculosomes in addition to PBS, pH7.4, and an NADPH regeneration system. Enzymatic incubations were terminated with 50 μl of ice-cold acetonitrile before centrifugation at 13,200 g for 15 min at 4˚C. The resulting supernatant was analyzed by ultra-pressure liquid chromatography paired with tandem mass spectrometry on a Waters ACQUITY platform configured with a 0.2 μm in-line filter preceding a 1.7 μm ACQUITY UPLC BEH C18 column (2.1 mm x 100 mm, Ireland). The UPLC gradient used to separate EXE and its phase I metabolites has been described previously [282]. 800 L/h nitrogen gas was used for drying while desolvation temperature was set at 500˚C. A targeted UPLC/MRM method was performed in positive mode using electrospray ionization to monitor mass transitions for EXE (*m/z* 297.34 → 185.07), 17α-DHE (*m/z* 299.14 → 135.07), 17β-DHE (*m/z* 299.20 → 135.13) and 6-HME (*m/z* 312.89 → 158.98). 0.01 s dwell time was optimal for all four compounds while 25 V of collision energy was used for EXE and 6-HME. 20 V of collision energy was used for 17α- and 17β-DHE. An additional non-targeted screening for phase I EXE metabolites was performed using UPLC/MS to detect positively charged molecular ions with *m/z* ranging from 100 to 450. The identity of all metabolites observed was verified by comparing the observed retention times and *m/z* with those of purified standards.

4.3.7 Enzyme kinetic assays

Wildtype and variant CYP450-mediated 17β-DHE production was measured in 45-min

incubations at 37˚C in PBS, pH 7.4 with varying concentrations of EXE (25-2500 μM). Each reaction included 20 μg of microsomal protein from CYP450-overexpressing HEK293, as well as an NADPH regeneration system. The chosen incubation length and protein concentration fell within the linear range of EXE reduction velocity curves for the seven wildtype CYP450s assayed (data not shown). Cold acetonitrile (50 μl) was used to terminate each reaction. After centrifugation for 15 min at 4˚C at 13,200 g, 17β-DHE formation was monitored in the supernatant according to a previously established UPLC/MS/MS method and quantitated against a standard curve constructed of known 17β-DHE concentrations [282].

4.3.8 Isoform-specific CYP450 inhibition

Reduction of EXE to 17β-DHE in the presence of isoform-specific CYP450 inhibitors was monitored in pooled human liver microsomes (HLM). Furafylline (1 μM) was used to inhibit CYP1A2 while 0.5 μM tranylcypromine (TCP) and 10 μM thioTEPA inhibited CYPs 2A6 and 2B6, respectively. Other compounds used to systematically inhibit hepatic CYP450s included 0.5 μM montelukast (CYP2C8 inhibitor), 1 μM sulfaphenazole (CYP2C9 inhibitor), 0.5 μM NBP (CYP2C19), 1 μM quinidine (CYP2D6 inhibitor), 5 μM clomethiazole (CYP2E1 inhibitor), and 1 μM ketoconazole (CYP3A inhibitor). Initial dosages were selected from the literature and then further titrated to determine the lowest dose producing maximum isoform-specific inhibition [310-312]. Each 50-μl inhibition reaction contained 12.5 μg of pooled HLM, one isoform-specific CYP450 inhibitor dissolved in ethanol, and 10 μM EXE in PBS, pH 7.4. Following a 15-min pre-incubation at 37˚C, the reactions were initiated by the addition of NADPH regeneration system and incubated for an additional 15 min before termination with 50 μl of cold acetonitrile. After refrigerated centrifugation for 15 min at 13,200 g, supernatants

were collected and dried at ambient temperature in a Jouan RC10.22 vacuum concentrator. Samples were resuspended in 20 µl of water/acetonitrile (1:1) and analyzed by UPLC/MS/MS using the aforementioned method. A negative control reaction was run in parallel and received ethanol vehicle rather than inhibitor. Organic solvent constituted less than 1% of each incubation.

4.3.9 Statistical Analyses

K_M and relative V_{max} values were calculated in GraphPad Prism 6 according to the Michaelis-Menten equation (GraphPad Software, Inc., San Diego, California). V_{max} is expressed as picomoles·min^{-1}·mg^{-1} and was normalized to total protein content to account for differences in CYP450 expression between cell lines as determined by Western blot analysis. Two-sided unpaired *t*-tests were used to compare the wildtype catalytic activity of CYP450s 1A2 and 3A4 to their respective variants. Wildtype CYP450s 2C8, 2C9, 2C19, and 2D6 were compared to their nonsynonymous variants using one-way ANOVA supplemented with Dunnett's multiple comparison test. In all instances, the threshold for statistical significance was set at a two-tailed p value < 0.05. The percent change in 17β-DHE formation associated with each inhibitor in pooled HLM was likewise calculated in GraphPad Prism 6. An uninhibited reaction receiving vehicle was considered maximum catalytic activity for the purposes of comparison. All experimental results represent triplicate assays performed independently.

4.4 RESULTS AND DISCUSSION

4.4.1 Identification of phase I exemestane metabolites

As shown in a representative Western blot analysis, significant levels of expression of

individual CYPs were obtained in all HEK293 overexpressing cell lines (Figure 4-1, panel A). Ponceau staining revealed no significant differences in total protein content between cell lines (Figure 4-1, panel B). The major metabolite formed in individual 45-min incubations of EXE with CYP2C9 (Figure 4-2, panel E) as well as overexpressed wildtype CYP450s 1A2, 2C8, 2C19, 2D6, 3A4, and 3A5 (results not shown) was 17β-DHE. Low levels of 6-HME and 17α-DHE formation were observed for all CYPs studied. In all cases, formation of the 17α-DHE and 6-HME metabolites exceeded the minimum threshold of detection. No EXE metabolite formation was observed in incubations using microsomes from the parent HEK293 cell line (Figure 4-2, panel F), but interestingly, significant 17β-DHE formation was observed using negative control baculosomes (Figure 4-2, panel G). Secondary metabolite formation was not observed when overexpressing CYP450 microsomes were presented with 6-HME or either stereoisomer of 17-DHE as substrate (results not shown).

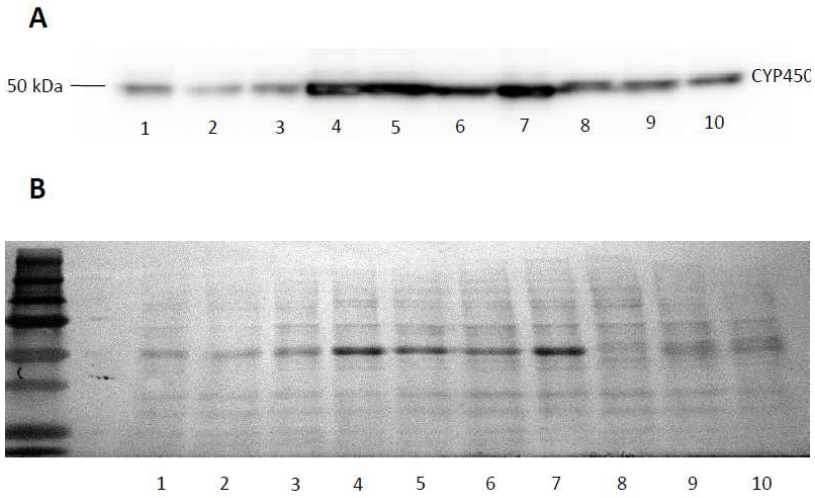

Figure 4-1: Relative quantification of overexpressed CYP450s in HEK293 microsomes. Panel (A) Detection of V5-tagged CYP450s by Western blotting. Panel (B) Ponceau total protein staining for CYP450 normalization. Lane 1, CYP2C19; lane 2, CYP2C19Glu92Asp; lane 3, CYP2C19Ile331Val; lane 4, CYP2D6; lane 5, CYP2D6Arg296Cys, Ser486Thr; lane 6, CYP2D6Pro34Ser, Ser486Thr; lane 7, CYP2D6Thr107Ile, Arg296Cys, Ser486Thr; lane 8, CYP3A4; lane 9, CYP3A4Arg162Gln; lane 10, CYP3A5.

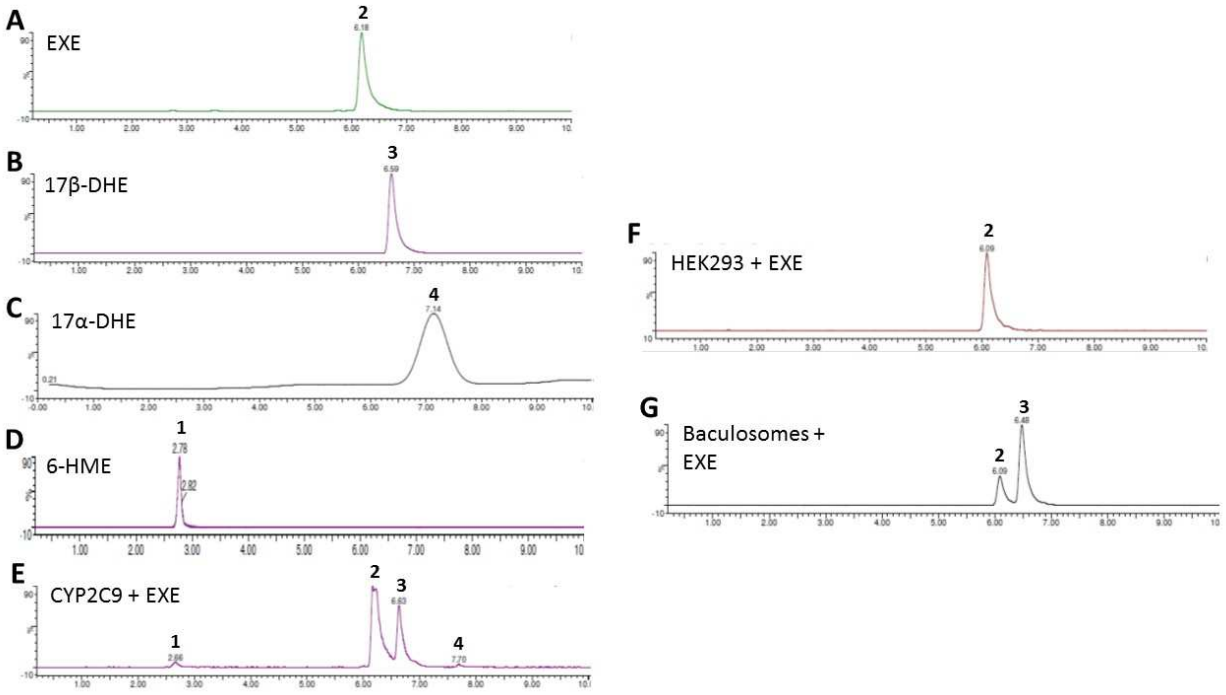

Figure 4-2: Identification of EXE metabolites. Panel (A), EXE (6-methyleneandrosta-1,4-diene-3,17-dione) standard; panel (B), 17β-DHE (17β-hydroxy-6-methyleneandrosta-1,4-dien-3-one) standard; panel (C), 17α-DHE (17α-hydroxy-6-methyleneandrosta-1,4-dien-3-one) standard; panel (D), 6-HME (6-hydroxymethylandrosta-1,4,6-triene-3,17-dione) standard; panel (E), EXE metabolite profile after incubating CYP2C9-overexpressing HEK293 microsomes with EXE; panel (F), EXE metabolite profile after incubating microsomes from the parent HEK293 cell line (no CYP450 overexpression) with EXE; panel (G), EXE metabolite profile after incubating negative control commercial baculosomes (no CYP450 overexpression) with EXE. Incubations were performed for 45 min at 37oC with 100 µM EXE and 20 µg of CYP450-overexpressing HEK293 microsomes, 50 µg of CYP450-overexpressing HEK293 microsomes or 50 µg of baculosomes. Peak 1, 6-HME; peak 2, EXE; peak 3, 17β-DHE; peak 4, 17α-DHE.

4.4.2 Kinetic analysis of 17β-dihydroexemestane formation

Representative kinetic curves of 17β-DHE formation for each wildtype hepatic CYP450 are shown in Figure 4-3. Kinetic assays using overexpressed CYP450 protein suggest that CYP2D6 exhibited the highest affinity for EXE (K_M = 0.57 ± 0.03 mM) followed by CYP2C8 (K_M = 0.66 ± 0.10 mM), CYP3A5 (K_M = 0.69 ± 0.18 mM), CYP1A2 (K_M = 0.74 ± 0.5 mM), and CYP3A4 (K_M = 0.83 ± 0.16 mM) (Table 4-4). CYP450s 2C9 and 2C19 had approximately the

same affinity for EXE with K_M values of 0.96 ± 0.22 mM and 0.92 ± 0.18 mM, respectively. CYP2C9 exhibited the slowest rate of EXE reduction while CYP2C8 reduced EXE approximately 5-fold faster (V_{max} = 26 ± 0.6 versus 128 ± 4 picomoles·min^{-1}·mg^{-1}). CYP1A2 catalyzed 17β-DHE production at a rate of 61 ± 17 picomoles·min^{-1}·mg^{-1} followed by CYP2C19 (51 ± 8 picomoles·min^{-1}·mg^{-1}) and CYP2D6 (49 ± 3 picomoles·min^{-1}·mg^{-1}). Catalytic velocities for CYP450s 3A4 and 3A5 were not significantly different (39 ± 7 and 36 ± 4 picomoles·min^{-1}·mg^{-1}). Intrinsic clearance (V_{max}/K_M) was calculated for each wildtype enzyme as an indication of its overall catalytic activity against EXE. CYP2C8 exhibited the highest intrinsic clearance value (194 nl·min^{-1}·mg^{-1}) followed by CYP2D6 (86 nl·min^{-1}·mg^{-1}), CYP1A2 (82 nl·min^{-1}·mg^{-1}), CYP2C19 (55 nl·min^{-1}·mg^{-1}), CYP3A5 (52 nl·min^{-1}·mg^{-1}), and CYP3A4 (47 nl·min^{-1}·mg^{-1}). In addition to having the slowest rate of EXE reduction, CYP2C9 also exhibited the lowest overall catalytic activity against EXE substrate (27 nl·min^{-1}·mg^{-1}).

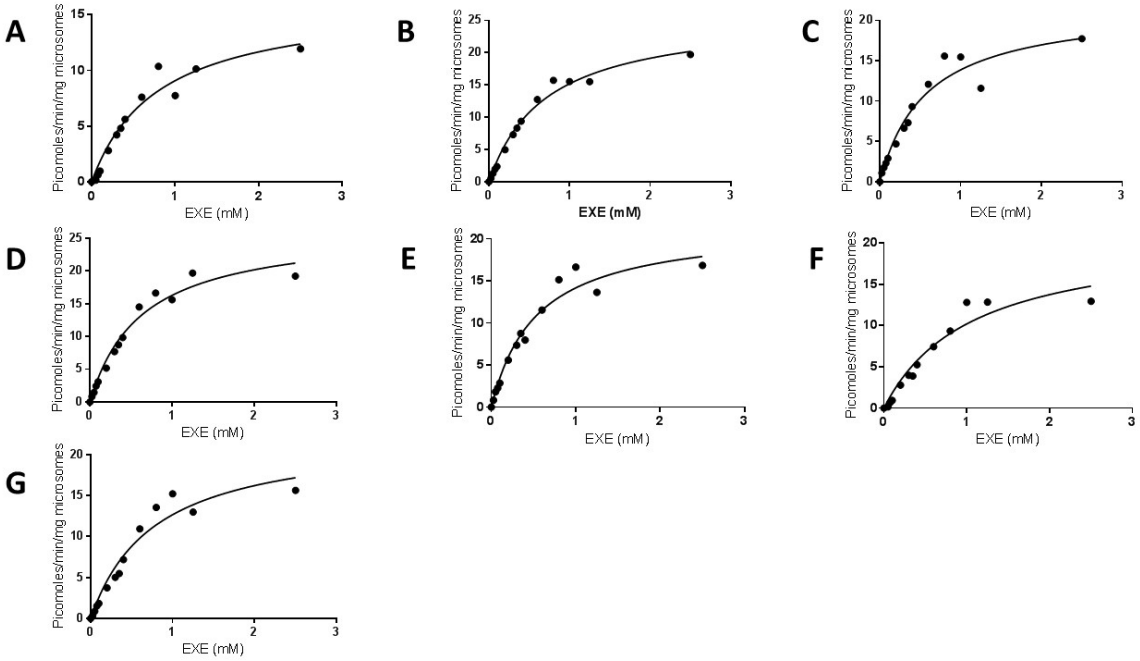

Figure 4-3: Representative kinetics curves for the reduction of EXE to 17β-DHE. Panel (A), CYP1A2; panel (B), CYP2C8; panel (C), CYP2C9; panel (D), CYP2C19; panel (E), CYP2D6; panel (F), CYP3A4; and panel (G), CYP3A5.

Table 4-4: Kinetic analysis of wildtype and variant CYP450s active against EXE.

Wildtype CYP450 or variant	NCBI dbSNP Identifier	Allele	K_M (mM)	V_{max} (picomoles·min^{-1}·mg^{-1})[a]	CL_{INT} (nl·min^{-1}·mg^{-1})
CYP1A2		CYP1A2*1A	0.74 ± 0.5	61 ± 17	82
CYP1A2^{Ser298Arg}	rs17861157		0.59 ± 0.2*	80 ± 7	136
CYP2C8		CYP2C8*1A	0.66 ± 0.10	128 ± 4	194
CYP2C8^{Ile269Phe}	rs11572103	CYP2C8*2	0.86 ± 0.8	280 ± 17*	326
CYP2C8$^{Arg139Lys,\ Lys399Arg}$	rs11572080, rs10509681	CYP2C8*3	0.77 ± 0.13	144 ± 7	187
CYP2C8^{Ile264Met}	rs1058930	CYP2C8*4	0.65 ± 0.3	218 ± 11*	335
CYP2C9		CYP2C9*1A	0.96 ± 0.22	26 ± 0.6	27
CYP2C9^{Arg144Cys}	rs1799853	CYP2C9*2	0.95 ± 0.4	58 ± 4	61
CYP2C9^{Ile359Leu}	rs1057910	CYP2C9*3	1.32 ± 0.16	36 ± 4	27
CYP2C9^{Arg150His}	rs7900194	CYP2C9*8	1.14 ± 0.25	73 ± 13*	64
CYP2C9^{His251Arg}	rs2256871	CYP2C9*9	1.07 ± 0.14	116 ± 13*	108
CYP2C19		CYP2C19*1A	0.92 ± 0.18	51 ± 8	55
CYP2C19^{Ile331Val}	rs3758581	CYP2C19*1B	0.92 ± 0.13	59 ± 16	64
CYP2C19^{Glu92Asp}	rs17878459		0.70 ± 0.10	59 ± 7	84
CYP2D6		CYP2D6*1A	0.57 ± 0.03	49 ± 3	86
CYP2D6$^{Arg296Cys,\ Ser486Thr}$	rs16947, rs1135840	CYP2D6*2	0.95 ± 0.10*	23 ± 0.6*	24
CYP2D6$^{Pro34Ser,\ Ser486Thr}$	rs1065852, rs1135840	CYP2D6*10	1.04 ± 0.01*	39 ± 6	38
CYP2D6$^{Thr107Ile,\ Arg296Cys,\ Ser486Thr}$	rs28371706, rs16947, rs1135840	CYP2D6*17	0.92 ± 0.15	40 ± 2	43
CYP3A4		CYP3A4*1A	0.83 ± 0.16	39 ± 7	47
CYP3A4^{Arg162Gln}	rs4986907	CYP3A4*15A	1.04 ± 0.09	46 ± 6	44
CYP3A5		CYP3A5*1A	0.69 ± 0.18	36 ± 4	52

[a] All V_{max} values were normalized to reflect the relative CYP450 content of microsomes assayed.
* Denotes that a variant exhibited statistically significant deviations ($p < 0.05$) from the activity of its respective wildtype CYP450.

4.4.3 Impact of functional polymorphisms on exemestane reduction

Twenty-three nonsynonymous polymorphisms with MAF > 0.01 were detected using the NCBI Variation Viewer to search for common variants in hepatic CYP450s involved in xenobiotic metabolism. Four polymorphisms of interest were identified for CYP2C9. Two variants were gleaned for CYP2C19 while a single variant was reported for both CYP450s 1A2

and 3A4. No variants matching the search criteria were listed for CYP3A5. Variation Viewer search filters returned four common SNPs in CYP2C8. In the present study, two of the CYP2C8 polymorphisms were investigated as a single haplotype (CYP2C8*3). 11 nonsynonymous polymorphisms occur in CYP2D6 at > 1%. Although CYP2D6 is notoriously polymorphic, only a handful of common haplotypes are associated with clinically relevant alterations in drug metabolism [313]. For this reason, only four of the SNPs identified in Variation Viewer were included in kinetic assays as the 2D6*2, 2D6*10, and 2D6*17 haplotypes.

Although V_{max} was comparable between wildtype CYP1A2 and CYP1A2^{Ser298Arg}, the variant enzyme exhibited significantly increased affinity for EXE with K_M values of 0.74 ± 0.5 and 0.59 ± 0.2 mM, respectively. No notable differences were observed in affinity between wildtype CYP450s 2C8, 2C9, 2C19 or 3A4 and their respective variants (Table 4-4). However, CYP2D6*2 (K_M = 0.95 ± 0.10 mM) and CYP2D6*10 (K_M = 1.04 ± 0.01 mM) were both associated with decreased affinity relative to wildtype CYP2D6 (K_M = 0.57 ± 0.03 mM). The CYP2C8*2 and CYP2C8*4 polymorphisms were associated with 2.2 and 1.7-fold increases in velocity of EXE reduction compared to wildtype. CYP2C9*8 and CYP2C9*9 variants were likewise associated with increased rates of 17β-DHE formation (V_{max} = 73 ± 13 and 116 ± 13 versus 26 ± 0.6 picomoles·min^{-1}·mg^{-1} for wildtype). The V_{max} for EXE reduction by CYP2D6*2 (23 ± 0.6 picomoles·min^{-1}·mg^{-1}) is 53% lower than that of wildtype CYP2D6 (49 ± 3 picomoles·min^{-1}·mg^{-1}). V_{max} values were comparable between CYP2C19 and its variants CYP2C19^{Ile331Val} and CYP2C19^{Glu92Asp}. No significant difference in V_{max} was observed between wildtype CYP3A4 and CYP3A4^{Arg162Gln} (V_{max} = 39 ± 7 and 46 ± 6 picomoles·min^{-1}·mg^{-1}).

4.4.4 Isoform-specific CYP450 inhibition

In incubations of EXE with pooled mixed gender HLMs, inhibition of CYP3A isoforms with ketoconazole resulted in a 39% decrease in 17β-DHE production (Figure 4-4). Isoform specific inhibition of CYP450s 2C8, 2C9, and 2C19 resulted in 27%, 12%, and 22% decreases in EXE reduction, respectively. Inclusion of TCP to inhibit CYP2A6 did not impact 17β-DHE production to any appreciable extent (100.5 ± 5.7% control activity). Similar results were obtained when either thioTEPA or clomethiazole were included to chemically inhibit CYP2B6 (112.5 ± 8.3% control activity) or CYP2E1 (97.3 ± 5.3% control activity). Inhibition of CYP2D6 decreased EXE reduction by 27% while furafylline-induced CYP1A2 inhibition reduced formation of the active 17β-DHE metabolite by 19%.

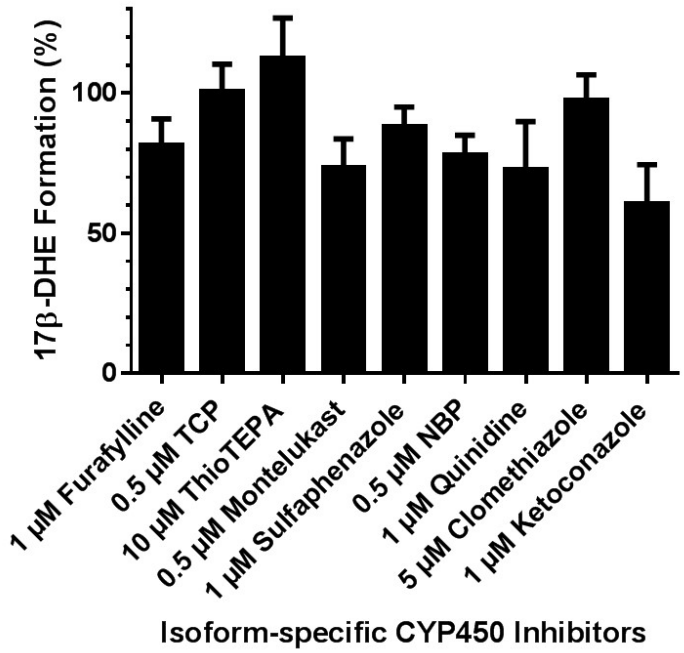

Figure 4-4: Isoform-specific chemical inhibition of CYP450-mediated EXE metabolism in pooled HLM. Data represent means of triplicate independent assays monitoring 17β-DHE formation.

4.4.5 Discussion of experimental results

Previous studies examining phase I exemestane metabolism strongly suggest that reduction of EXE at the C17 carbonyl moiety to produce 17β-DHE represents a major metabolic pathway for this commonly prescribed aromatase inhibitor [114, 269-271]. Manufacturer-supplied information regarding EXE metabolism is minimal and attributes metabolism in human liver preparations to CYP3A4 and members of the aldo-keto reductase (AKR) superfamily [108]. CYP3A4 is further identified as the principal enzyme catalyzing EXE oxidative metabolism with subsequent formation of multiple metabolites [108]. At present, a comprehensive roster of all metabolites observed in these studies has not been disclosed. A recent study has clarified the role of five cytosolic reductases in hepatic EXE metabolism *in vitro*, and multiple hepatic CYP450s may contribute to EXE metabolism as work by *Kamdem et al.* suggests [277, 282]. The present study examines the involvement of CYP450s in EXE metabolism *in vitro* and highlights the potential impact of common nonsynonymous CYP450 polymorphisms on 17β-DHE formation.

EXE reduction to form 17β-DHE was detected in incubations with HEK293-overexpressed CYP450s 1A2, 2C8, 2C9, 2C19, 2D6, 3A4 and 3A5. These results are in agreement with previous studies indicating that EXE reduction at C17 is a major metabolic pathway and confirm that CYP3A4 catalyzes the production of multiple phase I metabolites [108, 114, 269-271]. Due to overlapping substrate specificity, many currently marketed pharmaceuticals are metabolized by multiple CYP450s [308]. The data presented herein bolster previous observations regarding the capacity of multiple hepatic CYP450s to engage in *in vitro* oxidative metabolism of EXE [277, 282].

The relative contribution of each CYP450 to EXE metabolism *in vivo* is likely dependent

upon differential expression in human liver, as well as overall catalytic activity against EXE substrate (V_{max}/K_M). CYPs 3A4 and 3A5 exhibited intermediate intrinsic clearance values in the present study (47 and 52 nl·min^{-1}·mg^{-1}, respectively), but the literature indicates that CYP3A isoforms are well expressed in the liver comprising 30% of total CYP450 content and accounting for nearly 55% of xenobiotic metabolism [314]. The overall catalytic activity against EXE for CYP2D6 (86 nl·min^{-1}·mg^{-1}) was second only to that of CYP2C8 (194 nl·min^{-1}·mg^{-1}) in kinetic assays. CYP2D6 is estimated to account for 30% of drug metabolism despite constituting only 2% of total hepatic CYP450 content [314]. CYP1A2, while moderately active against EXE *in vitro* (CL_{INT} = 82 nl·min^{-1}·mg^{-1}), accounts for only 2% of overall CYP450-mediated xenobiotic metabolism in human liver [314]. CL_{INT} values for EXE ranged from 27 to 194 nl·min^{-1}·mg^{-1} for CYP450 2C isoforms, which make up 20% of total hepatic CYP450 proteins but contribute only 10% of total hepatic drug metabolism [314]. Therefore, CYP3A isoforms and CYP2D6 are potentially key enzymes in phase I EXE metabolism *in vivo* as they are well-expressed hepatically, make significant contributions to overall xenobiotic metabolism, and display activity against EXE *in vitro*.

To our knowledge, only one study to date had previously examined EXE metabolism by CYP450s. In incubations with HLMs, *Kamdem et al.* detected two primary EXE metabolites, 17-DHE and potentially 6-HME [277]. In incubations of EXE with CYP450-overexpressing HEK293 microsomes, we observed the formation of three EXE metabolites including 17α- and 17β-DHE, as well as 6-HME (Figure 4-2). Formation of several metabolites is unsurprising as CYP450s catalyze diverse reactions including carbon hydroxylation, dealkylation, and epoxidation [315]. Significantly decreased 17β-DHE formation (39% reduction) in the presence of the isoform-specific inhibitor ketoconazole suggests that CYP3As are the major hepatic

CYP450s responsible for EXE reduction in human liver microsomes (Figure 4-4). This result is in accordance with the manufacturer's limited description of the drug's phase I metabolism [108]. Isoform-specific inhibition of major hepatic CYP450s 1A2, 2C8, 2C9, 2C19, and 2D6 also decreased 17β-DHE formation by 12-27%, which suggests that multiple CYP isoforms in addition to CYP3As may be relevant to EXE metabolism. In contrast, a previously published CYP450 inhibition experiment found that treating pooled HLM with ketoconazole strongly inhibits 6-HME formation but had no significant effect on EXE reduction to 17β-DHE [277]. Furthermore, no effect on 17β-DHE formation was observed in HLM treated with any other CYP inhibitor [277]. The same *in vitro* study attributed 6-HME formation predominantly to CYP3As and CYP2B6 [277]. The present study cannot comment on the relative contribution of specific CYP450s to EXE oxidation to form 6-HME. Kinetic parameters were not collected for 6-HME formation as it is an inactive metabolite lacking the capacity to strongly inhibit aromatase (See Chapter 2). In addition, while 6-HME was possibly a major metabolite in a previous study, it was a minor metabolite formed by the seven hepatic CYP450s tested in our study [277]. Discrepancies between the two studies may reflect experimental differences. It is also feasible that significant decreases in 17β-DHE formation were undetectable in HLM subject to isoform-specific inhibition in the prior study due to redundancy in EXE clearance by multiple hepatic CYP450s. Of interest, *Kamdem et al*. found a significant correlation between 17-DHE formation and the rate of activity by CYP450s 1A2 and 4A11 in a panel of HLM [277]. CYP1A2 inhibition with furafylline decreased 17β-DHE formation by approximately 19% in pooled HLM in the present study and may indeed contribute to hepatic EXE metabolism to a previously unappreciated extent.

Unfortunately, the enzyme kinetics results presented herein are not comparable to those

of the previous *in vitro* enzyme kinetics study of EXE metabolism, which concluded that baculosome-expressed CYP1A1, CYP2A6, and CYP4A11 are most active in 17-DHE production [277]. In lieu of using a commercially available baculosome system, HEK293 cell lines constitutively overexpressing CYP450s were created for kinetics assays, because HEK293 are devoid of many drug metabolizing enzymes, including the CYP450s. In addition, significant reduction of EXE to 17β-DHE was observed in negative control baculosomes (see Figure 4-2). These results indicate that endogenous CYPs or active reductases are present in baculosome preparations, which is likely to confound the interpretation of kinetic assays. Background reduction in HEK293 microsomal fractions was undetectable by UPLC/MS/MS (see Figure 4-2). While overexpressed CYP2A6 was not directly tested for activity against EXE in the present study, the involvement of CYP2A6 is questionable as it has been shown to preferentially metabolize small substrates [316]. Furthermore, its inhibition did not appreciably decrease 17β-DHE generated by HLM incubated with EXE (100.5 ± 5.7% control activity). CYP1A1 expression, in turn, is low in human liver diminishing the likelihood that it is a key participant in phase I EXE metabolism [317].

Xenobiotic-metabolizing CYP450s are highly polymorphic [308]. Multiple nonsynonymous variants often exist within a single isoform at varying levels of penetrance in the human population. CYP2D6, for instance, can harbor > 100 distinct polymorphisms several of which are associated with altered drug metabolism and increased risk for life-threatening adverse reactions [308, 318-321]. In our enzyme kinetics assays, three variant CYP450s exhibited altered affinity for EXE while five deviated appreciably from their wildtype counterparts with respect to maximum velocity of EXE reduction.

Maximum velocity of EXE reduction to form 17β-DHE is similar between CYP1A2 and

CYP1A2^{Ser298Arg} (see Table 4-4). However, CYP1A2^{Ser298Arg} had approximately 25% higher affinity, which contributed to a 66% increase in intrinsic clearance of EXE compared to the wildtype isoform (CL_{INT} = 136 versus 82 nl·min^{-1}·mg^{-1}). Despite its high incidence in African populations (MAF = 0.0893), a three dimensional structure examining conformational changes in CYP1A2 arising from arginine substitution is currently unavailable [322, 323]. It is known, however, that amino acid residue 298 is located within a loop distal to the CYP1A2 active site [323]. *In silico* analyses by *Watanabe et al*. predict that when the adjacent glycine at residue 299 is mutated to serine, flexibility increases near Val487 in the C terminal loop [323]. While this particular mutation does not impact overall CYP1A2 enzymatic activity as assessed by 7-ethoxyresorufin O-deethylation, it is indicative that polymorphisms can alter structural flexibility in loop regions [323, 324]. Structural flexibility, in turn, may strongly impact ligand-binding induced conformational changes, substrate recognition, and overall CYP450 catalytic activity as several studies suggest [325-328]. Similar structural analyses are needed to determine if CYP1A2^{Ser298Arg} exhibits deviant flexibility, possibly underlying differences observed in kinetic parameters against EXE.

CYP2C8^{Ile269Phe} (*2), CYP2C8$^{Arg139Lys,\ Lys399Arg}$ (*3), and CYP2C8^{Ile264Met} (*4) are comparable to wildtype CYP2C8 in affinity for EXE substrate *in vitro*. *Kaspera et al.* likewise found only minor differences in apparent K_M values between recombinant wildtype CYP2C8 and its *2, *3, and *4 variants while monitoring oxidation of cerivastatin to form its O-desmethyl- (M-1) and 6-hydroxyl- (M-23) cerivastatin metabolites [329]. Although *E. coli*-expressed CYP2C8*2 yielded individual V_{max} values similar to wildtype CYP2C8 for M-1 and M-23 formation, a 53% increase in the sum of cerivastatin metabolite clearance was noted [329]. In the present study, CYP2C8*2 produced 17β-DHE 2.2-fold faster than wildtype contributing to a

68% increase in overall EXE clearance. CYP2C8*2 carriers reported abdominal pain more frequently than wildtype homozygotes in a small study of West African malaria patients taking amodiaquine, suggesting possible clinical relevance for the polymorphism [330]. The CYP2C8*3 genotype is likewise of considerable interest and has been examined extensively with regards to NSAIDS, antidiabetic agents, and HMG-CoA reductase inhibitors [331-336]. In clinical studies, CYP2C8*3 is associated with increased drug metabolism for several substrates as evidenced by significantly decreased plasma concentrations of rosiglitazone, pioglitazone, and repaglinide [334, 335, 337-339]. In contrast, decreased ibuprofen metabolism has also been noted, implying that the kinetic properties of CYP2C8*3 may be substrate-dependent [331, 332]. With regard to EXE, our *in vitro* results indicate that the CYP2C8*3 polymorphism doesn't alter the drug's overall intrinsic clearance. CYP2C8*4, on the other hand, was associated with a 1.7-fold increase in EXE clearance due to elevated V_{max} relative to wildtype (218 ± 11 versus 128 ± 4 $nl \cdot min^{-1} \cdot mg^{-1}$). *Kaspera et al*. estimated that recombinant CYP2C8*4 increased the combined clearance of the M-1 and M-23 cerivastatin metabolites by approximately 2.5-fold compared to wildtype [329]. Though CYP2C8*4 has demonstrated increased catalytic activity against both cerivastatin and EXE *in vitro*, human livers with the *4 genotype express lower levels of CYP2C8 protein [329, 340]. Differences in hepatic expression of variant CYPs may negate or exacerbate the overall metabolic effect of deviant catalytic activity observed in the present study. Thus, additional *in vivo* studies are needed to gauge what impact, if any, CYP2C8 polymorphisms have on clinical outcomes in postmenopausal breast cancer patients taking EXE.

Kinetic parameters for EXE metabolism by $CYP2C9^{Arg144Cys}$ (*2) and $CYP2C9^{Ile359Leu}$ (*3) were similar to those of wildtype CYP2C9. The CYP2C9*2 and *3 polymorphisms are relatively common (MAF > 0.01) in South Asian, European, and Hispanic populations (see

Table 4.1) and are associated with impaired warfarin metabolism [341, 342]. Although the *2 variant is associated with a poor metabolizer phenotype for certain substrates, its impact on catalytic activity is not entirely clear [341-345]. Several previous studies of the CYP2C9*2 variant are conflicting with fluvastatin and celecoxib metabolism unaffected while losartan and phenytoin clearance significantly decreased relative to wildtype [336, 346-348]. Impaired warfarin metabolism is likewise associated with CYP2C9*3 necessitating the need for genotype-based dose reductions in clinical settings [341, 342]. Work by *Wei et al.* suggests that CYP2C9*2 and *3 exhibit altered metabolism due to decreased coupling efficiency in the P450 catalytic cycle [349]. Another study posits that the substrate binding pocket of CYP2C9*3 is enlarged relative to wildtype, resulting in reduced enzymatic activity against warfarin [350]. $CYP2C9^{Arg150His}$ (*8) and $CYP2C9^{His251Arg}$ (*9) polymorphic protein reduced EXE to 17β-DHE 2.8- and 4.5-fold faster than wildtype CYP2C9, respectively. The CYP2C9*8 allele also increased clearance of the antidiabetic tolbutamide *in vitro* [351]. *In vivo*, the CYP2C9*8 allele is associated with decreased phenytoin metabolism due to strong linkage disequilibrium with SNPs in the gene promoter that downregulate expression [352, 353]. *In silico* analyses by *Matimba et al*. predicted reduced activity of CYP2C9*9 compared to wildtype [354]. However, a significant correlation between the CYP2C9*9 allele and phenytoin metabolism wasn't detected in African epilepsy patients [354]. Published discrepancies in variant CYP2C9 activity are common and likely arise from variations in experimental procedures between laboratories [355].

CYP2D6 is believed to be the most polymorphic of the major drug-metabolizing hepatic CYP450s [308]. A 72% decrease in EXE clearance was observed for $CYP2D6^{Arg296Cys,\ Ser486Thr}$ (*2) relative to wildtype CYP2D6 due to significant decreases in affinity and 17β-DHE

formation rate. *Sakuyama et al.* reported a similar 2-fold decrease in substrate affinity in transiently expressed CYP2D6*2 while monitoring bufuralol 1'-hydroxylation [356]. Although analysis of the crystal structure of CYP2D6 suggests that residue 296 may be involved in substrate recognition, a study of CYP2D6*2A in Europeans found no association with altered drug metabolism [126, 357]. In the present study, HEK293-expressed CYP2D6 $^{Pro34Ser, Ser486Thr}$ (*10) increased the K_M value for EXE substrate by 82% causing a 56% decrease in clearance compared to CYP2D6*1. CYP2D6*10 is highly prevalent in Asians and has previously been associated with decreased catalytic activity *in vitro* [356, 358-362]. *Shen et al*. estimated that CYP2D6*10 protein decreases catalytic activity in a substrate-dependent manner with intrinsic clearance of probe substrates reduced to 4-28% that of wildtype protein [362]. Diminished catalytic activity by the *10 variant is attributed to increased enzyme instability as a result of serine substitution in a proline-rich region near the N-terminus [356, 363]. CYP2D6 $^{Thr107Ile, Arg296Cys, Ser486Thr}$ (*17) is common in individuals of African heritage and is likewise considered a reduced function allele [313, 364-367]. CYP2D6*17 exhibits considerable variability in catalytic activity against various substrates [313]. Studies using recombinant CYP2D6*17 protein have reported increased metabolism of certain substrates, such as haloperidol, but decreased metabolism of others, including codeine [368, 369]. The Thr107Ile substitution (rs28371706) is believed to alter a highly conserved region of CYP2D6 involved in substrate recognition, perhaps explaining the substrate-dependent effects previously reported [370-372]. It is interesting to note that recombinant CYP2D7*17 protein yielded a 61% decrease in EXE affinity relative to wildtype, although this observation did not reach statistical significance.

Kinetic parameters measuring substrate affinity (K_M) and production of the major active metabolite 17β-DHE (V_{max}) indicate that EXE metabolism by common allelic variants of

CYP2C19 and CYP3A4 is comparable to that of their respective wildtype CYP450s. The neutral effect of the CYP2C19^{Ile331Val} (*1B) polymorphism on EXE reduction confirms prior observations of equivalent catalytic activity for the CYP2C19*1A and *1B alleles [373]. Although the CYP2C19^{Glu92Asp} SNP (rs17878459) didn't directly impact 17β-DHE formation, it cosegregates with approximately 20% of CYP2C19*2 poor metabolizing alleles in Caucasians [374]. Found predominantly in Africans, the CYP3A4^{Arg162Gln} (*15A) polymorphism doesn't appreciably impact EXE metabolism. However, kinetic studies of the variant enzyme with additional substrates are needed to confirm its overall effect on CYP3A4 activity.

The present *in vitro* study augments existing pharmaceutical knowledge by examining the role of hepatic CYP450s in the metabolism of EXE, a widely used endocrine therapy for hormone responsive breast cancer. Qualitative enzymatic incubations with EXE confirm that multiple hepatic monoxygenases from CYP450 families 1, 2, and 3 catalyze the production of 6-HME, 17α-DHE, as well as the active metabolite 17β-DHE. Earlier studies suggested that 17β-DHE may partially determine overall drug exposure by acting as an androgen agonist, contributing to estrogen blockade through aromatase inhibition, and by serving as a gateway to phase II conjugation and excretion [115, 272]. Thus, any genetic factors influencing 17β-DHE formation or clearance may contribute to inter-individual variation in the overall therapeutic efficacy of EXE by altering a major metabolic pathway. This possibility is bolstered by the observation that three of the variant CYP450s included in this study had altered affinity for EXE substrate leading to differential 17β-DHE production while five variants had deviant catalytic rates of EXE reduction. To our knowledge, this is the first study to report the impact of common nonsynonymous polymorphisms in CYP450s on EXE reduction to its 17β-DHE metabolite. A previous *in vitro* study demonstrated the capacity of genetic variation to alter EXE metabolism

by the cytosolic ketosteroid reductases CBR1 and AKR1C1-4 [282]. Although differences in experimental procedures preclude a direct comparison of kinetic parameters between the two studies, it appears that both cytosolic and microsomal phase I enzymes contribute to *in vitro* EXE metabolism. An important limitation of the overexpression model used in this study was the inability to assess the metabolic impact of copy number variations or polymorphisms in noncoding promoter regions. Additional studies are needed to determine if multiple hepatic CYP450s contribute to overall EXE metabolism *in vivo* and whether common genetic variants in phase I enzymes are associated with differential metabolite production or clinical outcomes in EXE-treated breast cancer patients.

CHAPTER FIVE

Conclusions and future directions

5.1 SUMMARY AND CONCLUSIONS

The studies described herein address significant gaps in the knowledge of the phase I metabolism of the anti-cancer drug, EXE. Initial *in vitro* experiments identified putative phase I EXE metabolites capable of suppressing estrogen synthesis through aromatase inhibition, a property that may contribute to the drug's overall efficacy or toxicity in postmenopausal breast cancer patients (Chapter 2). A novel, highly sensitive anti-aromatase activity assay was used to directly quantify estrone formation in incubations of EXE and ten potential phase I EXE metabolites with HEK293-overexpressed wildtype aromatase. The extreme potency of EXE in inhibiting aromatase (IC_{50} = 0.92 ± 0.17 μM) was experimentally confirmed via anti-aromatase activity assay. All of the EXE analogues assayed were less potent than the parent drug, including the major metabolite, 17β-DHE (IC_{50} = 4.3 ± 0.56 μM). The diminished potency observed for 17β-DHE relative to EXE agrees with prior studies [268, 309]. C17 reduction is a major known phase I EXE metabolic pathway so moderate aromatase inhibition by the 17β-DHE metabolite could feasibly contribute to *in vivo* clinical outcomes [114, 269-271]. Additional anti-aromatase assays were performed for two nonsynonymous polymorphic aromatase allozymes to determine if common aromatase variants are associated with altered EXE potency. The results suggest that common variant aromatase alleles are unlikely to account for inter-individual differences in 17β-DHE formation.

Another major objective completed throughout the course of these studies was to identify hepatic phase I EXE metabolites. Qualitative incubations revealed that 17β-DHE is the major phase I metabolite produced by EXE reduction in human liver cytosol although minor amounts of its inactive stereoisomer, 17α-DHE (IC_{50} > 100 μM) were also formed (Chapter 3). 17α-DHE was not detected in incubations of EXE with pooled human liver microsomes (Chapter 2).

However, its stereoisomer, 17β-DHE, was detected, as well as 6-HME (IC_{50} = 61 ± 20 μM), 6α/β-hydroxy-6α/β-hydroxy-methylandrosta-1,4-diene-3,17-dione (IC_{50} > 100 μM), and 6α/β,17β-dihydroxy-6α/β-hydroxymethyl-androsta-1,4-diene-3-one (IC_{50} > 100 μM). In similar incubations with EXE substrate, the purified ketosteroid reductases AKR1C1, AKR1C2, AKR1C3, AKR1C4, and CBR1 catalyzed 17β-DHE formation while AKR1C4 and CBR1 also reduced EXE to 17α-DHE (Chapter 3). When incubated with EXE, microsomes from HEK293 cell lines constitutively overexpressing CYP450s 1A2, 2C8, 2C9, 2C19, 2D6, 3A4, and 3A5 predominantly produced 17β-DHE with formation of minor amounts of 17α-DHE and 6-HME metabolites, as well (Chapter 4). Overall, it appears that 17β-DHE is the only major hepatic phase I EXE metabolite with moderate-to-potent anti-aromatase activity (IC50 ≤ 10 μM) that is produced *in vitro* by human liver fractions, AKR1Cs, CBR1 or xenobiotic-metabolizing CYP450s.

This body of work supplements the scant literature regarding EXE metabolism by identifying specific hepatic enzymes that catalyze the reduction of EXE to 17β-DHE and by reporting the effect of common nonsynonymous polymorphisms on the catalytic activity of EXE-metabolizing enzymes. Prescribing information for EXE tablets offers little data regarding the enzymes responsible for its phase I metabolism [108]. It discloses only that aldo-keto reductases and CYP3A4 are involved [108]. In hopes of clarifying this statement, *in vitro* enzyme kinetic studies were performed using purified hepatic cytosolic reductases. CBR1 and four members of the AKR1C subfamily were found to catalyze the formation of the active metabolite, 17β-DHE (Chapter 3). In keeping with the results of a previous study, *in vitro* assays monitoring 17β-DHE formation by HEK293-overexpressed CYP450s indicate that EXE metabolism may be more complex than described in the drug prescribing information [277]. Although CYP3A4

extensively metabolized EXE in these assays, 17β-DHE formation was also catalyzed by six additional hepatically-expressed CYP450s, including 1A2, 2C8, 2C9, 2C19, 2D6, and 3A5 (Chapter 4). Isoform-specific CYP450 inhibition experiments in human liver microsomes confirmed that CYP3A4 is not exclusively responsible for the reduction of EXE to 17β-DHE.

To assess the impact of naturally-occurring genetic variants in drug-metabolizing enzymes on EXE metabolism, enzyme kinetic studies were also completed for common nonsynonymous polymorphisms found in the AKR1Cs, CBR1, and CYP450s 1A2, 2C8, 2C9, 2C19, 2D6, 3A4, and 3A5 (Chapters 3 & 4). In comparison to their respective wildtype enzymes, variant forms of AKR1C3, AKR1C4, CYP1A2, CYP2C8, CYP2C9, and CYP2D6 were associated with significant deviations in 17β-DHE production *in vitro*. These pharmacogenetic studies complement a previous investigation of phase II EXE metabolism by *Sun et al*, which correlated a variant allele in the drug-metabolizing enzyme, UGT2B17, with altered catalytic activity [115]. Significantly lower rates of 17β-DHE glucuronidation have also been reported in human liver microsomes carrying the UGT2B17 deletion allele relative to homozygotes with functional UGT2B17 [115].

In summary, this body of work describes the identification of active EXE metabolites, as well as hepatic enzymes that may participate in *in vivo* phase I EXE metabolism through the production of metabolites with anti-aromatase activity, such as 17β-DHE. Altered catalytic activity in reducing EXE to 17β-DHE is reported for multiple variant alleles of CYP450 xenobiotic-metabolizing enzymes and cytosolic ketosteroid reductases. At present, the clinical significance of these polymorphisms is poorly understood. These studies confirmed that 17β-DHE is an abundant phase I EXE metabolite with moderate anti-aromatase activity and suggest that significant genotype-phenotype interactions may exist for hepatic cytosolic ketosteroid

reductases and CYP450s active in phase I EXE metabolism. In the literature, it has previously been suggested that genetic factors affecting 17β-DHE formation could potentially modify the extent of estrogen deprivation and thus, cause differential clinical outcomes in postmenopausal women taking EXE for breast cancer treatment or prevention [282]. Further research is needed to assess whether EXE efficacy or toxicity is correlated with genotypes for phase I drug-metabolizing enzymes included in these studies.

5.2 FUTURE DIRECTIONS

The successful identification of xenobiotic-metabolizing enzymes likely to participate in phase I EXE metabolism has laid the groundwork for targeted future studies of EXE pharmacogenetics. The *in vitro* kinetic results reported in Chapters 3 & 4 suggest that genetic variation in hepatic ketosteroid reductases and CYP450s may play a profound but currently unrecognized impact on clinical response to EXE by altering production of the active metabolite, 17β-DHE. Thus, future studies should be performed to identify any *in vivo* genotype-phenotype correlations that are predictive of drug response and can potentially be used to inform the selection of EXE as an endocrine hormonal therapy in postmenopausal women. One such study will utilize clinical samples from MAP.3, a large clinical trial investigating EXE for breast cancer chemoprevention, in hopes of elucidating any genotypic differences in drug-metabolizing enzymes that contribute to differential response to EXE between individuals [133]. Blood samples from high-risk postmenopausal women taking 25 mg/day EXE while enrolled in MAP.3 will be used to genotype participants for enzymes implicated in EXE metabolism, as well as quantitate serum metabolites, which may be significantly correlated with patient quality of life scores, drug efficacy or the incidence of serious adverse events.

REFERENCES

1. Nelson MR, Johnson T, Warren L, Hughes AR, Chissoe SL, Xu CF, et al. The genetics of drug efficacy: opportunities and challenges. Nat Rev Genet. 2016;17(4):197-206.

2. Ulrich RG. Idiosyncratic toxicity: a convergence of risk factors. Annu Rev Med. 2007;58:17-34.

3. Maronas O, Latorre A, Dopazo J, Pirmohamed M, Rodriguez-Antona C, Siest G, et al. Progress in pharmacogenetics: consortiums and new strategies. Drug Metab Pers Ther. 2016;31(1):17-23.

4. FDA Administration. Guideline for Industry Clinical Safety Data Management: Definitions and Standards for Expedited Reporting. In: Services USDoHaH, editor. 1995.

5. Iasella CJ, Johnson HJ, Dunn MA. Adverse Drug Reactions: Type A (Intrinsic) or Type B (Idiosyncratic). Clin Liver Dis. 2017;21(1):73-87.

6. Pirmohamed M, James S, Meakin S, Green C, Scott AK, Walley TJ, et al. Adverse drug reactions as cause of admission to hospital: prospective analysis of 18 820 patients. BMJ. 2004;329(7456):15-9.

7. Winterstein AG, Sauer BC, Hepler CD, Poole C. Preventable drug-related hospital admissions. Ann Pharmacother. 2002;36(7-8):1238-48.

8. Bouvy JC, De Bruin ML, Koopmanschap MA. Epidemiology of adverse drug reactions in Europe: a review of recent observational studies. Drug Saf. 2015;38(5):437-53.

9. Goettler M, Schneeweiss S, Hasford J. Adverse drug reaction monitoring--cost and benefit considerations. Part II: cost and preventability of adverse drug reactions leading to hospital admission. Pharmacoepidemiol Drug Saf. 1997;6 Suppl 3:S79-90.

10. Bohm R, Cascorbi I. Pharmacogenetics and Predictive Testing of Drug Hypersensitivity Reactions. Front Pharmacol. 2016;7:396.

11. Sammons HM, Choonara I. Learning Lessons from Adverse Drug Reactions in Children. Children (Basel). 2016;3(1).

12. Alagoz O, Durham D, Kasirajan K. Cost-effectiveness of one-time genetic testing to minimize lifetime adverse drug reactions. Pharmacogenomics J. 2016;16(2):129-36.

13. Lazarou J, Pomeranz BH, Corey PN. Incidence of adverse drug reactions in hospitalized patients: a meta-analysis of prospective studies. JAMA. 1998;279(15):1200-5.

14. Van Driest SL, Shi Y, Bowton EA, Schildcrout JS, Peterson JF, Pulley J, et al. Clinically actionable genotypes among 10,000 patients with preemptive pharmacogenomic testing. Clin Pharmacol Ther. 2014;95(4):423-31.

15. Masys DR. Effects of current and future information technologies on the health care workforce. Health Aff (Millwood). 2002;21(5):33-41.

16. Stead WW, Searle JR, Fessler HE, Smith JW, Shortliffe EH. Biomedical informatics: changing what physicians need to know and how they learn. Acad Med. 2011;86(4):429-34.

17. Green ED, Guyer MS, National Human Genome Research I. Charting a course for genomic medicine from base pairs to bedside. Nature. 2011;470(7333):204-13.

18. Bond CR, C.L. Adverse drug reactions in United States hospitals. Pharmacotherapy. 2006;26:601-108.

19. Spear BB, Heath-Chiozzi M, Huff J. Clinical application of pharmacogenetics. Trends Mol Med. 2001;7(5):201-4.

20. Schildcrout JS, Denny JC, Bowton E, Gregg W, Pulley JM, Basford MA, et al. Optimizing drug outcomes through pharmacogenetics: a case for preemptive genotyping. Clin Pharmacol Ther. 2012;92(2):235-42.

21. Hertz DL, Rae JM. Pharmacogenetic Predictors of Response. Adv Exp Med Biol. 2016;882:191-215.

22. International Warfarin Pharmacogenetics C, Klein TE, Altman RB, Eriksson N, Gage BF, Kimmel SE, et al. Estimation of the warfarin dose with clinical and pharmacogenetic data. N Engl J Med. 2009;360(8):753-64.

23. Hall-Flavin DK, Winner JG, Allen JD, Carhart JM, Proctor B, Snyder KA, et al. Utility of integrated pharmacogenomic testing to support the treatment of major depressive disorder in a psychiatric outpatient setting. Pharmacogenet Genomics. 2013;23(10):535-48.

24. Kapoor R, Tan-Koi WC, Teo YY. Role of pharmacogenetics in public health and clinical health care: a SWOT analysis. Eur J Hum Genet. 2016;24(12):1651-7.

25. Pulley JM, Denny JC, Peterson JF, Bernard GR, Vnencak-Jones CL, Ramirez AH, et al. Operational implementation of prospective genotyping for personalized medicine: the design of the Vanderbilt PREDICT project. Clin Pharmacol Ther. 2012;92(1):87-95.

26. Collins SL, Carr DF, Pirmohamed M. Advances in the Pharmacogenomics of Adverse Drug Reactions. Drug Saf. 2016;39(1):15-27.

27. O'Donnell PH, Danahey K, Ratain MJ. The Outlier in All of Us: Why Implementing Pharmacogenomics Could Matter for Everyone. Clin Pharmacol Ther. 2016;99(4):401-4.

28. Shotelersuk V, Limwongse C, Mahasirimongkol S. Genetics and genomics in Thailand: challenges and opportunities. Mol Genet Genomic Med. 2014;2(3):210-6.

29. Rabbani B, Nakaoka H, Akhondzadeh S, Tekin M, Mahdieh N. Next generation sequencing: implications in personalized medicine and pharmacogenomics. Mol Biosyst. 2016;12(6):1818-

30.

30. GWAS Catalog [Internet]. [cited January 24th, 2017]. Available from: https://www.ebi.ac.uk/gwas/.

31. Whirl-Carrillo M, McDonagh EM, Hebert JM, Gong L, Sangkuhl K, Thorn CF, et al. Pharmacogenomics knowledge for personalized medicine. Clin Pharmacol Ther. 2012;92(4):414-7.

32. Tuckson RVA, S.M.; Berry, C.E.; et al. Realizing the promise of pharmacogenomics: opportunities and challenges. Biotechnol Rep. 2007;26(3):261-91.

33. Valdes R, Jr., Yin DT. Fundamentals of Pharmacogenetics in Personalized, Precision Medicine. Clin Lab Med. 2016;36(3):447-59.

34. Fact Sheet: President Obama's Precision Medicine Initiative [press release]. January 30, 2015 2015.

35. Swen JJ, Nijenhuis M, de Boer A, Grandia L, Maitland-van der Zee AH, Mulder H, et al. Pharmacogenetics: from bench to byte--an update of guidelines. Clin Pharmacol Ther. 2011;89(5):662-73.

36. Relling MV, McDonagh EM, Chang T, Caudle KE, McLeod HL, Haidar CE, et al. Clinical Pharmacogenetics Implementation Consortium (CPIC) guidelines for rasburicase therapy in the context of G6PD deficiency genotype. Clin Pharmacol Ther. 2014;96(2):169-74.

37. Caudle KE, Klein TE, Hoffman JM, Muller DJ, Whirl-Carrillo M, Gong L, et al. Incorporation of pharmacogenomics into routine clinical practice: the Clinical Pharmacogenetics Implementation Consortium (CPIC) guideline development process. Curr Drug Metab. 2014;15(2):209-17.

38. Relling MV, Klein TE. CPIC: Clinical Pharmacogenetics Implementation Consortium of the Pharmacogenomics Research Network. Clin Pharmacol Ther. 2011;89(3):464-7.

39. Conley A, Hinshelwood M. Mammalian aromatases. Reproduction. 2001;121(5):685-95.

40. Schindler AE, Ebert A, Friedrich E. Conversion of androstenedione to estrone by human tissue. J Clin Endocrinol Metab. 1972;35(4):627-30.

41. Sasano H, Takashashi K, Satoh F, Nagura H, Harada N. Aromatase in the human central nervous system. Clin Endocrinol (Oxf). 1998;48(3):325-9.

42. Perez-Sepulveda A, Monteiro LJ, Dobierzewska A, Espana-Perrot PP, Venegas-Araneda P, Guzman-Rojas AM, et al. Placental Aromatase Is Deficient in Placental Ischemia and Preeclampsia. PLoS One. 2015;10(10):e0139682.

43. Biegon A, Alexoff DL, Kim SW, Logan J, Pareto D, Schlyer D, et al. Aromatase imaging with [N-methyl-11C]vorozole PET in healthy men and women. J Nucl Med. 2015;56(4):580-5.

44. Lambard S, Silandre D, Delalande C, Denis-Galeraud I, Bourguiba S, Carreau S. Aromatase in testis: expression and role in male reproduction. J Steroid Biochem Mol Biol. 2005;95(1-5):63-9.

45. Bulun SE, Sebastian S, Takayama K, Suzuki T, Sasano H, Shozu M. The human CYP19 (aromatase P450) gene: update on physiologic roles and genomic organization of promoters. J Steroid Biochem Mol Biol. 2003;86(3-5):219-24.

46. Means GD, Mahendroo MS, Corbin CJ, Mathis JM, Powell FE, Mendelson CR, et al. Structural analysis of the gene encoding human aromatase cytochrome P-450, the enzyme responsible for estrogen biosynthesis. J Biol Chem. 1989;264(32):19385-91.

47. Harada N, Yamada K, Saito K, Kibe N, Dohmae S, Takagi Y. Structural characterization of the human estrogen synthetase (aromatase) gene. Biochem Biophys Res Commun. 1990;166(1):365-72.

48. Toda K, Terashima M, Kawamoto T, Sumimoto H, Yokoyama Y, Kuribayashi I, et al. Structural and functional characterization of human aromatase P-450 gene. Eur J Biochem. 1990;193(2):559-65.

49. Means GD, Kilgore MW, Mahendroo MS, Mendelson CR, Simpson ER. Tissue-specific promoters regulate aromatase cytochrome P450 gene expression in human ovary and fetal tissues. Mol Endocrinol. 1991;5(12):2005-13.

50. Toda K, Shizuta Y. Molecular cloning of a cDNA showing alternative splicing of the 5'-untranslated sequence of mRNA for human aromatase P-450. Eur J Biochem. 1993;213(1):383-9.

51. Mahendroo MS, Means GD, Mendelson CR, Simpson ER. Tissue-specific expression of human P-450AROM. The promoter responsible for expression in adipose tissue is different from that utilized in placenta. J Biol Chem. 1991;266(17):11276-81.

52. Bulun SE, Takayama K, Suzuki T, Sasano H, Yilmaz B, Sebastian S. Organization of the human aromatase p450 (CYP19) gene. Semin Reprod Med. 2004;22(1):5-9.

53. NCBI Reference Sequence Database [Internet]. [cited January 21st, 2017].

54. Shimozawa O, Sakaguchi M, Ogawa H, Harada N, Mihara K, Omura T. Core glycosylation of cytochrome P-450(arom). Evidence for localization of N terminus of microsomal cytochrome P-450 in the lumen. J Biol Chem. 1993;268(28):21399-402.

55. Sethumadhavan K, Bellino FL, Thotakura NR. Estrogen synthetase (aromatase). The cytochrome P-450 component of the human placental enzyme is a glycoprotein. Mol Cell Endocrinol. 1991;78(1-2):25-32.

56. Lamb DC, Waterman MR. Unusual properties of the cytochrome P450 superfamily. Philos Trans R Soc Lond B Biol Sci. 2013;368(1612):20120434.

57. Sakaguchi M, Mihara K, Sato R. Signal recognition particle is required for co-translational insertion of cytochrome P-450 into microsomal membranes. Proc Natl Acad Sci U S A. 1984;81(11):3361-4.

58. Meyer AS. Conversion of 19-hydroxy-delta 4-androstene-3,17-dione to estrone by endocrine tissue. Biochim Biophys Acta. 1955;17(3):441-2.

59. Meyer AS, Hayano M, Lindberg MC, Gut M, Rodgers OG. The conversion of delta 4-androstene-3,17-dione-4-C14 and dehydroepiandrosterone by bovine adrenal homogenate preparations. Acta Endocrinol (Copenh). 1955;18(2):148-68.

60. Ryan KJ. Biological aromatization of steroids. J Biol Chem. 1959;234(2):268-72.

61. Baggett B, Dorfman RI, Engel LL, Savard K. The conversion of testosterone-3-C14 to C14-estradiol-17beta by human ovarian tissue. J Biol Chem. 1956;221(2):931-41.

62. Santen RJ, Brodie H, Simpson ER, Siiteri PK, Brodie A. History of aromatase: saga of an important biological mediator and therapeutic target. Endocr Rev. 2009;30(4):343-75.

63. Akhtar M, Calder MR, Corina DL, Wright JN. Mechanistic studies on C-19 demethylation in oestrogen biosynthesis. Biochem J. 1982;201(3):569-80.

64. Sgrignani J, Iannuzzi M, Magistrato A. Role of Water in the Puzzling Mechanism of the Final Aromatization Step Promoted by the Human Aromatase Enzyme. Insights from QM/MM MD Simulations. J Chem Inf Model. 2015;55(10):2218-26.

65. Akhtar M, Wright JN, Lee-Robichaud P. A review of mechanistic studies on aromatase (CYP19) and 17alpha-hydroxylase-17,20-lyase (CYP17). J Steroid Biochem Mol Biol. 2011;125(1-2):2-12.

66. Sen K, Hackett JC. Coupled electron transfer and proton hopping in the final step of CYP19-catalyzed androgen aromatization. Biochemistry. 2012;51(14):3039-49.

67. Manna PR, Molehin D, Ahmed AU. Dysregulation of Aromatase in Breast, Endometrial, and Ovarian Cancers: An Overview of Therapeutic Strategies. Prog Mol Biol Transl Sci. 2016;144:487-537.

68. Labrie F, Martel C, Balser J. Wide distribution of the serum dehydroepiandrosterone and sex steroid levels in postmenopausal women: role of the ovary? Menopause. 2011;18(1):30-43.

69. Wang S, Paris F, Sultan CS, Song RX, Demers LM, Sundaram B, et al. Recombinant cell ultrasensitive bioassay for measurement of estrogens in postmenopausal women. J Clin Endocrinol Metab. 2005;90(3):1407-13.

70. Labrie F. All sex steroids are made intracellularly in peripheral tissues by the mechanisms of intracrinology after menopause. J Steroid Biochem Mol Biol. 2015;145:133-8.

71. Tulandi T, Martin J, Al-Fadhli R, Kabli N, Forman R, Hitkari J, et al. Congenital

malformations among 911 newborns conceived after infertility treatment with letrozole or clomiphene citrate. Fertil Steril. 2006;85(6):1761-5.

72. Soysal S, Soysal ME, Ozer S, Gul N, Gezgin T. The effects of post-surgical administration of goserelin plus anastrozole compared to goserelin alone in patients with severe endometriosis: a prospective randomized trial. Hum Reprod. 2004;19(1):160-7.

73. Coombes RC, Hall E, Gibson LJ, Paridaens R, Jassem J, Delozier T, et al. A randomized trial of exemestane after two to three years of tamoxifen therapy in postmenopausal women with primary breast cancer. N Engl J Med. 2004;350(11):1081-92.

74. Riepe FG, Baus I, Wiest S, Krone N, Sippell WG, Partsch CJ. Treatment of pubertal gynecomastia with the specific aromatase inhibitor anastrozole. Horm Res. 2004;62(3):113-8.

75. Lonning PE. The potency and clinical efficacy of aromatase inhibitors across the breast cancer continuum. Ann Oncol. 2011;22(3):503-14.

76. Goodman & Gilman's Manual of Pharmacology and Therapeutics. Brunton LL, Parker KL, Blumenthal DK, Buxton ILO, editors: The McGraw Hill Companies, Inc.; 2008.

77. Simpson ER, Clyne C, Rubin G, Boon WC, Robertson K, Britt K, et al. Aromatase--a brief overview. Annu Rev Physiol. 2002;64:93-127.

78. Bulun SE, Lin Z, Zhao H, Lu M, Amin S, Reierstad S, et al. Regulation of aromatase expression in breast cancer tissue. Ann N Y Acad Sci. 2009;1155:121-31.

79. Bulun SE, Lin Z, Imir G, Amin S, Demura M, Yilmaz B, et al. Regulation of aromatase expression in estrogen-responsive breast and uterine disease: from bench to treatment. Pharmacol Rev. 2005;57(3):359-83.

80. Zhao H, Zhou L, Shangguan AJ, Bulun SE. Aromatase expression and regulation in breast and endometrial cancer. J Mol Endocrinol. 2016;57(1):R19-33.

81. Xu S, Linher-Melville K, Yang BB, Wu D, Li J. Micro-RNA378 (miR-378) regulates ovarian estradiol production by targeting aromatase. Endocrinology. 2011;152(10):3941-51.

82. Hayashi T, Harada N. Post-translational dual regulation of cytochrome P450 aromatase at the catalytic and protein levels by phosphorylation/dephosphorylation. FEBS J. 2014;281(21):4830-40.

83. Charlier TD, Harada N, Balthazart J, Cornil CA. Human and quail aromatase activity is rapidly and reversibly inhibited by phosphorylating conditions. Endocrinology. 2011;152(11):4199-210.

84. Martin LL, Holien JK, Mizrachi D, Corbin CJ, Conley AJ, Parker MW, et al. Evolutionary comparisons predict that dimerization of human cytochrome P450 aromatase increases its enzymatic activity and efficiency. J Steroid Biochem Mol Biol. 2015;154:294-301.

85. Praporski S, Ng SM, Nguyen AD, Corbin CJ, Mechler A, Zheng J, et al. Organization of cytochrome P450 enzymes involved in sex steroid synthesis: PROTEIN-PROTEIN INTERACTIONS IN LIPID MEMBRANES. J Biol Chem. 2009;284(48):33224-32.

86. Agarwal VR, Bulun SE, Leitch M, Rohrich R, Simpson ER. Use of alternative promoters to express the aromatase cytochrome P450 (CYP19) gene in breast adipose tissues of cancer-free and breast cancer patients. J Clin Endocrinol Metab. 1996;81(11):3843-9.

87. Bulun SE, Price TM, Aitken J, Mahendroo MS, Simpson ER. A link between breast cancer and local estrogen biosynthesis suggested by quantification of breast adipose tissue aromatase cytochrome P450 transcripts using competitive polymerase chain reaction after reverse transcription. J Clin Endocrinol Metab. 1993;77(6):1622-8.

88. Boudot A, Kerdivel G, Habauzit D, Eeckhoute J, Le Dily F, Flouriot G, et al. Differential estrogen-regulation of CXCL12 chemokine receptors, CXCR4 and CXCR7, contributes to the growth effect of estrogens in breast cancer cells. PLoS One. 2011;6(6):e20898.

89. Sommer S, Fuqua SA. Estrogen receptor and breast cancer. Semin Cancer Biol. 2001;11(5):339-52.

90. Larionov AA, Berstein LM, Miller WR. Local uptake and synthesis of oestrone in normal and malignant postmenopausal breast tissues. J Steroid Biochem Mol Biol. 2002;81(1):57-64.

91. Simpson E, Jones M, Misso M, Hewitt K, Hill R, Maffei L, et al. Estrogen, a fundamental player in energy homeostasis. J Steroid Biochem Mol Biol. 2005;95(1-5):3-8.

92. Chen D, Reierstad S, Lu M, Lin Z, Ishikawa H, Bulun SE. Regulation of breast cancer-associated aromatase promoters. Cancer Lett. 2009;273(1):15-27.

93. Utsumi T, Harada N, Maruta M, Takagi Y. Presence of alternatively spliced transcripts of aromatase gene in human breast cancer. J Clin Endocrinol Metab. 1996;81(6):2344-9.

94. Zhou C, Zhou D, Esteban J, Murai J, Siiteri PK, Wilczynski S, et al. Aromatase gene expression and its exon I usage in human breast tumors. Detection of aromatase messenger RNA by reverse transcription-polymerase chain reaction. J Steroid Biochem Mol Biol. 1996;59(2):163-71.

95. Irahara N, Miyoshi Y, Taguchi T, Tamaki Y, Noguchi S. Quantitative analysis of aromatase mRNA expression derived from various promoters (I.4, I.3, PII and I.7) and its association with expression of TNF-alpha, IL-6 and COX-2 mRNAs in human breast cancer. Int J Cancer. 2006;118(8):1915-21.

96. Sebastian S, Takayama K, Shozu M, Bulun SE. Cloning and characterization of a novel endothelial promoter of the human CYP19 (aromatase P450) gene that is up-regulated in breast cancer tissue. Mol Endocrinol. 2002;16(10):2243-54.

97. Harada N, Utsumi T, Takagi Y. Tissue-specific expression of the human aromatase cytochrome P-450 gene by alternative use of multiple exons 1 and promoters, and switching of

tissue-specific exons 1 in carcinogenesis. Proc Natl Acad Sci U S A. 1993;90(23):11312-6.

98. Mor G, Yue W, Santen RJ, Gutierrez L, Eliza M, Berstein LM, et al. Macrophages, estrogen and the microenvironment of breast cancer. J Steroid Biochem Mol Biol. 1998;67(5-6):403-11.

99. Leek RD, Lewis CE, Whitehouse R, Greenall M, Clarke J, Harris AL. Association of macrophage infiltration with angiogenesis and prognosis in invasive breast carcinoma. Cancer Res. 1996;56(20):4625-9.

100. Li H, Yang B, Huang J, Lin YS, Xiang T, Wan J, et al. Cyclooxygenase-2 in tumor-associated macrophages promotes breast cancer cell survival by triggering a positive-feedback loop between macrophages and cancer cells. Oncotarget. 2015;6(30):29637–50.

101. Zhao Y, Agarwal VR, Mendelson CR, Simpson ER. Estrogen biosynthesis proximal to a breast tumor is stimulated by PGE2 via cyclic AMP, leading to activation of promoter II of the CYP19 (aromatase) gene. Endocrinology. 1996;137(12):5739-42.

102. Brueggemeier RW. Overview of the pharmacology of the aromatase inactivator exemestane. Breast Cancer Res Treat. 2002;74(2):177-85.

103. [cited January 25th, 2017]. Available from: https://www.drugs.com/.

104. Geisler J. Differences between the non-steroidal aromatase inhibitors anastrozole and letrozole--of clinical importance? Br J Cancer. 2011;104(7):1059-66.

105. Steroid Chemistry and Steroid Hormone Action [cited 2017 March 22nd]. Available from: https://www.rose-hulman.edu/~brandt/Chem330/EndocrineNotes/Chapter_1_Steroids.pdf.

106. Ghosh D, Griswold J, Erman M, Pangborn W. Structural basis for androgen specificity and oestrogen synthesis in human aromatase. Nature. 2009;457(7226):219-23.

107. Lonning PE, Geisler J. Indications and limitations of third-generation aromatase inhibitors. Expert Opin Investig Drugs. 2008;17(5):723-39.

108. Pfizer. Aromasin Exemestane Tablets 2016 [updated October 2016; cited 2016 December 14th]. Available from: http://www.pfizer.com/files/products/uspi_aromasin.pdf.

109. di Salle E, Ornati G, Giudici D, Lassus M, Evans TR, Coombes RC. Exemestane (FCE 24304), a new steroidal aromatase inhibitor. J Steroid Biochem Mol Biol. 1992;43(1-3):137-43.

110. Bryant HU. Selective estrogen receptor modulators. Rev Endocr Metab Disord. 2002;3(3):231-41.

111. AstraZeneca Pharmaceuticals LP. Nolvadex (tamoxifen citrate) tablets. 2004.

112. Di Salle E, Briatico G, Giudici D, Ornati G, Zaccheo T, Buzzetti F, et al. Novel aromatase and 5 alpha-reductase inhibitors. J Steroid Biochem Mol Biol. 1994;49(4-6):289-94.

113. Ma CX, Adjei AA, Salavaggione OE, Coronel J, Pelleymounter L, Wang L, et al. Human aromatase: gene resequencing and functional genomics. Cancer Res. 2005;65(23):11071-82.

114. Evans TR, Di Salle E, Ornati G, Lassus M, Benedetti MS, Pianezzola E, et al. Phase I and endocrine study of exemestane (FCE 24304), a new aromatase inhibitor, in postmenopausal women. Cancer Res. 1992;52(21):5933-9.

115. Sun D, Chen G, Dellinger RW, Sharma AK, Lazarus P. Characterization of 17-dihydroexemestane glucuronidation: potential role of the UGT2B17 deletion in exemestane pharmacogenetics. Pharmacogenet Genomics. 2010;20(10):575-85.

116. Spinelli R JM, Poggesi I, et al. Pharmacokinetics (PK) of Aromasin (exemestane, EXE) after single and repeated doses in healthy postmenopausal volunteers. Eur J Cancer. 1999;35(Suppl 4):S295.

117. Zilembo N, Noberasco C, Bajetta E, Martinetti A, Mariani L, Orefice S, et al. Endocrinological and clinical evaluation of exemestane, a new steroidal aromatase inhibitor. Br J Cancer. 1995;72(4):1007-12.

118. Ghosh D, Lo J, Egbuta C. Recent Progress in the Discovery of Next Generation Inhibitors of Aromatase from the Structure-Function Perspective. J Med Chem. 2016;59(11):5131-48.

119. Graham-Lorence S, Amarneh B, White RE, Peterson JA, Simpson ER. A three-dimensional model of aromatase cytochrome P450. Protein Sci. 1995;4(6):1065-80.

120. Karkola S, Holtje HD, Wahala K. A three-dimensional model of CYP19 aromatase for structure-based drug design. J Steroid Biochem Mol Biol. 2007;105(1-5):63-70.

121. Favia AD, Cavalli A, Masetti M, Carotti A, Recanatini M. Three-dimensional model of the human aromatase enzyme and density functional parameterization of the iron-containing protoporphyrin IX for a molecular dynamics study of heme-cysteinato cytochromes. Proteins. 2006;62(4):1074-87.

122. Ghosh D, Griswold J, Erman M, Pangborn W. X-ray structure of human aromatase reveals an androgen-specific active site. J Steroid Biochem Mol Biol. 2010;118(4-5):197-202.

123. Cojocaru V, Winn PJ, Wade RC. The ins and outs of cytochrome P450s. Biochim Biophys Acta. 2007;1770(3):390-401.

124. Jiang W, Ghosh D. Motion and flexibility in human cytochrome p450 aromatase. PLoS One. 2012;7(2):e32565.

125. Williams PA, Cosme J, Vinkovic DM, Ward A, Angove HC, Day PJ, et al. Crystal structures of human cytochrome P450 3A4 bound to metyrapone and progesterone. Science. 2004;305(5684):683-6.

126. Rowland P, Blaney FE, Smyth MG, Jones JJ, Leydon VR, Oxbrow AK, et al. Crystal structure of human cytochrome P450 2D6. J Biol Chem. 2006;281(11):7614-22.

127. Viciano I, Marti S. Theoretical Study of the Mechanism of Exemestane Hydroxylation Catalyzed by Human Aromatase Enzyme. J Phys Chem B. 2016;120(13):3331-43.

128. Ghosh D, Lo J, Morton D, Valette D, Xi J, Griswold J, et al. Novel aromatase inhibitors by structure-guided design. J Med Chem. 2012;55(19):8464-76.

129. Di Nardo G, Breitner M, Bandino A, Ghosh D, Jennings GK, Hackett JC, et al. Evidence for an elevated aspartate pK(a) in the active site of human aromatase. J Biol Chem. 2015;290(2):1186-96.

130. Covey DF, Hood WF. A new hypothesis based on suicide substrate inhibitor studies for the mechanism of action of aromatase. Cancer Res. 1982;42(8 Suppl):3327s-33s.

131. Hong Y, Rashid R, Chen S. Binding features of steroidal and nonsteroidal inhibitors. Steroids. 2011;76(8):802-6.

132. Hong Y, Yu B, Sherman M, Yuan YC, Zhou D, Chen S. Molecular basis for the aromatization reaction and exemestane-mediated irreversible inhibition of human aromatase. Mol Endocrinol. 2007;21(2):401-14.

133. Goss PE, Ingle JN, Ales-Martinez JE, Cheung AM, Chlebowski RT, Wactawski-Wende J, et al. Exemestane for breast-cancer prevention in postmenopausal women. N Engl J Med. 2011;364(25):2381-91.

134. Cuzick J, Forbes J, Edwards R, Baum M, Cawthorn S, Coates A, et al. First results from the International Breast Cancer Intervention Study (IBIS-I): a randomised prevention trial. Lancet. 2002;360(9336):817-24.

135. Waters EA, Cronin KA, Graubard BI, Han PK, Freedman AN. Prevalence of tamoxifen use for breast cancer chemoprevention among U.S. women. Cancer Epidemiol Biomarkers Prev. 2010;19(2):443-6.

136. Freedman OC, Verma S, Clemons MJ. Using aromatase inhibitors in the neoadjuvant setting: evolution or revolution? Cancer Treat Rev. 2005;31(1):1-17.

137. Takei H, Kurosumi M, Yoshida T, Hayashi Y, Higuchi T, Uchida S, et al. Neoadjuvant endocrine therapy of breast cancer: which patients would benefit and what are the advantages? Breast Cancer. 2011;18(2):85-91.

138. Fontein DB, Charehbili A, Nortier JW, Meershoek-Klein Kranenbarg E, Kroep JR, Putter H, et al. Efficacy of six month neoadjuvant endocrine therapy in postmenopausal, hormone receptor-positive breast cancer patients--a phase II trial. Eur J Cancer. 2014;50(13):2190-200.

139. Grassadonia A, Di Nicola M, Grossi S, Noccioli P, Tavoletta S, Politi R, et al. Long-term outcome of neoadjuvant endocrine therapy with aromatase inhibitors in elderly women with hormone receptor-positive breast cancer. Ann Surg Oncol. 2014;21(5):1575-82.

140. Seo JH, Kim YH, Kim JS. Meta-analysis of pre-operative aromatase inhibitor versus

tamoxifen in postmenopausal woman with hormone receptor-positive breast cancer. Cancer Chemother Pharmacol. 2009;63(2):261-6.

141. Meier CR, Jick H. Tamoxifen and risk of idiopathic venous thromboembolism. Br J Clin Pharmacol. 1998;45(6):608-12.

142. Fornander T, Rutqvist LE, Cedermark B, Glas U, Mattsson A, Silfversward C, et al. Adjuvant tamoxifen in early breast cancer: occurrence of new primary cancers. Lancet. 1989;1(8630):117-20.

143. Smith IE, Dowsett M. Aromatase inhibitors in breast cancer. N Engl J Med. 2003;348(24):2431-42.

144. Eiermann W, Paepke S, Appfelstaedt J, Llombart-Cussac A, Eremin J, Vinholes J, et al. Preoperative treatment of postmenopausal breast cancer patients with letrozole: A randomized double-blind multicenter study. Ann Oncol. 2001;12(11):1527-32.

145. Smith IE, Dowsett M, Ebbs SR, Dixon JM, Skene A, Blohmer JU, et al. Neoadjuvant treatment of postmenopausal breast cancer with anastrozole, tamoxifen, or both in combination: the Immediate Preoperative Anastrozole, Tamoxifen, or Combined with Tamoxifen (IMPACT) multicenter double-blind randomized trial. J Clin Oncol. 2005;23(22):5108-16.

146. Cataliotti L, Buzdar AU, Noguchi S, Bines J, Takatsuka Y, Petrakova K, et al. Comparison of anastrozole versus tamoxifen as preoperative therapy in postmenopausal women with hormone receptor-positive breast cancer: the Pre-Operative "Arimidex" Compared to Tamoxifen (PROACT) trial. Cancer. 2006;106(10):2095-103.

147. Hojo T, Kinoshita T, Imoto S, Shimizu C, Isaka H, Ito H, et al. Use of the neo-adjuvant exemestane in post-menopausal estrogen receptor-positive breast cancer: a randomized phase II trial (PTEX46) to investigate the optimal duration of preoperative endocrine therapy. Breast. 2013;22(3):263-7.

148. Torrisi R, Rota S, Losurdo A, Zuradelli M, Masci G, Santoro A. Aromatase inhibitors in premenopause: Great expectations fulfilled? Crit Rev Oncol Hematol. 2016;107:82-9.

149. Rossi E, Morabito A, De Maio E, Di Rella F, Esposito G, Gravina A, et al. Endocrine effects of adjuvant letrozole + triptorelin compared with tamoxifen + triptorelin in premenopausal patients with early breast cancer. J Clin Oncol. 2008;26(2):264-70.

150. Pagani O, Regan MM, Walley BA, Fleming GF, Colleoni M, Lang I, et al. Adjuvant exemestane with ovarian suppression in premenopausal breast cancer. N Engl J Med. 2014;371(2):107-18.

151. Bernhard J, Luo W, Ribi K, Colleoni M, Burstein HJ, Tondini C, et al. Patient-reported outcomes with adjuvant exemestane versus tamoxifen in premenopausal women with early breast cancer undergoing ovarian suppression (TEXT and SOFT): a combined analysis of two phase 3 randomised trials. Lancet Oncol. 2015;16(7):848-58.

152. Coates AS, Winer EP, Goldhirsch A, Gelber RD, Gnant M, Piccart-Gebhart M, et al. Tailoring therapies--improving the management of early breast cancer: St Gallen International Expert Consensus on the Primary Therapy of Early Breast Cancer 2015. Ann Oncol. 2015;26(8):1533-46.

153. Bellet M, Gray KP, Francis PA, Lang I, Ciruelos E, Lluch A, et al. Twelve-Month Estrogen Levels in Premenopausal Women With Hormone Receptor-Positive Breast Cancer Receiving Adjuvant Triptorelin Plus Exemestane or Tamoxifen in the Suppression of Ovarian Function Trial (SOFT): The SOFT-EST Substudy. J Clin Oncol. 2016;34(14):1584-93.

154. Bonneterre J, Thurlimann B, Robertson JF, Krzakowski M, Mauriac L, Koralewski P, et al. Anastrozole versus tamoxifen as first-line therapy for advanced breast cancer in 668 postmenopausal women: results of the Tamoxifen or Arimidex Randomized Group Efficacy and Tolerability study. J Clin Oncol. 2000;18(22):3748-57.

155. Nabholtz JM, Buzdar A, Pollak M, Harwin W, Burton G, Mangalik A, et al. Anastrozole is superior to tamoxifen as first-line therapy for advanced breast cancer in postmenopausal women: results of a North American multicenter randomized trial. Arimidex Study Group. J Clin Oncol. 2000;18(22):3758-67.

156. Mouridsen H, Gershanovich M, Sun Y, Perez-Carrion R, Boni C, Monnier A, et al. Superior efficacy of letrozole versus tamoxifen as first-line therapy for postmenopausal women with advanced breast cancer: results of a phase III study of the International Letrozole Breast Cancer Group. J Clin Oncol. 2001;19(10):2596-606.

157. Paridaens RJ, Dirix LY, Beex LV, Nooij M, Cameron DA, Cufer T, et al. Phase III study comparing exemestane with tamoxifen as first-line hormonal treatment of metastatic breast cancer in postmenopausal women: the European Organisation for Research and Treatment of Cancer Breast Cancer Cooperative Group. J Clin Oncol. 2008;26(30):4883-90.

158. Mauri D, Pavlidis N, Polyzos NP, Ioannidis JP. Survival with aromatase inhibitors and inactivators versus standard hormonal therapy in advanced breast cancer: meta-analysis. J Natl Cancer Inst. 2006;98(18):1285-91.

159. van de Velde CJ, Rea D, Seynaeve C, Putter H, Hasenburg A, Vannetzel JM, et al. Adjuvant tamoxifen and exemestane in early breast cancer (TEAM): a randomised phase 3 trial. Lancet. 2011;377(9762):321-31.

160. Coombes RC, Kilburn LS, Snowdon CF, Paridaens R, Coleman RE, Jones SE, et al. Survival and safety of exemestane versus tamoxifen after 2-3 years' tamoxifen treatment (Intergroup Exemestane Study): a randomised controlled trial. Lancet. 2007;369(9561):559-70.

161. Van Asten K, Neven P, Lintermans A, Wildiers H, Paridaens R. Aromatase inhibitors in the breast cancer clinic: focus on exemestane. Endocr Relat Cancer. 2014;21(1):R31-49.

162. Goss PE, Ingle JN, Pritchard KI, Ellis MJ, Sledge GW, Budd GT, et al. Exemestane versus anastrozole in postmenopausal women with early breast cancer: NCIC CTG MA.27--a

randomized controlled phase III trial. J Clin Oncol. 2013;31(11):1398-404.

163. Goss PE, Ingle JN, Pater JL, Martino S, Robert NJ, Muss HB, et al. Late extended adjuvant treatment with letrozole improves outcome in women with early-stage breast cancer who complete 5 years of tamoxifen. J Clin Oncol. 2008;26(12):1948-55.

164. Arimidex TAoiCTG, Forbes JF, Cuzick J, Buzdar A, Howell A, Tobias JS, et al. Effect of anastrozole and tamoxifen as adjuvant treatment for early-stage breast cancer: 100-month analysis of the ATAC trial. Lancet Oncol. 2008;9(1):45-53.

165. Coates AS, Keshaviah A, Thurlimann B, Mouridsen H, Mauriac L, Forbes JF, et al. Five years of letrozole compared with tamoxifen as initial adjuvant therapy for postmenopausal women with endocrine-responsive early breast cancer: update of study BIG 1-98. J Clin Oncol. 2007;25(5):486-92.

166. Henry NL, Azzouz F, Desta Z, Li L, Nguyen AT, Lemler S, et al. Predictors of aromatase inhibitor discontinuation as a result of treatment-emergent symptoms in early-stage breast cancer. J Clin Oncol. 2012;30(9):936-42.

167. Gluck S, von Minckwitz G, Untch M. Aromatase inhibitors in the treatment of elderly women with metastatic breast cancer. Breast. 2013;22(2):142-9.

168. Kaufmann M, Bajetta E, Dirix LY, Fein LE, Jones SE, Zilembo N, et al. Exemestane is superior to megestrol acetate after tamoxifen failure in postmenopausal women with advanced breast cancer: results of a phase III randomized double-blind trial. The Exemestane Study Group. J Clin Oncol. 2000;18(7):1399-411.

169. Iaffaioli RV, Formato R, Tortoriello A, Del Prete S, Caraglia M, Pappagallo G, et al. Phase II study of sequential hormonal therapy with anastrozole/exemestane in advanced and metastatic breast cancer. Br J Cancer. 2005;92(9):1621-5.

170. Lonning PE, Bajetta E, Murray R, Tubiana-Hulin M, Eisenberg PD, Mickiewicz E, et al. Activity of exemestane in metastatic breast cancer after failure of nonsteroidal aromatase inhibitors: a phase II trial. J Clin Oncol. 2000;18(11):2234-44.

171. Steele N, Zekri J, Coleman R, Leonard R, Dunn K, Bowman A, et al. Exemestane in metastatic breast cancer: effective therapy after third-generation non-steroidal aromatase inhibitor failure. Breast. 2006;15(3):430-6.

172. Yardley DA, Noguchi S, Pritchard KI, Burris HA, 3rd, Baselga J, Gnant M, et al. Everolimus plus exemestane in postmenopausal patients with HR(+) breast cancer: BOLERO-2 final progression-free survival analysis. Adv Ther. 2013;30(10):870-84.

173. Coleman RE, Banks LM, Girgis SI, Kilburn LS, Vrdoljak E, Fox J, et al. Skeletal effects of exemestane on bone-mineral density, bone biomarkers, and fracture incidence in postmenopausal women with early breast cancer participating in the Intergroup Exemestane Study (IES): a randomised controlled study. Lancet Oncol. 2007;8(2):119-27.

174. Cheung AM, Tile L, Cardew S, Pruthi S, Robbins J, Tomlinson G, et al. Bone density and structure in healthy postmenopausal women treated with exemestane for the primary prevention of breast cancer: a nested substudy of the MAP.3 randomised controlled trial. Lancet Oncol. 2012;13(3):275-84.

175. Cummings SR, Browner WS, Bauer D, Stone K, Ensrud K, Jamal S, et al. Endogenous hormones and the risk of hip and vertebral fractures among older women. Study of Osteoporotic Fractures Research Group. N Engl J Med. 1998;339(11):733-8.

176. Bundred NJ. Aromatase inhibitors and bone health. Curr Opin Obstet Gynecol. 2009;21(1):60-7.

177. Frenkel B, Hong A, Baniwal SK, Coetzee GA, Ohlsson C, Khalid O, et al. Regulation of adult bone turnover by sex steroids. J Cell Physiol. 2010;224(2):305-10.

178. Hadji P, Bundred N. Reducing the risk of cancer treatment-associated bone loss in patients with breast cancer. Semin Oncol. 2007;34(6 Suppl 4):S4-10.

179. Kalder M, Hans D, Kyvernitakis I, Lamy O, Bauer M, Hadji P. Effects of Exemestane and Tamoxifen treatment on bone texture analysis assessed by TBS in comparison with bone mineral density assessed by DXA in women with breast cancer. J Clin Densitom. 2014;17(1):66-71.

180. Lonning PE, Geisler J, Krag LE, Erikstein B, Bremnes Y, Hagen AI, et al. Effects of exemestane administered for 2 years versus placebo on bone mineral density, bone biomarkers, and plasma lipids in patients with surgically resected early breast cancer. J Clin Oncol. 2005;23(22):5126-37.

181. Goss PE, Hadji P, Subar M, Abreu P, Thomsen T, Banke-Bochita J. Effects of steroidal and nonsteroidal aromatase inhibitors on markers of bone turnover in healthy postmenopausal women. Breast Cancer Res. 2007;9(4):R52.

182. Love RR, Mazess RB, Barden HS, Epstein S, Newcomb PA, Jordan VC, et al. Effects of tamoxifen on bone mineral density in postmenopausal women with breast cancer. N Engl J Med. 1992;326(13):852-6.

183. Powles TJ, Hickish T, Kanis JA, Tidy A, Ashley S. Effect of tamoxifen on bone mineral density measured by dual-energy x-ray absorptiometry in healthy premenopausal and postmenopausal women. J Clin Oncol. 1996;14(1):78-84.

184. Fisher B, Costantino JP, Wickerham DL, Cecchini RS, Cronin WM, Robidoux A, et al. Tamoxifen for the prevention of breast cancer: current status of the National Surgical Adjuvant Breast and Bowel Project P-1 study. J Natl Cancer Inst. 2005;97(22):1652-62.

185. Hadji P, Asmar L, van Nes JG, Menschik T, Hasenburg A, Kuck J, et al. The effect of exemestane and tamoxifen on bone health within the Tamoxifen Exemestane Adjuvant Multinational (TEAM) trial: a meta-analysis of the US, German, Netherlands, and Belgium sub-studies. J Cancer Res Clin Oncol. 2011;137(6):1015-25.

186. Sambrook P, Cooper C. Osteoporosis. Lancet. 2006;367(9527):2010-8.

187. Coleman RE, Banks LM, Girgis SI, al. e, editors. Reversal of skeletal effects of endocrine treatments in the intergroup exemestane study. San Antonio Breast Cancer Symposium (SABCS); 2008; San Antonio, Texas, USA.

188. Coombes RC, Kilburn LS, Beare S, al. e, editors. Survival and safety post study treatment completion: an updated analysis of the intergroup exemestane study (IES)—submitted on behalf of the IES investigators. ECCO 15-ESMO 34 meeting; 2009; Berlin, Germany.

189. Cigler T, Richardson H, Yaffe MJ, Fabian CJ, Johnston D, Ingle JN, et al. A randomized, placebo-controlled trial (NCIC CTG MAP.2) examining the effects of exemestane on mammographic breast density, bone density, markers of bone metabolism and serum lipid levels in postmenopausal women. Breast Cancer Res Treat. 2011;126(2):453-61.

190. Gatti-Mays ME, Venzon D, Galbo CE, Singer A, Reynolds J, Makariou E, et al. Exemestane Use in Postmenopausal Women at High Risk for Invasive Breast Cancer: Evaluating Biomarkers of Efficacy and Safety. Cancer Prev Res (Phila). 2016;9(3):225-33.

191. Atalay G, Dirix L, Biganzoli L, Beex L, Nooij M, Cameron D, et al. The effect of exemestane on serum lipid profile in postmenopausal women with metastatic breast cancer: a companion study to EORTC Trial 10951, 'Randomized phase II study in first line hormonal treatment for metastatic breast cancer with exemestane or tamoxifen in postmenopausal patients'. Ann Oncol. 2004;15(2):211-7.

192. Montagnani A, Gonnelli S, Cadirni A, Caffarelli C, Del Santo K, Pieropan C, et al. The effects on lipid serum levels of a 2-year adjuvant treatment with exemestane after tamoxifen in postmenopausal women with early breast cancer. Eur J Intern Med. 2008;19(8):592-7.

193. Bruning PF, Bonfrer JM, Hart AA, de Jong-Bakker M, Linders D, van Loon J, et al. Tamoxifen, serum lipoproteins and cardiovascular risk. Br J Cancer. 1988;58(4):497-9.

194. Cuzick J, Allen D, Baum M, Barrett J, Clark G, Kakkar V, et al. Long term effects of tamoxifen. Biological effects of Tamoxifen Working Party. Eur J Cancer. 1992;29A(1):15-21.

195. Dewar JA, Horobin JM, Preece PE, Tavendale R, Tunstall-Pedoe H, Wood RA. Long term effects of tamoxifen on blood lipid values in breast cancer. BMJ. 1992;305(6847):225-6.

196. Guetta V, Lush RM, Figg WD, Waclawiw MA, Cannon RO, 3rd. Effects of the antiestrogen tamoxifen on low-density lipoprotein concentrations and oxidation in postmenopausal women. Am J Cardiol. 1995;76(14):1072-3.

197. Gylling H, Pyrhonen S, Mantyla E, Maenpaa H, Kangas L, Miettinen TA. Tamoxifen and toremifene lower serum cholesterol by inhibition of delta 8-cholesterol conversion to lathosterol in women with breast cancer. J Clin Oncol. 1995;13(12):2900-5.

198. Holleran AL, Lindenthal B, Aldaghlas TA, Kelleher JK. Effect of tamoxifen on cholesterol synthesis in HepG2 cells and cultured rat hepatocytes. Metabolism. 1998;47(12):1504-13.

199. de Medina P, Payre BL, Bernad J, Bosser I, Pipy B, Silvente-Poirot S, et al. Tamoxifen is a potent inhibitor of cholesterol esterification and prevents the formation of foam cells. J Pharmacol Exp Ther. 2004;308(3):1165-73.

200. Love RR, Wiebe DA, Newcomb PA, Cameron L, Leventhal H, Jordan VC, et al. Effects of tamoxifen on cardiovascular risk factors in postmenopausal women. Ann Intern Med. 1991;115(11):860-4.

201. Lamon-Fava S, Micherone D. Regulation of apoA-I gene expression: mechanism of action of estrogen and genistein. J Lipid Res. 2004;45(1):106-12.

202. Saarto T, Blomqvist C, Ehnholm C, Taskinen MR, Elomaa I. Antiatherogenic effects of adjuvant antiestrogens: a randomized trial comparing the effects of tamoxifen and toremifene on plasma lipid levels in postmenopausal women with node-positive breast cancer. J Clin Oncol. 1996;14(2):429-33.

203. Khosrow-Khavar F, Filion KB, Al-Qurashi S, Torabi N, Bouganim N, Suissa S, et al. Cardiotoxicity of Aromatase Inhibitors and Tamoxifen in Post-Menopausal Women with Breast Cancer: A Systematic Review and Meta-Analysis of Randomized Controlled Trials. Ann Oncol. 2016.

204. Bliss JM, Kilburn LS, Coleman RE, Forbes JF, Coates AS, Jones SE, et al. Disease-related outcomes with long-term follow-up: an updated analysis of the intergroup exemestane study. J Clin Oncol. 2012;30(7):709-17.

205. Boccardo F, Guglielmini P, Bordonaro R, Fini A, Massidda B, Porpiglia M, et al. Switching to anastrozole versus continued tamoxifen treatment of early breast cancer: long term results of the Italian Tamoxifen Anastrozole trial. Eur J Cancer. 2013;49(7):1546-54.

206. Colleoni M, Giobbie-Hurder A, Regan MM, Thurlimann B, Mouridsen H, Mauriac L, et al. Analyses adjusting for selective crossover show improved overall survival with adjuvant letrozole compared with tamoxifen in the BIG 1-98 study. J Clin Oncol. 2011;29(9):1117-24.

207. Wiseman H, Laughton MJ, Arnstein HR, Cannon M, Halliwell B. The antioxidant action of tamoxifen and its metabolites. Inhibition of lipid peroxidation. FEBS Lett. 1990;263(2):192-4.

208. Wiseman H. Tamoxifen as an antioxidant and cardioprotectant. Biochem Soc Symp. 1995;61:209-19.

209. Love RR, Wiebe DA, Feyzi JM, Newcomb PA, Chappell RJ. Effects of tamoxifen on cardiovascular risk factors in postmenopausal women after 5 years of treatment. J Natl Cancer Inst. 1994;86(20):1534-9.

210. Cushman M, Costantino JP, Tracy RP, Song K, Buckley L, Roberts JD, et al. Tamoxifen and cardiac risk factors in healthy women: Suggestion of an anti-inflammatory effect. Arterioscler Thromb Vasc Biol. 2001;21(2):255-61.

211. Ellis AJ, Hendrick VM, Williams R, Komm BS. Selective estrogen receptor modulators in

clinical practice: a safety overview. Expert Opin Drug Saf. 2015;14(6):921-34.

212. Cuzick J, Forbes JF, Sestak I, Cawthorn S, Hamed H, Holli K, et al. Long-term results of tamoxifen prophylaxis for breast cancer--96-month follow-up of the randomized IBIS-I trial. J Natl Cancer Inst. 2007;99(4):272-82.

213. Burstein HJ. Aromatase inhibitor-associated arthralgia syndrome. Breast. 2007;16(3):223-34.

214. Burstein HJ, Winer EP. Aromatase inhibitors and arthralgias: a new frontier in symptom management for breast cancer survivors. J Clin Oncol. 2007;25(25):3797-9.

215. Henry NL, Jacobson JA, Banerjee M, Hayden J, Smerage JB, Van Poznak C, et al. A prospective study of aromatase inhibitor-associated musculoskeletal symptoms and abnormalities on serial high-resolution wrist ultrasonography. Cancer. 2010;116(18):4360-7.

216. Henry NL, Pchejetski D, A'Hern R, Nguyen AT, Charles P, Waxman J, et al. Inflammatory cytokines and aromatase inhibitor-associated musculoskeletal syndrome: a case-control study. Br J Cancer. 2010;103(3):291-6.

217. Lintermans A, Van Calster B, Van Hoydonck M, Pans S, Verhaeghe J, Westhovens R, et al. Aromatase inhibitor-induced loss of grip strength is body mass index dependent: hypothesis-generating findings for its pathogenesis. Ann Oncol. 2011;22(8):1763-9.

218. Winters L, Habin K, Flanagan J, Cashavelly BJ. "I feel like I am 100 years old!" managing arthralgias from aromatase inhibitors. Clin J Oncol Nurs. 2010;14(3):379-82.

219. Dizdar O, Ozcakar L, Malas FU, Harputluoglu H, Bulut N, Aksoy S, et al. Sonographic and electrodiagnostic evaluations in patients with aromatase inhibitor-related arthralgia. J Clin Oncol. 2009;27(30):4955-60.

220. Mao JJ, Stricker C, Bruner D, Xie S, Bowman MA, Farrar JT, et al. Patterns and risk factors associated with aromatase inhibitor-related arthralgia among breast cancer survivors. Cancer. 2009;115(16):3631-9.

221. Helzlsouer KJ, Gallicchio L, MacDonald R, Wood B, Rushovich E. A prospective study of aromatase inhibitor therapy, vitamin D, C-reactive protein and musculoskeletal symptoms. Breast Cancer Res Treat. 2012;131(1):277-85.

222. Gaillard S, Stearns V. Aromatase inhibitor-associated bone and musculoskeletal effects: new evidence defining etiology and strategies for management. Breast Cancer Res. 2011;13(2):205.

223. Henry NL, Giles JT, Ang D, Mohan M, Dadabhoy D, Robarge J, et al. Prospective characterization of musculoskeletal symptoms in early stage breast cancer patients treated with aromatase inhibitors. Breast Cancer Res Treat. 2008;111(2):365-72.

224. Park JY, Lee SK, Bae SY, Kim J, Kim MK, Kil WH, et al. Aromatase inhibitor-associated

musculoskeletal symptoms: incidence and associated factors. J Korean Surg Soc. 2013;85(5):205-11.

225. Singer O, Cigler T, Moore AB, Levine AB, Hentel K, Belfi L, et al. Defining the aromatase inhibitor musculoskeletal syndrome: a prospective study. Arthritis Care Res (Hoboken). 2012;64(12):1910-8.

226. Robidoux A, Rich E, Bureau NJ, Mader S, Laperriere D, Bail M, et al. A prospective pilot study investigating the musculoskeletal pain in postmenopausal breast cancer patients receiving aromatase inhibitor therapy. Curr Oncol. 2011;18(6):285-94.

227. Moxley G. Rheumatic disorders and functional disability with aromatase inhibitor therapy. Clin Breast Cancer. 2010;10(2):144-7.

228. Kidwell KM, Harte SE, Hayes DF, Storniolo AM, Carpenter J, Flockhart DA, et al. Patient-reported symptoms and discontinuation of adjuvant aromatase inhibitor therapy. Cancer. 2014;120(16):2403-11.

229. Mieog JS, Morden JP, Bliss JM, Coombes RC, van de Velde CJ, Committee IESS. Carpal tunnel syndrome and musculoskeletal symptoms in postmenopausal women with early breast cancer treated with exemestane or tamoxifen after 2-3 years of tamoxifen: a retrospective analysis of the Intergroup Exemestane Study. Lancet Oncol. 2012;13(4):420-32.

230. Khan QJ, O'Dea AP, Sharma P. Musculoskeletal adverse events associated with adjuvant aromatase inhibitors. J Oncol. 2010;2010.

231. Tomao F, Spinelli G, Vici P, Pisanelli GC, Cascialli G, Frati L, et al. Current role and safety profile of aromatase inhibitors in early breast cancer. Expert Rev Anticancer Ther. 2011;11(8):1253-63.

232. Morandi P, Rouzier R, Altundag K, Buzdar AU, Theriault RL, Hortobagyi G. The role of aromatase inhibitors in the adjuvant treatment of breast carcinoma: the M. D. Anderson Cancer Center evidence-based approach. Cancer. 2004;101(7):1482-9.

233. Presant CA, Bosserman L, Young T, Vakil M, Horns R, Upadhyaya G, et al. Aromatase inhibitor-associated arthralgia and/ or bone pain: frequency and characterization in non-clinical trial patients. Clin Breast Cancer. 2007;7(10):775-8.

234. Younus J, Kligman L. Management of aromatase inhibitor-induced arthralgia. Curr Oncol. 2010;17(1):87-90.

235. Mishra G, Kuh D. Perceived change in quality of life during the menopause. Soc Sci Med. 2006;62(1):93-102.

236. Ingle JN, Schaid DJ, Goss PE, Liu M, Mushiroda T, Chapman JA, et al. Genome-wide associations and functional genomic studies of musculoskeletal adverse events in women receiving aromatase inhibitors. J Clin Oncol. 2010;28(31):4674-82.

237. Shanmugam VK, McCloskey J, Elston B, Allison SJ, Eng-Wong J. The CIRAS study: a case control study to define the clinical, immunologic, and radiographic features of aromatase inhibitor-induced musculoskeletal symptoms. Breast Cancer Res Treat. 2012;131(2):699-708.

238. Felson DT, Cummings SR. Aromatase inhibitors and the syndrome of arthralgias with estrogen deprivation. Arthritis Rheum. 2005;52(9):2594-8.

239. Toesca A, Pagnotta A, Zumbo A, Sadun R. Estrogen and progesterone receptors in carpal tunnel syndrome. Cell Biol Int. 2008;32(1):75-9.

240. Claassen H, Hassenpflug J, Schunke M, Sierralta W, Thole H, Kurz B. Immunohistochemical detection of estrogen receptor alpha in articular chondrocytes from cows, pigs and humans: in situ and in vitro results. Ann Anat. 2001;183(3):223-7.

241. Richette P, Corvol M, Bardin T. Estrogens, cartilage, and osteoarthritis. Joint Bone Spine. 2003;70(4):257-62.

242. Morales L, Pans S, Verschueren K, Van Calster B, Paridaens R, Westhovens R, et al. Prospective study to assess short-term intra-articular and tenosynovial changes in the aromatase inhibitor-associated arthralgia syndrome. J Clin Oncol. 2008;26(19):3147-52.

243. De Logu F, Tonello R, Materazzi S, Nassini R, Fusi C, Coppi E, et al. TRPA1 Mediates Aromatase Inhibitor-Evoked Pain by the Aromatase Substrate Androstenedione. Cancer Res. 2016;76(23):7024-35.

244. Biglia N, Bounous VE, Sgro LG, D'Alonzo M, Pecchio S, Nappi RE. Genitourinary Syndrome of Menopause in Breast Cancer Survivors: Are We Facing New and Safe Hopes? Clin Breast Cancer. 2015;15(6):413-20.

245. Fallowfield L, Cella D, Cuzick J, Francis S, Locker G, Howell A. Quality of life of postmenopausal women in the Arimidex, Tamoxifen, Alone or in Combination (ATAC) Adjuvant Breast Cancer Trial. J Clin Oncol. 2004;22(21):4261-71.

246. Baumgart J, Nilsson K, Evers AS, Kallak TK, Poromaa IS. Sexual dysfunction in women on adjuvant endocrine therapy after breast cancer. Menopause. 2013;20(2):162-8.

247. Cella D, Fallowfield L, Barker P, Cuzick J, Locker G, Howell A, et al. Quality of life of postmenopausal women in the ATAC ("Arimidex", tamoxifen, alone or in combination) trial after completion of 5 years' adjuvant treatment for early breast cancer. Breast Cancer Res Treat. 2006;100(3):273-84.

248. Jones SE, Cantrell J, Vukelja S, Pippen J, O'Shaughnessy J, Blum JL, et al. Comparison of menopausal symptoms during the first year of adjuvant therapy with either exemestane or tamoxifen in early breast cancer: report of a Tamoxifen Exemestane Adjuvant Multicenter trial substudy. J Clin Oncol. 2007;25(30):4765-71.

249. Duffy S, Jackson TL, Lansdown M, Philips K, Wells M, Pollard S, et al. The ATAC ('Arimidex', Tamoxifen, Alone or in Combination) adjuvant breast cancer trial: first results of the

endometrial sub-protocol following 2 years of treatment. Hum Reprod. 2006;21(2):545-53.

250. Duffy SR, Distler W, Howell A, Cuzick J, Baum M. A lower incidence of gynecologic adverse events and interventions with anastrozole than with tamoxifen in the ATAC trial. Am J Obstet Gynecol. 2009;200(1):80 e1-7.

251. Loret de Mola JR. Endometrial changes with chronic tamoxifen use. Curr Opin Obstet Gynecol. 1997;9(3):160-4.

252. Neven P, De Muylder X, Van Belle Y, Vanderick G, De Muylder E. Tamoxifen and the uterus and endometrium. Lancet. 1989;1(8634):375.

253. Tamoxifen for early breast cancer: an overview of the randomised trials. Early Breast Cancer Trialists' Collaborative Group. Lancet. 1998;351(9114):1451-67.

254. Kedar RP, Bourne TH, Powles TJ, Collins WP, Ashley SE, Cosgrove DO, et al. Effects of tamoxifen on uterus and ovaries of postmenopausal women in a randomised breast cancer prevention trial. Lancet. 1994;343(8909):1318-21.

255. Kieback DG, Harbeck N, Bauer W, Hadji P, Weyer G, Menschik T, et al. Endometrial effects of exemestane compared to tamoxifen within the Tamoxifen Exemestane Adjuvant Multicenter (TEAM) trial: results of a prospective gynecological ultrasound substudy. Gynecol Oncol. 2010;119(3):500-5.

256. Bertelli G HE, Bliss JM et al., editor Intergroup Exemestane Study: results of the endometrial sub-protocol [abstract]. San Antonio Breast Cancer Symposium; 2004; San Antonio, TX, USA.

257. McCowan C, Shearer J, Donnan PT, Dewar JA, Crilly M, Thompson AM, et al. Cohort study examining tamoxifen adherence and its relationship to mortality in women with breast cancer. Br J Cancer. 2008;99(11):1763-8.

258. Hershman DL, Shao T, Kushi LH, Buono D, Tsai WY, Fehrenbacher L, et al. Early discontinuation and non-adherence to adjuvant hormonal therapy are associated with increased mortality in women with breast cancer. Breast Cancer Res Treat. 2011;126(2):529-37.

259. Murphy CC, Bartholomew LK, Carpentier MY, Bluethmann SM, Vernon SW. Adherence to adjuvant hormonal therapy among breast cancer survivors in clinical practice: a systematic review. Breast Cancer Res Treat. 2012;134(2):459-78.

260. Cheung WY, Lai EC, Ruan JY, Chang JT, Setoguchi S. Comparative adherence to oral hormonal agents in older women with breast cancer. Breast Cancer Res Treat. 2015;152(2):419-27.

261. Partridge AH, LaFountain A, Mayer E, Taylor BS, Winer E, Asnis-Alibozek A. Adherence to initial adjuvant anastrozole therapy among women with early-stage breast cancer. J Clin Oncol. 2008;26(4):556-62.

262. Huiart L, Dell'Aniello S, Suissa S. Use of tamoxifen and aromatase inhibitors in a large population-based cohort of women with breast cancer. Br J Cancer. 2011;104(10):1558-63.

263. Rae JM, Sikora MJ, Henry NL, Li L, Kim S, Oesterreich S, et al. Cytochrome P450 2D6 activity predicts discontinuation of tamoxifen therapy in breast cancer patients. Pharmacogenomics J. 2009;9(4):258-64.

264. Lash TL, Fox MP, Westrup JL, Fink AK, Silliman RA. Adherence to tamoxifen over the five-year course. Breast Cancer Res Treat. 2006;99(2):215-20.

265. Fink AK, Gurwitz J, Rakowski W, Guadagnoli E, Silliman RA. Patient beliefs and tamoxifen discontinuance in older women with estrogen receptor--positive breast cancer. J Clin Oncol. 2004;22(16):3309-15.

266. Gotay C, Dunn J. Adherence to long-term adjuvant hormonal therapy for breast cancer. Expert Rev Pharmacoecon Outcomes Res. 2011;11(6):709-15.

267. Geisler J, King N, Anker G, Ornati G, Di Salle E, Lonning PE, et al. In vivo inhibition of aromatization by exemestane, a novel irreversible aromatase inhibitor, in postmenopausal breast cancer patients. Clin Cancer Res. 1998;4(9):2089-93.

268. Buzzetti F, Di Salle E, Longo A, Briatico G. Synthesis and aromatase inhibition by potential metabolites of exemestane (6-methylenandrosta-1,4-diene-3,17-dione). Steroids. 1993;58(11):527-32.

269. Lonning PE. Pharmacological profiles of exemestane and formestane, steroidal aromatase inhibitors used for treatment of postmenopausal breast cancer. Breast Cancer Res Treat. 1998;49 Suppl 1:S45-52; discussion S73-7.

270. Mareck U, Geyer H, Guddat S, Haenelt N, Koch A, Kohler M, et al. Identification of the aromatase inhibitors anastrozole and exemestane in human urine using liquid chromatography/tandem mass spectrometry. Rapid Commun Mass Spectrom. 2006;20(12):1954-62.

271. Traina TA, Poggesi I, Robson M, Asnis A, Duncan BA, Heerdt A, et al. Pharmacokinetics and tolerability of exemestane in combination with raloxifene in postmenopausal women with a history of breast cancer. Breast Cancer Res Treat. 2008;111(2):377-88.

272. Ariazi EA, Leitao A, Oprea TI, Chen B, Louis T, Bertucci AM, et al. Exemestane's 17-hydroxylated metabolite exerts biological effects as an androgen. Mol Cancer Ther. 2007;6(11):2817-27.

273. Corona G, Elia C, Casetta B, Diana C, Rosalen S, Bari M, et al. A liquid chromatography-tandem mass spectrometry method for the simultaneous determination of exemestane and its metabolite 17-dihydroexemestane in human plasma. J Mass Spectrom. 2009;44(6):920-8.

274. Kalow W, Tang BK, Endrenyi L. Hypothesis: comparisons of inter- and intra-individual variations can substitute for twin studies in drug research. Pharmacogenetics. 1998;8(4):283-9.

275. Penning TM. The aldo-keto reductases (AKRs): Overview. Chem Biol Interact. 2015;234:236-46.

276. Penning TM, Burczynski ME, Jez JM, Hung CF, Lin HK, Ma H, et al. Human 3alpha-hydroxysteroid dehydrogenase isoforms (AKR1C1-AKR1C4) of the aldo-keto reductase superfamily: functional plasticity and tissue distribution reveals roles in the inactivation and formation of male and female sex hormones. Biochem J. 2000;351(Pt 1):67-77.

277. Kamdem LK, Flockhart DA, Desta Z. In vitro cytochrome P450-mediated metabolism of exemestane. Drug Metab Dispos. 2011;39(1):98-105.

278. Cavalcanti Gde A, Garrido BC, Leal FD, Padilha MC, de la Torre X, de Aquino Neto FR. Detection of new urinary exemestane metabolites by gas chromatography coupled to mass spectrometry. Steroids. 2011;76(10-11):1010-5.

279. Cocchiari G, Allievi C, Berardi A, Zugnoni P, Strolin Benedetti M, Dostert P. Urinary metabolism of exemestane, a new aromatase inhibitor, in rat, dog, monkey, and human volunteers. J Endocrinol Invest. 1994;17(Suppl. 1 to no. 3).

280. Thompson EA, Jr., Siiteri PK. Utilization of oxygen and reduced nicotinamide adenine dinucleotide phosphate by human placental microsomes during aromatization of androstenedione. J Biol Chem. 1974;249(17):5364-72.

281. The Human Protein Atlas [Internet]. 2015 [cited December 14th, 2016]. Available from: http://www.proteinatlas.org/.

282. Platt A, Xia Z, Liu Y, Chen G, Lazarus P. Impact of nonsynonymous single nucleotide polymorphisms on in-vitro metabolism of exemestane by hepatic cytosolic reductases. Pharmacogenet Genomics. 2016;26(8):370-80.

283. Marcos-Escribano A. BFA, Bonde-Larsen A.L., Retuerto J.I., Sierra I.H. 1,2-Dehydrogenation of steroidal 6-methylen derivatives. Tetrahedron. 2009;65(36):7587-90.

284. Vatèle J. 2-(Prenyloxymethyl)benzoyl (POMB) group: a new temporary protecting group removable by intramolecular cyclization. Tetrahedron. 2007;63(45):10921-9.

285. Baxter SW, Choong DY, Eccles DM, Campbell IG. Polymorphic variation in CYP19 and the risk of breast cancer. Carcinogenesis. 2001;22(2):347-9.

286. Meier M, Moller G, Adamski J. Perspectives in understanding the role of human 17beta-hydroxysteroid dehydrogenases in health and disease. Ann N Y Acad Sci. 2009;1155:15-24.

287. Matsunaga T, Shintani S, Hara A. Multiplicity of mammalian reductases for xenobiotic carbonyl compounds. Drug Metab Pharmacokinet. 2006;21(1):1-18.

288. Jin Y, Penning TM. Aldo-keto reductases and bioactivation/detoxication. Annu Rev Pharmacol Toxicol. 2007;47:263-92.

289. Penning TM, Drury JE. Human aldo-keto reductases: Function, gene regulation, and single nucleotide polymorphisms. Arch Biochem Biophys. 2007;464(2):241-50.

290. Variation Viewer [Internet]. National Center for Biotechnology Information, U.S. National Library of Medicine. [cited 2015]. Available from: http://www.ncbi.nlm.nih.gov/variation/view/.

291. Steckelbroeck S, Jin Y, Oyesanmi B, Kloosterboer HJ, Penning TM. Tibolone is metabolized by the 3alpha/3beta-hydroxysteroid dehydrogenase activities of the four human isozymes of the aldo-keto reductase 1C subfamily: inversion of stereospecificity with a delta5(10)-3-ketosteroid. Mol Pharmacol. 2004;66(6):1702-11.

292. Jin Y, Penning TM. Molecular docking simulations of steroid substrates into human cytosolic hydroxysteroid dehydrogenases (AKR1C1 and AKR1C2): insights into positional and stereochemical preferences. Steroids. 2006;71(5):380-91.

293. Jin Y, Mesaros AC, Blair IA, Penning TM. Stereospecific reduction of 5beta-reduced steroids by human ketosteroid reductases of the AKR (aldo-keto reductase) superfamily: role of AKR1C1-AKR1C4 in the metabolism of testosterone and progesterone via the 5beta-reductase pathway. Biochem J. 2011;437(1):53-61.

294. Askonas LJ, Ricigliano JW, Penning TM. The kinetic mechanism catalysed by homogeneous rat liver 3 alpha-hydroxysteroid dehydrogenase. Evidence for binary and ternary dead-end complexes containing non-steroidal anti-inflammatory drugs. Biochem J. 1991;278 (Pt 3):835-41.

295. Neuhauser W, Haltrich D, Kulbe KD, Nidetzky B. NAD(P)H-dependent aldose reductase from the xylose-assimilating yeast Candida tenuis. Isolation, characterization and biochemical properties of the enzyme. Biochem J. 1997;326 (Pt 3):683-92.

296. Trauger JW, Jiang A, Stearns BA, LoGrasso PV. Kinetics of allopregnanolone formation catalyzed by human 3 alpha-hydroxysteroid dehydrogenase type III (AKR1C2). Biochemistry. 2002;41(45):13451-9.

297. Cooper WC, Jin Y, Penning TM. Elucidation of a complete kinetic mechanism for a mammalian hydroxysteroid dehydrogenase (HSD) and identification of all enzyme forms on the reaction coordinate: the example of rat liver 3alpha-HSD (AKR1C9). J Biol Chem. 2007;282(46):33484-93.

298. Arthur JW, Reichardt JK. Modeling single nucleotide polymorphisms in the human AKR1C1 and AKR1C2 genes: implications for functional and genotyping analyses. PLoS One. 2010;5(12):e15604.

299. Kume T, Iwasa H, Shiraishi H, Yokoi T, Nagashima K, Otsuka M, et al. Characterization of a novel variant (S145C/L311V) of 3alpha-hydroxysteroid/dihydrodiol dehydrogenase in human liver. Pharmacogenetics. 1999;9(6):763-71.

300. Lan Q, Mumford JL, Shen M, Demarini DM, Bonner MR, He X, et al. Oxidative damage-

related genes AKR1C3 and OGG1 modulate risks for lung cancer due to exposure to PAH-rich coal combustion emissions. Carcinogenesis. 2004;25(11):2177-81.

301. Bains OS, Grigliatti TA, Reid RE, Riggs KW. Naturally occurring variants of human aldo-keto reductases with reduced in vitro metabolism of daunorubicin and doxorubicin. J Pharmacol Exp Ther. 2010;335(3):533-45.

302. Takahashi RH, Grigliatti TA, Reid RE, Riggs KW. The effect of allelic variation in aldo-keto reductase 1C2 on the in vitro metabolism of dihydrotestosterone. J Pharmacol Exp Ther. 2009;329(3):1032-9.

303. Jez JM, Bennett MJ, Schlegel BP, Lewis M, Penning TM. Comparative anatomy of the aldo-keto reductase superfamily. Biochem J. 1997;326 (Pt 3):625-36.

304. Jakobsson J, Palonek E, Lorentzon M, Ohlsson C, Rane A, Ekstrom L. A novel polymorphism in the 17beta-hydroxysteroid dehydrogenase type 5 (aldo-keto reductase 1C3) gene is associated with lower serum testosterone levels in caucasian men. Pharmacogenomics J. 2007;7(4):282-9.

305. Figueroa JD, Malats N, Garcia-Closas M, Real FX, Silverman D, Kogevinas M, et al. Bladder cancer risk and genetic variation in AKR1C3 and other metabolizing genes. Carcinogenesis. 2008;29(10):1955-62.

306. Matsuura K, Hara A, Deyashiki Y, Iwasa H, Kume T, Ishikura S, et al. Roles of the C-terminal domains of human dihydrodiol dehydrogenase isoforms in the binding of substrates and modulators: probing with chimaeric enzymes. Biochem J. 1998;336 (Pt 2):429-36.

307. Guengerich FP. Cytochrome p450 and chemical toxicology. Chem Res Toxicol. 2008;21(1):70-83.

308. Preissner SC, Hoffmann MF, Preissner R, Dunkel M, Gewiess A, Preissner S. Polymorphic cytochrome P450 enzymes (CYPs) and their role in personalized therapy. PLoS One. 2013;8(12):e82562.

309. Varela CL, Amaral C, Tavares da Silva E, Lopes A, Correia-da-Silva G, Carvalho RA, et al. Exemestane metabolites: Synthesis, stereochemical elucidation, biochemical activity and anti-proliferative effects in a hormone-dependent breast cancer cell line. Eur J Med Chem. 2014;87:336-45.

310. Bourrie M, Meunier V, Berger Y, Fabre G. Cytochrome P450 isoform inhibitors as a tool for the investigation of metabolic reactions catalyzed by human liver microsomes. J Pharmacol Exp Ther. 1996;277(1):321-32.

311. Khojasteh SC, Prabhu S, Kenny JR, Halladay JS, Lu AY. Chemical inhibitors of cytochrome P450 isoforms in human liver microsomes: a re-evaluation of P450 isoform selectivity. Eur J Drug Metab Pharmacokinet. 2011;36(1):1-16.

312. Administration USFaD. Drug Development and Drug Interactions: Table of Substrate,

Inhibitors and Inducers. 2006.

313. Zhou SF. Polymorphism of human cytochrome P450 2D6 and its clinical significance: Part I. Clin Pharmacokinet. 2009;48(11):689-723.

314. Chang GW, Kam PC. The physiological and pharmacological roles of cytochrome P450 isoenzymes. Anaesthesia. 1999;54(1):42-50.

315. Guengerich FP. Common and uncommon cytochrome P450 reactions related to metabolism and chemical toxicity. Chem Res Toxicol. 2001;14(6):611-50.

316. Zhou S. Cytochrome P450 CYP2D6: Structure, Function, Regulation and Polymorphism. Boca Raton, FL: Taylor & Francis Group, LLC; 2016.

317. Stiborova M, Martinek V, Rydlova H, Koblas T, Hodek P. Expression of cytochrome P450 1A1 and its contribution to oxidation of a potential human carcinogen 1-phenylazo-2-naphthol (Sudan I) in human livers. Cancer Lett. 2005;220(2):145-54.

318. Wan YJ, Poland RE, Han G, Konishi T, Zheng YP, Berman N, et al. Analysis of the CYP2D6 gene polymorphism and enzyme activity in African-Americans in southern California. Pharmacogenetics. 2001;11(6):489-99.

319. Raimundo S, Toscano C, Klein K, Fischer J, Griese EU, Eichelbaum M, et al. A novel intronic mutation, 2988G>A, with high predictivity for impaired function of cytochrome P450 2D6 in white subjects. Clin Pharmacol Ther. 2004;76(2):128-38.

320. Dalen P, Frengell C, Dahl ML, Sjoqvist F. Quick onset of severe abdominal pain after codeine in an ultrarapid metabolizer of debrisoquine. Ther Drug Monit. 1997;19(5):543-4.

321. Gasche Y, Daali Y, Fathi M, Chiappe A, Cottini S, Dayer P, et al. Codeine intoxication associated with ultrarapid CYP2D6 metabolism. N Engl J Med. 2004;351(27):2827-31.

322. 1000 Genomes Browser [Internet]. [cited Aug. 25 2016]. Available from: http://www.ncbi.nlm.nih.gov/variation/tools/1000genomes/.

323. Watanabe Y, Fukuyoshi S, Hiratsuka M, Yamaotsu N, Hirono S, Takahashi O, et al. Prediction of three-dimensional structures and structural flexibilities of wild-type and mutant cytochrome P450 1A2 using molecular dynamics simulations. J Mol Graph Model. 2016;68:48-56.

324. Ito M, Katono Y, Oda A, Hirasawa N, Hiratsuka M. Functional characterization of 20 allelic variants of CYP1A2. Drug Metab Pharmacokinet. 2015;30(3):247-52.

325. Kobayashi K, Takahashi O, Hiratsuka M, Yamaotsu N, Hirono S, Watanabe Y, et al. Evaluation of influence of single nucleotide polymorphisms in cytochrome P450 2B6 on substrate recognition using computational docking and molecular dynamics simulation. PLoS One. 2014;9(5):e96789.

326. Zhang T, Liu LA, Lewis DF, Wei DQ. Long-range effects of a peripheral mutation on the enzymatic activity of cytochrome P450 1A2. J Chem Inf Model. 2011;51(6):1336-46.

327. de Waal PW, Sunden KF, Furge LL. Molecular dynamics of CYP2D6 polymorphisms in the absence and presence of a mechanism-based inactivator reveals changes in local flexibility and dominant substrate access channels. PLoS One. 2014;9(10):e108607.

328. Skopalik J, Anzenbacher P, Otyepka M. Flexibility of human cytochromes P450: molecular dynamics reveals differences between CYPs 3A4, 2C9, and 2A6, which correlate with their substrate preferences. J Phys Chem B. 2008;112(27):8165-73.

329. Kaspera R, Naraharisetti SB, Tamraz B, Sahele T, Cheesman MJ, Kwok PY, et al. Cerivastatin in vitro metabolism by CYP2C8 variants found in patients experiencing rhabdomyolysis. Pharmacogenet Genomics. 2010;20(10):619-29.

330. Parikh S, Ouedraogo JB, Goldstein JA, Rosenthal PJ, Kroetz DL. Amodiaquine metabolism is impaired by common polymorphisms in CYP2C8: implications for malaria treatment in Africa. Clin Pharmacol Ther. 2007;82(2):197-203.

331. Martinez C, Garcia-Martin E, Blanco G, Gamito FJ, Ladero JM, Agundez JA. The effect of the cytochrome P450 CYP2C8 polymorphism on the disposition of (R)-ibuprofen enantiomer in healthy subjects. Br J Clin Pharmacol. 2005;59(1):62-9.

332. Garcia-Martin E, Martinez C, Tabares B, Frias J, Agundez JA. Interindividual variability in ibuprofen pharmacokinetics is related to interaction of cytochrome P450 2C8 and 2C9 amino acid polymorphisms. Clin Pharmacol Ther. 2004;76(2):119-27.

333. Lopez-Rodriguez R, Novalbos J, Gallego-Sandin S, Roman-Martinez M, Torrado J, Gisbert JP, et al. Influence of CYP2C8 and CYP2C9 polymorphisms on pharmacokinetic and pharmacodynamic parameters of racemic and enantiomeric forms of ibuprofen in healthy volunteers. Pharmacol Res. 2008;58(1):77-84.

334. Kirchheiner J, Thomas S, Bauer S, Tomalik-Scharte D, Hering U, Doroshyenko O, et al. Pharmacokinetics and pharmacodynamics of rosiglitazone in relation to CYP2C8 genotype. Clin Pharmacol Ther. 2006;80(6):657-67.

335. Aquilante CL, Bushman LR, Knutsen SD, Burt LE, Rome LC, Kosmiski LA. Influence of SLCO1B1 and CYP2C8 gene polymorphisms on rosiglitazone pharmacokinetics in healthy volunteers. Hum Genomics. 2008;3(1):7-16.

336. Kirchheiner J, Kudlicz D, Meisel C, Bauer S, Meineke I, Roots I, et al. Influence of CYP2C9 polymorphisms on the pharmacokinetics and cholesterol-lowering activity of (-)-3S,5R-fluvastatin and (+)-3R,5S-fluvastatin in healthy volunteers. Clin Pharmacol Ther. 2003;74(2):186-94.

337. Tornio A, Niemi M, Neuvonen PJ, Backman JT. Trimethoprim and the CYP2C8*3 allele have opposite effects on the pharmacokinetics of pioglitazone. Drug Metab Dispos. 2008;36(1):73-80.

338. Niemi M, Leathart JB, Neuvonen M, Backman JT, Daly AK, Neuvonen PJ. Polymorphism in CYP2C8 is associated with reduced plasma concentrations of repaglinide. Clin Pharmacol Ther. 2003;74(4):380-7.

339. Niemi M, Backman JT, Kajosaari LI, Leathart JB, Neuvonen M, Daly AK, et al. Polymorphic organic anion transporting polypeptide 1B1 is a major determinant of repaglinide pharmacokinetics. Clin Pharmacol Ther. 2005;77(6):468-78.

340. Naraharisetti SB, Lin YS, Rieder MJ, Marciante KD, Psaty BM, Thummel KE, et al. Human liver expression of CYP2C8: gender, age, and genotype effects. Drug Metab Dispos. 2010;38(6):889-93.

341. Aithal GP, Day CP, Kesteven PJ, Daly AK. Association of polymorphisms in the cytochrome P450 CYP2C9 with warfarin dose requirement and risk of bleeding complications. Lancet. 1999;353(9154):717-9.

342. Lindh JD, Holm L, Andersson ML, Rane A. Influence of CYP2C9 genotype on warfarin dose requirements--a systematic review and meta-analysis. Eur J Clin Pharmacol. 2009;65(4):365-75.

343. Mosher CM, Tai G, Rettie AE. CYP2C9 amino acid residues influencing phenytoin turnover and metabolite regio- and stereochemistry. J Pharmacol Exp Ther. 2009;329(3):938-44.

344. Rosemary J, Surendiran A, Rajan S, Shashindran CH, Adithan C. Influence of the CYP2C9 AND CYP2C19 polymorphisms on phenytoin hydroxylation in healthy individuals from south India. Indian J Med Res. 2006;123(5):665-70.

345. van der Weide J, Steijns LS, van Weelden MJ, de Haan K. The effect of genetic polymorphism of cytochrome P450 CYP2C9 on phenytoin dose requirement. Pharmacogenetics. 2001;11(4):287-91.

346. Sandberg M, Yasar U, Stromberg P, Hoog JO, Eliasson E. Oxidation of celecoxib by polymorphic cytochrome P450 2C9 and alcohol dehydrogenase. Br J Clin Pharmacol. 2002;54(4):423-9.

347. Yasar U, Forslund-Bergengren C, Tybring G, Dorado P, Llerena A, Sjoqvist F, et al. Pharmacokinetics of losartan and its metabolite E-3174 in relation to the CYP2C9 genotype. Clin Pharmacol Ther. 2002;71(1):89-98.

348. Aynacioglu AS, Brockmoller J, Bauer S, Sachse C, Guzelbey P, Ongen Z, et al. Frequency of cytochrome P450 CYP2C9 variants in a Turkish population and functional relevance for phenytoin. Br J Clin Pharmacol. 1999;48(3):409-15.

349. Wei L, Locuson CW, Tracy TS. Polymorphic variants of CYP2C9: mechanisms involved in reduced catalytic activity. Mol Pharmacol. 2007;72(5):1280-8.

350. Sano E, Li W, Yuki H, Liu X, Furihata T, Kobayashi K, et al. Mechanism of the decrease in catalytic activity of human cytochrome P450 2C9 polymorphic variants investigated by

computational analysis. J Comput Chem. 2010;31(15):2746-58.

351. Blaisdell J, Jorge-Nebert LF, Coulter S, Ferguson SS, Lee SJ, Chanas B, et al. Discovery of new potentially defective alleles of human CYP2C9. Pharmacogenetics. 2004;14(8):527-37.

352. Allabi AC, Gala JL, Horsmans Y. CYP2C9, CYP2C19, ABCB1 (MDR1) genetic polymorphisms and phenytoin metabolism in a Black Beninese population. Pharmacogenet Genomics. 2005;15(11):779-86.

353. Cavallari LH, Vaynshteyn D, Freeman KM, Wang D, Perera MA, Takahashi H, et al. CYP2C9 promoter region single-nucleotide polymorphisms linked to the R150H polymorphism are functional suggesting their role in CYP2C9*8-mediated effects. Pharmacogenet Genomics. 2013;23(4):228-31.

354. Matimba A, Del-Favero J, Van Broeckhoven C, Masimirembwa C. Novel variants of major drug-metabolising enzyme genes in diverse African populations and their predicted functional effects. Hum Genomics. 2009;3(2):169-90.

355. Jarrar YB, Lee SJ. Molecular functionality of CYP2C9 polymorphisms and their influence on drug therapy. Drug Metabol Drug Interact. 2014;29(4):211-20.

356. Sakuyama K, Sasaki T, Ujiie S, Obata K, Mizugaki M, Ishikawa M, et al. Functional characterization of 17 CYP2D6 allelic variants (CYP2D6.2, 10, 14A-B, 18, 27, 36, 39, 47-51, 53-55, and 57). Drug Metab Dispos. 2008;36(12):2460-7.

357. Marez D, Legrand M, Sabbagh N, Lo Guidice JM, Spire C, Lafitte JJ, et al. Polymorphism of the cytochrome P450 CYP2D6 gene in a European population: characterization of 48 mutations and 53 alleles, their frequencies and evolution. Pharmacogenetics. 1997;7(3):193-202.

358. Bradford LD. CYP2D6 allele frequency in European Caucasians, Asians, Africans and their descendants. Pharmacogenomics. 2002;3(2):229-43.

359. Ji L, Pan S, Marti-Jaun J, Hanseler E, Rentsch K, Hersberger M. Single-step assays to analyze CYP2D6 gene polymorphisms in Asians: allele frequencies and a novel *14B allele in mainland Chinese. Clin Chem. 2002;48(7):983-8.

360. Johansson I, Oscarson M, Yue QY, Bertilsson L, Sjoqvist F, Ingelman-Sundberg M. Genetic analysis of the Chinese cytochrome P4502D locus: characterization of variant CYP2D6 genes present in subjects with diminished capacity for debrisoquine hydroxylation. Mol Pharmacol. 1994;46(3):452-9.

361. Ishiguro A, Kubota T, Sasaki H, Iga T. A long PCR assay to distinguish CYP2D6*5 and a novel CYP2D6 mutant allele associated with an 11-kb EcoRI haplotype. Clin Chim Acta. 2004;347(1-2):217-21.

362. Shen H, He MM, Liu H, Wrighton SA, Wang L, Guo B, et al. Comparative metabolic capabilities and inhibitory profiles of CYP2D6.1, CYP2D6.10, and CYP2D6.17. Drug Metab Dispos. 2007;35(8):1292-300.

363. Yokota H, Tamura S, Furuya H, Kimura S, Watanabe M, Kanazawa I, et al. Evidence for a new variant CYP2D6 allele CYP2D6J in a Japanese population associated with lower in vivo rates of sparteine metabolism. Pharmacogenetics. 1993;3(5):256-63.

364. Masimirembwa C, Persson I, Bertilsson L, Hasler J, Ingelman-Sundberg M. A novel mutant variant of the CYP2D6 gene (CYP2D6*17) common in a black African population: association with diminished debrisoquine hydroxylase activity. Br J Clin Pharmacol. 1996;42(6):713-9.

365. Wennerholm A, Johansson I, Massele AY, Lande M, Alm C, Aden-Abdi Y, et al. Decreased capacity for debrisoquine metabolism among black Tanzanians: analyses of the CYP2D6 genotype and phenotype. Pharmacogenetics. 1999;9(6):707-14.

366. Griese EU, Asante-Poku S, Ofori-Adjei D, Mikus G, Eichelbaum M. Analysis of the CYP2D6 gene mutations and their consequences for enzyme function in a West African population. Pharmacogenetics. 1999;9(6):715-23.

367. Aklillu E, Persson I, Bertilsson L, Johansson I, Rodrigues F, Ingelman-Sundberg M. Frequent distribution of ultrarapid metabolizers of debrisoquine in an ethiopian population carrying duplicated and multiduplicated functional CYP2D6 alleles. J Pharmacol Exp Ther. 1996;278(1):441-6.

368. Bogni A, Monshouwer M, Moscone A, Hidestrand M, Ingelman-Sundberg M, Hartung T, et al. Substrate specific metabolism by polymorphic cytochrome P450 2D6 alleles. Toxicol In Vitro. 2005;19(5):621-9.

369. Oscarson M, Hidestrand M, Johansson I, Ingelman-Sundberg M. A combination of mutations in the CYP2D6*17 (CYP2D6Z) allele causes alterations in enzyme function. Mol Pharmacol. 1997;52(6):1034-40.

370. Koymans LM, Vermeulen NP, Baarslag A, Donne-Op den Kelder GM. A preliminary 3D model for cytochrome P450 2D6 constructed by homology model building. J Comput Aided Mol Des. 1993;7(3):281-9.

371. Gotoh O. Substrate recognition sites in cytochrome P450 family 2 (CYP2) proteins inferred from comparative analyses of amino acid and coding nucleotide sequences. J Biol Chem. 1992;267(1):83-90.

372. Hasler JA, Harlow GR, Szklarz GD, John GH, Kedzie KM, Burnett VL, et al. Site-directed mutagenesis of putative substrate recognition sites in cytochrome P450 2B11: importance of amino acid residues 114, 290, and 363 for substrate specificity. Mol Pharmacol. 1994;46(2):338-45.

373. Blaisdell J, Mohrenweiser H, Jackson J, Ferguson S, Coulter S, Chanas B, et al. Identification and functional characterization of new potentially defective alleles of human CYP2C19. Pharmacogenetics. 2002;12(9):703-11.

374. Ibeanu GC, Blaisdell J, Ghanayem BI, Beyeler C, Benhamou S, Bouchardy C, et al. An additional defective allele, CYP2C19*5, contributes to the S-mephenytoin poor metabolizer

phenotype in Caucasians. Pharmacogenetics. 1998;8(2):129-35.